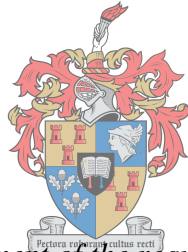


Formwork Pressures by Self-Compacting Concrete: A Practical Perspective

by

Jean-Claude Labuschagne



*Thesis presented in fulfilment of the requirements for the degree of
Master of Engineering in Civil Engineering in the Faculty of Engineering
at Stellenbosch University*

STELLENBOSCH
UNIVERSITY



Supervisor: Prof Jan Wium
Department of Civil Engineering
Co-supervisor: Mr Chris Jurgens
Department of Civil Engineering

March 2018

Declaration

By submitting this thesis electronically, I declare that the entirety of the work contained therein is my own, original work, that I am the sole author thereof (save to the extent explicitly otherwise stated), that reproduction and publication thereof by Stellenbosch University will not infringe any third party rights and that I have not previously in its entirety or in part submitted it for obtaining any qualification.

March 2018

Copyright © 2018 Stellenbosch University

All rights reserved



UNIVERSITEIT • STELLENBOSCH • UNIVERSITY
jou kennisvenoot • your knowledge partner

Plagiaatverklaring / Plagiarism Declaration

- 1 Plagiaat is die oorneem en gebruik van die idees, materiaal en ander intellektuele eiendom van ander persone asof dit jou eie werk is.
Plagiarism is the use of ideas, material and other intellectual property of another's work and to present is as my own.
- 2 Ek erken dat die pleeg van plagiaat 'n strafbare oortreding is aangesien dit 'n vorm van diefstal is.
I agree that plagiarism is a punishable offence because it constitutes theft.
- 3 Ek verstaan ook dat direkte vertalings plagiaat is.
I also understand that direct translations are plagiarism.
- 4 Dienooreenkomstig is alle aanhalings en bydraes vanuit enige bron (ingesluit die internet) volledig verwys (erken). Ek erken dat die woordelike aanhaal van teks sonder aanhalingstekens (selfs al word die bron volledig erken) plagiaat is.
Accordingly all quotations and contributions from any source whatsoever (including the internet) have been cited fully. I understand that the reproduction of text without quotation marks (even when the source is cited) is plagiarism.
- 5 Ek verklaar dat die werk in hierdie skryfstuk vervat, behalwe waar anders aangedui, my eie oorspronklike werk is en dat ek dit nie vantevore in die geheel of gedeeltelik ingehandig het vir bepunting in hierdie module/werkstuk of 'n ander module/werkstuk nie.
I declare that the work contained in this assignment, except where otherwise stated, is my original work and that I have not previously (in its entirety or in part) submitted it for grading in this module/assignment or another module/assignment.

Studentenommer / Student number	Handtekening / Signature
Voorletters en van / Initials and surname	Datum / Date

Abstract

One of the challenges facing the South African construction industry is the prediction of lateral formwork pressure exerted by Self-Compacting Concrete. A major hindrance to the increased use of Self-Compacting Concrete (SCC) in cast-in-place applications in the South African construction industry is the lack of information about and understanding of, lateral formwork pressure exerted by SCC.

There are no accepted standardised codes or guidelines for the local construction industry that can be used to facilitate the design of formwork for predicting formwork pressure exerted by SCC. Formwork systems designers have been encouraged to design formwork to withstand full hydrostatic pressures, unless a method based on appropriate and reliable experimental data is available. This generally limits contractors to low wall or extremely strong formwork, which can lead to extra formwork costs. Numerous parameters, including placement conditions, material properties and formwork characteristics can influence lateral formwork pressure.

This study presents the results of an experimental investigation undertaken using on-site conditions, aimed at studying the influence of placement methods (top-down and bottom-up pumping), of various casting rates, as well as implementing predetermined waiting periods of 10 and 15 minutes between castings. The influence of each of these parameters was evaluated by using six vertical instrumented wall elements. All six walls were fitted with eight flush diaphragms transducers and were identical in dimensions (5.4 m x 2.0 m x 0.25 m).

The test results show that with high casting rates from the top of the formwork system, hydrostatic pressure can be expected. It was shown that by interrupting the casting procedure and implementing waiting periods to allow the fresh SCC to set, decreased the lateral pressure exerted. It was found that, when pumping from the base of the formwork system at high casting rates, hydrostatic pressure could be expected during the casting process and that lateral pressures above the hydrostatic pressure could be expected during the casting of the SCC. The knowledge gained in this study can therefore be used to lay the foundation for future studies for the prediction of lateral pressure exerted on formwork by SCC under South African conditions.

Opsomming

Een van die uitdagings vir die Suid Afrikaanse konstruksie industrie is tans in die gebied van die laterale druk wat op bekisting uitgeoefen word deur selfkompaktende beton (SCC), en spesifiek die akkurate voorspelling van hierdie druk. 'n Groot hindernis tot die meer algemene gebruik van SCC in die giet van beton in die Suid Afrikaanse konstruksie industrie is die gebrek aan inligting oor, en die begrip van, die laterale druk wat op bekisting uitgeoefen word deur SCC.

Daar bestaan geen aanvaarde standaard kodes of riglyne vir die plaaslike konstruksie industrie om die ontwerp van bekisting te vergemaklik deur die laterale druk van SCC op bekisting te voorspel nie. Bekisting stelselontwerpers word aangemoedig om bekisting te ontwerp om die volle hidrostatiese druk te kan weerstaan, tensy 'n ander metode beskikbaar is wat op toepaslik en betroubare data gebaseer is. Dit beperk kontrakteurs gewoonlik tot of lae muur of uiters sterk bekisting, wat tot hoë bekistingskoste kan lei. Verskeie parameters, insluitend plasingstoestande, material eienskappe en bekistingseienskappe, kan die laterale druk van SCC op bekisting beïnvloed.

Hierdie studie verskaf resultate van 'n eksperimentele ondersoek wat onder terrein toestande onderneem is, met die doel om die invloed van plasingsmethodes te bepaal (van bo na onder gepomp, sowel as van onder na bo), van verskillende giet-tempos, sowel as voorafbepaalde wagperiodes met duurtes van 10 en 15 minute tussen gietperiodes. Die invloed van elk van die parameters is evalueer deur die gebruik van ses vertikale muurelemente met gemonteerde drukmeters. Op elke muurelement is agt diafragma sensors gemonteer. Die afmetings van al die mure was dieselfde (5.4 m x 2.0 m x 0.25 m).

Die toetsresultate toon dat 'n hoë giet-tempo vanaf die bokant van die bekistingstelsel, 'n hidrostatiese druk tot gevolg het. Dit is bewys dat onderbreking van hierdie gietproses met wagperiodes, wat toelaat dat die vars SCC kan set, die laterale druk op die bekisting verminder. Dit is gevind dat, wanneer SCC vanaf die onderkant van die bekisting gepomp word teen 'n hoë tempo, hidrostatiese druk verwag kan word teen die einde van die gietproses en dat laterale druk op die bekisting bo hidrostatiese druk sal styg tydens die gietproses. Die kennis verwerf tydens hierdie studie kan dus van nut wees as die basis vir toekomstige studies wat kan lei tot die akkurate voorspelling van die laterale druk van SCC op die bekisting onder verskillende omstandighede in Suid Afrika.

Acknowledgements

Without the significant time and support of all those directly or indirectly involved within the research study, this thesis would not have been successfully completed. It is to the following people I owe my sincere appreciation:

First and foremost, I would like to thank my Lord and Saviour, Jesus Christ for His grace, protection and love, and for giving me the opportunity and ability to perform and complete my master's studies.

Secondly, I would like to extend my sincere appreciation to my study leader, Prof Wium, who expertly guided me through my research study. His unwavering enthusiasm for the project kept me constantly engaged with my research. His wisdom, knowledge, and commitment to the highest standards motivated and inspired me to complete this thesis. I am also grateful for his quick responses to all my queries and requests for advice during the research study. His office door was always open whenever I had a question about my research. I am particularly grateful for the comments of Prof Wium with respect to suggested areas of improvement of the testing procedures, equipment and the enhancement of the thesis.

Next, I would like to thank Mr Chris Jurgens for his advice, patience, support, assistance and guidance. I truly appreciate all the encouragements and suggestions during our bi-weekly meeting discussions.

Special thanks go to PERI Formwork Scaffolding Engineering Pty Ltd. (Mr Riaan Brits) for generously sponsoring the formwork system, testing equipment and finance of the concrete pumps. My appreciation also extends to Lafarge South Africa (Mr Hennis van Zyl), for supplying the Self-Compacting Concrete to perform the experiments. I would also like to thank Mr Hennie Karsten of Ekcon and Mr Tobie Cilliers of NMC Construction Pty Ltd for providing the testing space and making it possible to perform full-scale form filling tests at a construction site near Val-de-Vie estate in Paarl, Western Cape. I would also like to extend my appreciation and thanks to Mr Geoffrey McGiven of Pumping Readymix and NMC Construction Pty Ltd for their sponsorships.

For their assistance in completing this study, I would like to thank Johan van der Merwe for his meticulous assistance in the construction of the jackets for the pressor transducers (Civil Workshop), Dr Ousmane Sawadogo (Institute for Water and Environmental Engineering) and Mr Danie Wium (Mechanical Engineering) for their input into establishing a model designed using ANSYS, and Stefan Erasmus (Electrical Engineering) for his assistance in building the data logger.

I would like to acknowledge with gratitude, the prayers, support and love of my family – they kept me going. Finally, I want to express my deepest love and appreciation to my parents for all the sacrifices they have made to insure my success. I would not be where I am today if I had not had their love, encouragement and support while completing my graduate studies.

Dedication:

To the One who loved me, died for me, and who was raised from the dead – ***JESUS CHRIST*** my Saviour. (Bible: 2 Corinthians 5:15)

“Scientists investigate that which already is; Engineers create that which has never been.”

Albert Einstein

Table of Contents

Declaration	i
Abstract	iii
Opsomming	iv
Acknowledgements	v
List of Figures	xi
List of Tables	xvi
Nomenclature	xvii
Chapter 1 : Introduction	1
1.1 Introduction	1
1.2 Motivation	3
1.3 Problem Statement	4
1.4 Research Scope.....	4
1.5 Research Strengths and Limitations	5
1.6 Research Aim and Objectives	5
1.6.1 Research Aim.....	5
1.6.2 Research Objectives	6
1.7 Research Methodology	6
1.8 Sponsors	7
1.9 Thesis Overview	7
Chapter 2 : Literature Review	9
2.1 Introduction	9
2.2 Definitions	11
2.2.1 Lateral Formwork Pressure	11
2.2.2 Self-Compacting Concrete	11
2.2.3 Hydration	12
2.2.4 Trixotropy	12
2.2.5 Viscosity.....	13

2.2.6	Yield Stress	13
2.2.7	Formwork Systems	13
2.3	Overview of Lateral Formwork Pressure	14
2.4	Placement Characteristics.....	16
2.4.1	Method of Placement	16
2.4.1	Casting Rate	22
2.4.2	Concrete Temperature.....	23
2.4.3	Waiting Period between casting.....	24
2.4.4	Consistency Level (Slump Flow).....	25
2.5	Material Properties	26
2.5.1	SCC Binder Composition.....	26
2.5.2	Concrete Aggregate Characteristics.....	27
2.5.3	Water-Cementitious Material Ratio (w/cm)	27
2.5.4	Yield stress and Viscosity	28
2.5.5	Thixotropy.....	29
2.6	Formwork Characteristics	30
2.6.1	Formwork Dimension and Shape.....	30
2.6.2	Presence of reinforcing bars.....	30
2.6.3	Formwork System Material Type	31
2.7	Lateral Pressure Measuring Systems.....	31
2.8	Existing Models.....	35
2.1	Conclusion.....	41
Chapter 3	: Research Equipment	45
3.1	Introduction	45
3.2	Overview of Experiment	46
3.3	Experimental Recording Equipment	46
3.3.1	Pressure Transducers.....	46
3.3.2	Water Column Test	47

3.3.3	Pressure Transducer Adaptor	49
3.3.4	Data Logger.....	50
3.4	Concrete Pumping Equipment.....	53
3.4.1	Truck-Mounted Concrete Boom Pump.....	53
3.4.2	Portable Pump.....	55
3.5	Conclusion.....	56
Chapter 4 : Experimental Methodology		57
4.1	Introduction	57
4.2	Concrete Information	58
4.3	Concrete Properties Testing Methods	58
4.3.1	Slump Flow Test	58
4.3.2	Compressive Strength Test	60
4.3.3	Lafarge V-Funnel Test	61
4.4	Formwork System	61
4.5	Experimental Procedure	64
4.5.1	Experimental Set-up and Management	64
4.5.2	Top-down Casting Experiments.....	67
4.5.3	Bottom-up Casting Experiments.....	70
4.6	Conclusion.....	74
Chapter 5 : Experimental Results		76
5.1	Introduction	76
5.2	Top-down Pumping.....	77
5.2.1	Lateral Pressure Distribution for Wall 1	77
5.2.2	Lateral Pressure Distribution for Wall 2	82
5.2.3	Lateral Pressure Distribution for Wall 3	84
5.3	Bottom-up Pumping	86
5.3.1	Lateral Pressure Distribution for Wall 4	86
5.3.2	Lateral Pressure Distribution for Wall 5	91

5.3.3	Lateral Pressure Distribution for Wall 6	97
5.4	Results Comparison and Site Observations.....	102
5.4.1	Comparing the Results of Wall 1, Wall 2 and Wall 3.....	102
5.4.2	Comparing the Results of Wall 1 and Wall 5	104
5.4.3	Comparing the Results of Wall 4, Wall 5 and Wall 6.....	107
5.4.4	Comparing of Results to Existing Models	110
5.4.5	Site Observations	116
5.5	Conclusion.....	117
Chapter 6	: Conclusion and Recommendations	119
6.1	Introduction	119
6.2	Research Conclusion	119
6.3	Limitations of Experimental Results.....	121
6.4	Research Recommendations.....	122
References	123
Bibliography	134
Annexure A	: Additional CIFA K31L Information	135
Annexure B	: Additional Putzmeister 36Z-Meter Information.....	137
Annexure C	: Experimental Formwork System Design Drawing.....	139
Annexure D	: Pressure Readings for Wall 1	141
Annexure E	: Pressure Readings for Wall 2 and Wall 3	144
Annexure F	: Pressure Readings for Wall 4.....	146
Annexure G	: Pressure Readings for Wall 5	149
Annexure H	: Pressure Readings for Wall 6	152
Annexure I	: Humanities Ethical Approval.....	155
Annexure J	: Institutional Permission letter (PERI).....	158
Annexure K	: Institutional Permission letter (Lafarge)	160
Annexure L	: Institutional Permission letter (NMC)	162

List of Figures

Figure 1-1: Nelson Mandela Bridge (DYWIDAG Systems International).....	2
Figure 1-2: N4 Bakwena Toll Road Bridge Extension (Delf Consulting Engineers).....	2
Figure 1-3: Deck 2235 cross section (Jooste, 2004).	3
Figure 2-1: Layout and overview of Chapter 2.	10
Figure 2-2: The slump flow of CVC (left) and the slump flow of SCC (right) (Thrane <i>et al.</i> , 2008).	11
Figure 2-3: A typical formwork set-up for a concrete wall (The Constructor).....	14
Figure 2-4: Pumping from the top (left) and bottom (right) of the formwork (Khrapko, 2007).	16
Figure 2-5: Base and top placement locations influence thixotropic behaviour (Szecsy & Mohler, 2009).	17
Figure 2-6: Test set-up and position of the measuring anchors (Brameshuber & Uebachs, 2003). ..	18
Figure 2-7: Force of the lower anchor (Brameshuber & Uebachs, 2003).....	19
Figure 2-8: Lateral Pressure of SCC at the end of the casting (Leeman et al., 2006).....	19
Figure 2-9: Relative formwork pressure for low casting rates (Billberg, 2003).....	22
Figure 2-10: Influence of casting rate on the lateral pressure (Assaad and Khayat, 2006).	23
Figure 2-11: Effect of the SCC temperature on the lateral pressure (Khayat & Assaad, 2006).	24
Figure 2-12: Variations of lateral pressure with time for casting constantly, and after one and two Waiting Periods (Omran, et al., 2014).	25
Figure 2-13: Effect of consistency on the lateral pressure (Assaad& Khayat, 2006).....	25
Figure 2-14: Lateral pressure for SCC made with of various binders (Assaad & Khayat, 2005a)....	26
Figure 2-15: Variations of lateral pressure with regard to mixtures made with 10 mm MSA (Assaad & Khayat, 2005c).....	27
Figure 2-16: w/cm effect on the lateral pressure (PC-based HRWRA) (Khayat & Assaad, 2006)....	28
Figure 2-17: w/cm effect on relative pressure (PNS-based HRWRA) (Khayat & Assaad, 2006). ...	28
Figure 2-18: Lateral formwork pressure reduction 20 minutes after casting according to static and dynamic yield stress changes.	29
Figure 2-19: Dilatometer pressure cell (left) and test layout implemented (right) (Giammatteo, et al., 2007).	32
Figure 2-20: Dilatometer cell diagram (left) and control unit (right). (Giammatteo, et al., 2007). ...	33
Figure 2-21: Lateral pressure transducer (left) and pore-water pressure transducer (right). (Khayat & Assaad, 2008).....	33
Figure 2-22: Schematic diagram showing the strain gauge system used for measuring lateral pressure. (Khayat & Assaad, 2008).	34

Figure 2-23: Comparison of lateral pressure determined using the pressure sensor and strain gauge systems until cancellation in the hardened state (R: sand-to-total coarse aggregate ratio) (Khayat & Assaad, 2008).....	34
Figure 2-24: Schematic of UodS2 portable pressure column (left), and of UodS2 portable pressure column (right) (Khayat & Omran, 2009).	35
Figure 3-1: Layout and overview of Chapter 3.....	45
Figure 3-2: Stainless steel flush diaphragm pressure transducer – Series 1701.	47
Figure 3-3: Water column testing equipment.	48
Figure 3-4: Drawing of the PVC adaptor with dimensions (mm).....	49
Figure 3-5: Pressure transducer in the PVC Adaptor.....	50
Figure 3-6: Drilled hole in the formwork panel (left) and PVC adaptor mounted in the formwork panel (right).....	50
Figure 3-7: 24 v dc power supply.	51
Figure 3-8: The current loop between the transducers and the XR5-SE Data Logger.	52
Figure 3-9: XR5-SE data logger housing unit and pressure transducers	52
Figure 3-10: CIFA K31L Truck-Mounted Concrete Boom Pump.	53
Figure 3-11: The Putzmeister 36Z-Meter Truck-Mounted Concrete Boom Pump.	54
Figure 3-12: CIFA S8 Series PC 907 Portable Pump.	55
Figure 4-1: Layout and overview of Chapter 4.....	57
Figure 4-2: Base plate and Abrams cone used to measure the slump flow (De Schutter 2005).....	60
Figure 4-3: Typical image and dimensions of the V-funnel (De Schutter 2005).	61
Figure 4-4: Lightweight steel formwork panels.....	62
Figure 4-5: The 5.4 m high experimental wall element.	62
Figure 4-6: The DRS alignment coupler (left) and rigid tie (right).	63
Figure 4-7: The construction process of the modified Domino formwork system.	63
Figure 4-8: The wall inlet and shut-off valve.	64
Figure 4-9: A 3D Autocad design drawing of the wall inlet and shut-off value.....	64
Figure 4-10: Flush diaphragm transducer mounted in the PVC jacket.....	65
Figure 4-11 Drawing of the pressure transducer heights and layout (mm)	66
Figure 4-12: Extended CIFA K31L boom pump arm.....	68
Figure 4-13: The end hose placed within the wall element (left), Agilia Vertical concrete being placed into the wall element (right).	68
Figure 4-14: The CIFA S8 Series PC 907 Portable Pump set up near the wall.....	72
Figure 4-15: The pipe from the pump connecting the wall element inlet.	72
Figure 5-1: Overview and layout of Chapter 5.	76

Figure 5-2: Lateral pressure profile at various casting heights during casting for Wall 1 (SCC-TP-R80).....	77
Figure 5-3: Pressure comparison at a casting height of 2.2 m for Wall 1 (SCC-TP-R80).	78
Figure 5-4: Pressure comparison at the casting height of 2.6 m for Wall 1 (SCC-TP-R80).	79
Figure 5-5: Pressure comparison at the casting height of 3 m for Wall 1 (SCC-TP-R80).	79
Figure 5-6: Pressure comparison at the casting height of 3.4 m for Wall 1 (SCC-TP-R80).	80
Figure 5-7: Pressure comparison at the casting height of 3.8 m for Wall 1 (SCC-TP-R80).	81
Figure 5-8: Pressure comparison at the casting height of 4.2m to 5.4 m for Wall 1 (SCC-TP-R80).	82
Figure 5-9: Maximum lateral pressure profile at end of casting for Wall 2 (SCC-TP-WP10-R27)..	83
Figure 5-10: Pressure comparison at the end of casting for Wall 2 (SCC-TP-WP10-R27).	84
Figure 5-11: Maximum lateral pressure distribution at end of casting for Wall 3 (SCC-TP-WP15-R27).....	85
Figure 5-12: Pressure comparison at the end of casting for Wall 3 (SCC-TP-WP15-R27).	85
Figure 5-13: Lateral pressure distribution at various heights during casting for Wall 4 (SCC-BP-R65).....	87
Figure 5-14: Pressure comparison at the casting height of 2.2 m for Wall 4 (SCC-BP-R65).	87
Figure 5-15: Pressure comparison at the casting height of 2.6 m for Wall 4 (SCC-BP-R65).	88
Figure 5-16: Pressure comparison at the casting height of 3 m for Wall 4 (SCC-BP-R65).	89
Figure 5-17: Pressure comparison at the casting height of 3.4 m for Wall 4 (SCC-BP-R65).	89
Figure 5-18: Pressure comparison at the casting height of 3.8 m to 5 m for Wall 4 (SCC-BP-R65).	90
Figure 5-19: Pressure comparison at the casting height of 5.4 m for Wall 4 (SCC-BP-R65).	91
Figure 5-20: Lateral pressure distribution at various heights during casting for Wall 5 (SCC-BP-R80).....	92
Figure 5-21: Pressure comparison at the casting height of 2.2 m for Wall 5 (SCC-BP-R80).	93
Figure 5-22: Pressure comparison at the casting height of 2.6 m for Wall 5 (SCC-BP-R80).	93
Figure 5-23: Pressure comparison at the casting height of 3 m for Wall 5 (SCC-BP-R80).	94
Figure 5-24: Pressure comparison at the casting height of 3.4 m to 4.6 m for Wall 5 (SCC-BP-R80).	95
Figure 5-25: Pressure comparison at the casting height of 5 m for Wall 5 (SCC-BP-R80).	96
Figure 5-26: Pressure comparison at the casting height of 5.4 m for Wall 5 (SCC-BP-R80).	97
Figure 5-27: Lateral pressure distribution at various heights during casting for Wall 6 (SCC-BP-R55).....	98
Figure 5-28: Pressure comparison at the casting height of 2.2 m for Wall 6 (SCC-BP-R55).	98
Figure 5-29: Pressure comparison at the height of 2.6 m for Wall 6 (SCC-BP-R55).	99

Figure 5-30: Pressure comparison at the casting height of 3 m for Wall 6 (SCC-BP-R55).	100
Figure 5-31: Pressure comparison at the casting height of 3.4 m for Wall 6 (SCC-BP-R55).	100
Figure 5-32: Pressure comparison at the casting height of 5 m for Wall 6 (SCC-BP-R55).	101
Figure 5-34: Pressure comparison at the casting height of 5.4 m for Wall 6 (SCC-BP-R55).	101
Figure 5-33: Pressure comparison at the casting height of 3.8 m to 4.6 m for Wall 6 (SCC-BP-R55).	102
Figure 5-35: Comparison between the maximum lateral pressure distribution at end of casting for Wall 1 (SCC-TP-R80), Wall 2 (SCC-TP-WP10-R27) and Wall 3 (SCC-TP-WP15-R27).	103
Figure 5-36: Comparison between the maximum lateral pressure distribution at end of casting for Wall 1 (SCC-TP-R80), Wall 2 (SCC-TP-WP10-R27) and Wall 3 (SCC-TP-WP15-R27).	104
Figure 5-37: Comparison between the maximum lateral pressure distribution at end of casting for Wall 1 (SCC- TP-R80) and Wall 5 (SCC-BP-R80).....	105
Figure 5-38: Comparison between pressures at the end of casting for Wall 1 (SCC- TP-R80) and Wall 5 (SCC-BP-R80).	105
Figure 5-39: Comparison between the maximum lateral pressure distribution at a casting height of 4.2 meters for Wall 1 (SCC- TP-R80) and Wall 5 (SCC-BP-R80).	106
Figure 5-40: Comparison between pressures at casting height of 4.2 meters for wall 1 (SCC- TP- R80) and wall 5 (SCC-BP-R80).....	106
Figure 5-41: Ansys model simulating pumping pressures using water.	107
Figure 5-42: Comparison between the maximum lateral pressure distribution at end of casting for Wall 4 (SCC-BP-R55), Wall 5 (SCC-BP-R80), and Wall 6 (SCC-BP-R65).	108
Figure 5-43: Comparison between pressures at the end of casting for Wall 4 (SCC-BP-R55), Wall 5 (SCC-BP-R80), and Wall 6 (SCC-BP-R65).	108
Figure 5-44: Comparison between the maximum lateral pressure distribution at a casting height of 4.2 meters for Wall 4 (SCC-BP-R55), Wall 5 (SCC-BP-R80), and Wall 6 (SCC-BP-R65).....	109
Figure 5-45: Comparison between pressures at a casting height of 4.2 meters for Wall 4 (SCC-BP- R55), Wall 5 (SCC-BP-R80), and Wall 6 (SCC-BP-R65).	109
Figure 5-46: Measured pressure at the end of casting vs. CIRIA Report 108 (1985) Eq.1.....	111
Figure 5-47: Measured pressure at a casting height of 4.2 meters vs. CIRIA Report 108 (1985) Eq.1.	112
Figure 5-48: Pressures from the modified casting rates at the end of casting vs. CIRIA Report 108 (1985) Eq.1.....	113
Figure 5-49: Measured pressure at the end of casting vs. Gardner (2014) Eq.13.....	114
Figure 5-50: Measured pressure at a casting height of 4.2 meters vs. Gardner (2014) Eq.13.....	115

Figure 5-51: Pressures from the modified casting rates at the end of casting vs. Gardner (2014)	
Eq.13.	116

List of Tables

Table 2-1: Summary of the Parameters affecting Lateral Formwork Pressure.....	9
Table 2-2: Advantages of Top and Bottom placement methods (De Schutter <i>et al.</i> , 2010).	20
Table 2-3: Disadvantages of Top and Bottom placement methods (De Schutter <i>et al.</i> , 2010).....	21
Table 2-4: Parameters of the models to predict lateral pressure on formwork.	43
Table 2-5: Parameters of the models to predict lateral pressure on formwork (cont.).	44
Table 3-1: Summary of the pressure transducer specifications.	47
Table 3-2: Water column readings and transducer accuracy (v: voltage).....	48
Table 3-3: CIFA K31L - HP1606H Technical data sheet.....	54
Table 3-4: Putzmeister 36Z.12H - Technical data sheet.	55
Table 3-5: The CIFA S8 Series PC 907 - Technical data sheet.	56
Table 4-1: Agilia Vertical: Composition Materials.	59
Table 4-2: Agilia Vertical: Information on Mix Design.	59
Table 4-3: Summary of the experimental casting for Walls 1 to 3.	67
Table 4-4: Summary of concrete properties recorded for Walls 1 to 3.....	71
Table 4-5: Summary of the experimental casting for Walls 4 to 6.	71
Table 4-6: Summary of concrete properties recorded for Walls 4 to 6.....	74
Table 5-1: Percentage hydrostatic (K_0) for the casting heights of 4.2 m to 5.4 m for Wall 1 (SCC-TP-R80).....	81
Table 5-2: Percentage hydrostatic (K_0) for the casting heights of 3.8 m to 5 m for Wall 4 (SCC-BP-R65).....	90
Table 5-3: Percentage hydrostatic (K_0) for the casting heights of 3.4 m to 4.6 m for Wall 5 (SCC-BP-R80).	95
Table 5-4: Percentage hydrostatic (K_0) for the casting heights of 3.8 m to 4.6 m for Wall 6 (SCC-BP-R55).	101
Table 5-5: CIRIA Report 108 (1985) parameters for Wall 1 to 6 at the end of casting.	110
Table 5-6: CIRIA Report 108 (1985) parameters for Walls 1 to 6 at a casting height of 4.2 meters.	111
Table 5-7: Gardner (2014) parameters for Wall 1 to Wall 6 at the end of casting.	113
Table 5-8: Gardner (2014) parameters for Wall 1 to Wall 6 at a casting height of 4.2 meters.	114

Nomenclature

Latin letters

Latin letter	Units	Description
K_0	%	Percentage of hydrostatic pressure
$P_{(maximum)}$	kPa	Maximum Lateral Pressure
$P_{(hydrostatic)}$	kPa	Hydrostatic Pressure

Acronyms

Acronym	Description
ACI	American Concrete Institute
AEA	Air Entrained Agent
ASTM	American Society for Testing Materials
BP	Bottom-up Pumping
BIN	Binary Cement
BS	British Standards
CP	Cone Penetration
CVC	Conventional Vibrated Concrete
CIRIA	Construction Industry Research and Information Association
DIN	Deutsche Institut für Normung
EN	European Standards
FEM	Finite-Element Method
GGBFS	Ground-granulated Blast Furnace Slag
HRWRA	High-range Water Reducing Admixture
IP	Incline Plane

MSA	Maximum-size Aggregate
NRMCA	National Ready Mix Concrete Association
PV	Portable Vane
PVC	Polyvinyl Chloride
RILEM	International Union of Laboratories and Experts in Construction Materials, Systems and Structures. (French Reunion Internationale des Laboratoires et Experts des Matériaux, Systemes de Construction et Ouvrages)
S/A	sand-to-total aggregate ratio
SANS	South African National Standards
SCC	Self-Compacting Concrete / Self-Consolidating Concrete
SLC	Self-Levelling Concrete
SP	Superplasticiser
TER	Ternary Cement
TP	Top-down Pumping
QUA	Quaternary Cement
USS	Undisturbed Slump Spread
R	Casting Rate
VMA	Viscosity-modifying Admixture
W/C	water-cement ratio
W/CM	Water-Cementitious Material Ratio
WP	Waiting Period

Chapter 1 : Introduction

1.1 Introduction

Self-Compacting Concrete (SCC) can be classified as a high-performance material which acts as an alternative to Conventional Vibrated Concrete (CVC). The lateral pressure exerted by SCC onto concrete formwork is a major issue that relates to cost, construction rate, quality, safety and potential delays in construction (Lange, 2012). Since SCC was first developed in the 1980s, there has been extensive research on lateral formwork pressure exerted by SCC (Ozawa, et al., 1989 (Japanese) as cited by Ouchi, 2001). Because of the shortage of information regarding lateral formwork pressure induced by SCC during casting, and pressure decay following placement, the American Concrete Institute (ACI) (ACI Committee 347R-14, 2014) has prompted formwork system engineers to design the formwork used for SCC to resist full hydrostatic pressures.

Appropriate forecasting of the maximum lateral pressure induced by freshly cast concrete against the formwork systems is essential to ensure the safety of formwork systems and to reduce formwork costs (Nemati, 2005). Miscalculating pressure can lead to extra formwork costs, and underestimating the pressure may cause formwork failure or distortion of the structural elements (Cauberg and Desmyter, 2007).

A limited investigation into the South African concrete industry's use of SCC was carried out by Geel and co-authors (Geel *et al.*, 2007). They reported that the use of SCC has gradually increased internationally; however, despite the clear advantages of shifting from CVC to SCC, its adoption in the South African construction industry has progressed at a very slow pace, due in part to the limited knowledge of the lateral formwork pressures exerted by SCC, the formwork design constraints, the formwork design codes and the methods of quality control (Geel *et al.*, 2007). Additionally, despite the fact that all major Readymix suppliers in South Africa utilize pumping equipment, pumping from the base of the element with pumping equipment is not a standard form of concrete placement readily available in the local construction industry.

Although progress has been made, there are no accepted standardised codes or guidelines for the South African construction industry to use in predicting the pressure exerted by SCC on formwork and which can then be used in the design of formwork for SCC. (Malherbe and Wium, 2016). Geel *et al.* (2007) recommended that a local set of guidelines needs to be developed for the production and application of SCC in South African conditions.

In South Africa, SCC was used on a large scale for the first time in 2002, during construction of the Nelson Mandela Bridge in Johannesburg, shown in Figure 1-1 (Malherbe and Wium, 2016). Pylon supports were built by filling two steel tubes 30.5 and 45.7 m in height with SCC.



Figure 1-1: Nelson Mandela Bridge (DYWIDAG Systems International).

Geel *et al.* (2007) revealed that SCC was chiefly used in South Africa for constructing high-rise buildings because of the technical advantages of the concrete. According to Jooste (2009), during the construction of a Bakwena Highway Bridge Deck 2235 at the N4 Platinum Toll Highway in Midrand, shown in Figure 1-2, the use of SCC gained some ground in the South African construction industry.



Figure 1-2: N4 Bakwena Toll Road Bridge Extension (Delf Consulting Engineers).

Bridge Deck 2235 is a post-tensioned two-cell box girder type structure. Challenges during the construction were the placing of concrete in the densely reinforced bottom slab, shown in Figure 1-3 and compaction; thus, it was decided to use SCC to eliminate the problems.

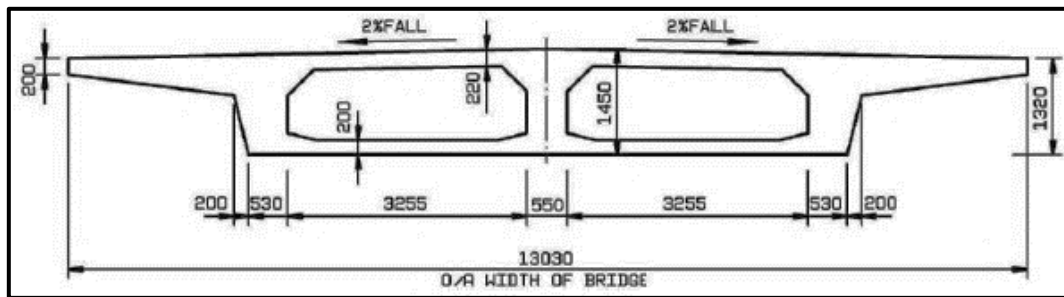


Figure 1-3: Deck 2235 cross section (Jooste, 2004).

SCC was also used in 2010 during the Soccer World Cup to upgrade the Soccer City Stadium in Soweto. The structure comprised 120 slender concrete columns each 16.3 m in height. Because of the dense reinforcement in these columns, which made their vibration extremely difficult, it was also decided to use SCC (Bokelman *et al.*, 2011).

Most researchers have accepted that fresh concrete, when placed in a vertical form, exerts a lateral pressure on the formwork (Assaad *et al.*, 2003a and Gardner, 1980). To identify a means to predict lateral formwork pressure, it is important to understand the various parameters influencing the lateral pressure. This study investigates the parameters which can be controlled under field conditions namely: casting rate by setting the pump's rpms, method of placement by utilising top-down casting by means of a boom pump and bottom-up casting by using a static pump, and implementing waiting periods between castings.

This thesis presents the experiments that were executed to measure the lateral pressure exerted by SCC on formwork as well as the results of these experiments. The results reported here could be of significance to engineers in the design of formwork and to contractors for the calculation of lateral pressure on formwork.

1.2 Motivation

The lateral pressure exerted by SCC on the formwork significantly influences the design of the formwork. A strong and secure formwork system is needed for high lateral pressure values (Van Waarde, 2007). Formwork costs can contribute anywhere between 40% - 60% of the overall cost of construction projects (Robert, 2007). There are possibilities of saving considerable amounts of money when constructing formwork systems for SCC, because the lateral pressures measured both on site, by Billberg, (2003) and Galeota *et al.*, (2007) and in the laboratory, by Assaad and Khayat, (2005c), often resulted values that were lower than hydrostatic pressure.

Omran (2009) reported that the main reasons for the use of SCC were the reduction of labour costs and the increase of productivity. Any formwork cost savings by for instance decreasing the lateral

pressure exerted by SCC will decrease the design loads and materials used to design the formwork would be of advantage to the construction industry.

Unfortunately, the recommendations applicable to CVC do not apply to SCC (Ozawa *et al.*, 1989). The rather high lateral formwork pressure exerted by SCC is believed to be the main technical hindrance that slows down the general use of SCC in cast-in-place applications (Giammatteo *et al.*, 2007). Lateral formwork pressure exerted by SCC is a concern to engineers as overestimation of this pressure results in unnecessary costs, as a result of the construction of over dimensioned formwork, while underestimating the pressure could cause deformation of the formwork or, in severe situations, collapse of the whole formwork system. High lateral pressure on formwork pressure also poses potential risk issues (Puente *et al.*, 2010). Therefore, any effort to reduce the cost of a concrete structure must be thoroughly investigated to ensure both the efficacy and the safety of the method. It is essential to investigate the lateral pressure exerted on formwork by SCC and to develop a theoretical model that can be used to predict this lateral pressure for the South African construction industry.

1.3 Problem Statement

The limited knowledge and data available in the South African construction industry on the lateral pressure on formwork exerted by SCC has created a need for more research on the topic of lateral formwork pressure exerted by SCC (Geel *et al.*, 2007). The introduction of SCC has created potential problems associated with the inability to accurately predict the lateral pressures exerted by SCC on the formwork. It is commonly known that the pressures of SCC are greater than that of CVC, but due to the numerous types of SCC available in the construction industry and the various parameters that can influence lateral pressure, prediction of the pressure has been difficult (Khayat and Omran, 2009). Often full hydrostatic pressure is assumed, which would require the strengthening of formwork and the associated cost. This is unlike CVC, where a reduction in pressure head occurs as a concrete pour continues (Billberg, 2006). An investigation is required to determine whether the lateral pressure exerted by fresh SCC always reaches the levels of hydrostatic pressure in the formwork, and to understand how and why this occurs, and how it differs during the different casting methods.

1.4 Research Scope

The scope of the research study is the investigation of the influence of various casting methods (both constant casting and using waiting periods) and placement methods (bottom-up and top-down

placement) on the lateral pressure exerted by SCC on wall formwork systems in the South African construction environment.

This study includes field tests on six walls, identical in dimensions with the aid of eight flush diaphragm pressure transducers. All eight pressure transducers were placed in the formwork by using machined polyvinyl chloride (PVC) adaptors to mount the transducers to the formwork panels.

The scope of the study is limited by the following: first, not all the parameters that influence lateral formwork pressure are investigated in this study, including the material properties characteristics of the formwork. However, these can be investigated in future research studies. Secondly, the study focuses on vertical wall elements only and does not examine columns or other concrete elements of formwork. Finally, the study focuses on field tests and not laboratory tests.

1.5 Research Strengths and Limitations

The strength of the proposed research is to have recorded and illustrated the potential lateral pressure profiles of SCC which can be seen under site conditions. It can become a framework for future researchers to elaborate and improve upon.

A limitation to the study is that the number of parameters influencing the formwork pressure of SCC is large and many of them could not be investigated in this study. This included the fact that the researcher did not have access to the SCC mix design proportions and was not able to change the material properties of the SCC used in the investigation, thus not having control over many of the SCC parameters that affect the lateral pressure exerted on the formwork systems. Because of the scale of the experiments, funds and time were limited, which limited the number of specimens, potentially limiting the possible conclusions.

1.6 Research Aim and Objectives

1.6.1 Research Aim

This research project aims to perform a practical investigation into the lateral formwork pressure exerted by SCC Agilia Vertical (Agilia is a complete range of Self-Compacting concretes for vertical and horizontal applications manufactured by Lafarge South Africa) on wall elements under site conditions, by studying the placement methods, casting rates and any interruptions in casting the concrete and implemented waiting periods as well as comparing the results to theoretical models.

The research outcomes provides the construction industry with real data generated within South Africa that can be used as the basis for further studies, potentially aiding in the design and planning involved in the use of SCC.

The provisions of the British Standard Codes BS 5975: 2011 (BS 5975:2008+A1, 2011) recommends that formwork be designed to withstand the full hydrostatic head of fluid concrete, except if a technique based on appropriate experimental data is available. Standard formwork cannot be used and special formwork has to be constructed, which comes at a high cost. In essence, this research study could potentially enable the construction industry to design formwork more cost effectively in accordance with requirements of the actual lateral pressures exerted by SCC in every case.

1.6.2 Research Objectives

The objectives set to satisfy the aim of the research are the following:

- Perform an investigation of the literature for existing research on the subject and experiments done throughout the world regarding the lateral pressure exerted by SCC on formwork systems.
- Find a SCC mix which is suitable for use in full-scale wall elements by the South African construction industry.
- Investigate the currently accepted placement methods by which SCC is cast in the South African construction industry.
- Perform field tests on full-scale walls elements under site conditions (using project labour and equipment) and measure the lateral formwork pressure of SCC.
- Develop practical, usable data from the raw experimental data and identify the lessons to be learned from the practical use of SCC in construction projects.

1.7 Research Methodology

To address the proposed research, a methodology was developed that comprised of the following steps:

1. Identify the research problem.
2. Perform a comprehensive literature study to gain a broader view of SCC, lateral pressure, formwork systems and their application in the construction industry.
3. Identify which of the relevant parameters can be addressed in the study, and then formulate the scope of the research and problem statement.

4. Establish the study's objectives within the area of the identified scope.
5. Perform a series of field tests on large scale wall elements to investigate the parameters identified.
6. Observe how SCC is cast under construction conditions in the field.
7. Analyse the results of the field experiments.
8. Provide a comprehensive conclusion based on the results and observations of the field experiments.
9. Formulate guidelines to increase the understanding of and improve the behaviour of lateral pressure exerted on formwork by SCC in the South African construction environment, so that formwork systems could potentially be designed more cost effectively.

The methodology for the mentioned field tests is described in detail in Chapter 4 of this report.

1.8 Sponsors

PERI Formwork and Scaffolding Engineering Pty Ltd. and Lafarge South Africa engaged in this research study to enable the South African construction industry to design formwork systems that would be more cost effective. This would enable contractors and others to make an informed decision on when to select SCC in preference to CVC solutions.

PERI Formwork and Scaffolding Engineering Pty Ltd sponsored the experimental part of this research study on lateral pressure on formwork exerted by SCC. PERI sponsored the Domino formwork system, pressure transducers, data logger, and donated funds for the cost of the boom and static pumps.

Lafarge South Africa (Cape Town) sponsored the SCC concrete for this study. Lafarge South Africa produces cement, concrete, aggregates, ready-mix concrete, gypsum plasterboard and interior building fittings.

NMC Construction Pty Ltd supplied the construction site for the tests and sponsored cleaning up costs and Pumping Readymix sponsored some of the pumping equipment.

1.9 Thesis Overview

Chapter 2: Literature Study

Chapter 2 consists of a study of the literature available on the lateral formwork pressure exerted by SCC. A detailed review of all the parameters which affect the lateral pressure exerted by SCC is also presented, and currently used lateral pressure measuring systems and management procedures

are covered and, finally, a conclusion of the literature review is presented. A list and comparison of the previously proposed SCC lateral pressure models are provided in this chapter.

Chapter 3: Research Equipment

This chapter covers all the equipment used in the investigation. The chapter is sub-divided into two sections. The first section covers the flush diaphragm pressure transducers, the PVC adaptors used to mount the transducers to the formwork system and the data loggers used to measure and record the lateral pressure exerted. The second section covers the pumping equipment.

Chapter 4: Experimental Methodology

The experimental procedures used to monitor and measure the lateral pressure exerted by the SCC is discussed in this chapter. Information of the material properties and the design of the mix are documented, as well as the tests used to measure and record the slump, filling ability and compressive strength. The formwork system used in the investigation is discussed. Procedures related to the setting up of the experiment, as well as the managerial process used to bring all relevant parties together are covered. Lastly, the experimental procedure itself is documented and explained.

Chapter 5: Experimental Results

Chapter 5 provides the recorded pressure data from the field experiments. A comparison of the pressure data, and the conclusions arrive at from the results are then provided in the form of comparative tables and graphs. The pressure data recorded is compared with the lateral pressure models provided in the literature. Finally, the observations made on site are presented.

Chapter 6: Conclusions and Recommendations

In the last chapter of the report, the research study is concluded by summarising all the findings, as well as listing the limitations of the presented results. Suggestions are made for future research based on the observations made and results recorded.

Chapter 2 : Literature Review

2.1 Introduction

The aim of this chapter is to identify any information that may be available in published sources reporting previous research on the lateral formwork pressure exerted by Self-Compacting Concrete (SCC). The literature review was conducted to find information reported from previous research results that would identify the key parameters affecting the lateral pressure on formwork.

Seven sections are addressed in the literature review. In the first section, definitions are discussed, thereafter a brief overview is given of lateral pressure on formwork, and then the effect of several parameters affecting lateral pressure is discussed in sections 3-5. All the parameters mentioned are tabulated in Table 2-1.

Table 2-1: Summary of the Parameters affecting Lateral Formwork Pressure.

Placement Characteristics	Material Properties	Formwork Characteristics
Method of placement	SCC binder composition	Formwork dimension and shape
Casting rate	Water-cementitious material ratio (w/cm)	Presence of reinforcing bars
Concrete temperature	Concrete aggregate properties	Leakage of water through the formwork panel surface
Waiting period between castings	Consistency level (slump flow)	Type of formwork surface material
	Yield stress and Viscosity	
	Thixotropy	

The sixth section covers the measurement systems which can be used to monitor and record the lateral formwork pressure exerted by SCC on formwork wall panels. Finally, the seventh section concludes the chapter with existing models used by previous researchers to predict the lateral formwork pressure exerted by SCC. See Figure 2-1 for the layout and overview of the chapter.

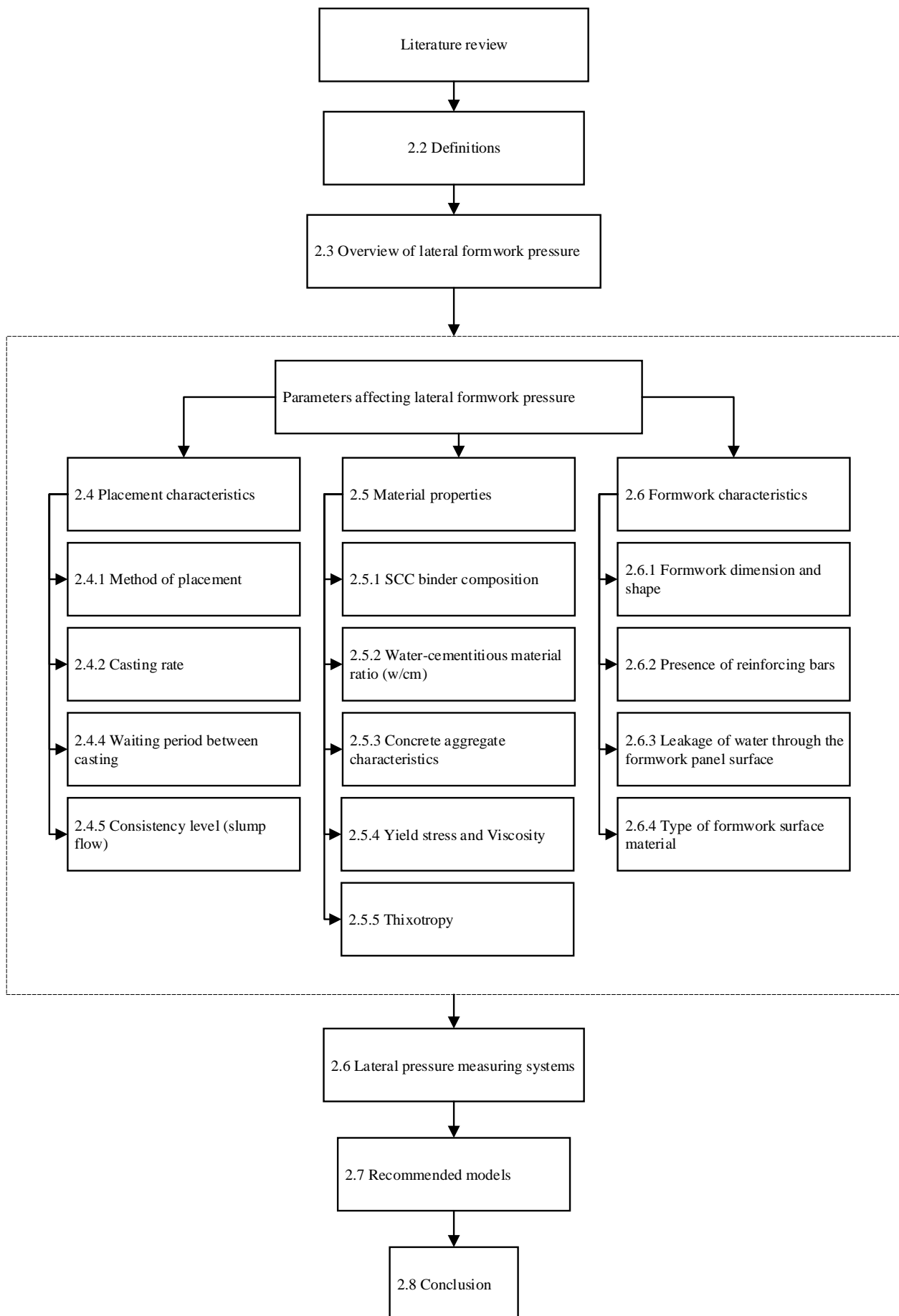


Figure 2-1: Layout and overview of Chapter 2.

2.2 Definitions

2.2.1 Lateral Formwork Pressure

Lateral pressure can generally be classified as the pressure that fresh concrete exerts in a horizontal direction. The lower the plastic viscosity and yield stress the more the original lateral pressure will be; however, faster rates of hardening will lead to faster rates of decay in the lateral pressure. Lateral pressure occurs only as long as the concrete is in a fresh state.

Nemati (2005) defines lateral pressure of concrete in a fresh state as follows:

“Loads imposed by fresh concrete against wall or column forms differ from the gravity load on a horizontal slab form. The freshly placed concrete behaves temporarily like a fluid, producing a hydrostatic pressure that acts laterally on the vertical forms. This lateral pressure is comparable to a full liquid head when concrete is placed to full height within the period required for its initial set”.

2.2.2 Self-Compacting Concrete

Self-Compacting Concrete (SCC), also referred to as Self-Consolidating Concrete (SCC) or Self-Levelling Concrete (SLC) is a relatively new type of high performance concrete, which was created in Japan in the early 1980s (Ozawa *et al.*, 1989). ACI Committee 237R-07 (2007) stated that:

“SCC is a highly flowable, non-segregating concrete that can spread in place, fill formwork, and encapsulate the reinforcement without any mechanical consolidation”.

The biggest difference between CVC and SCC is the consistency in its fresh state. Figure 2-2 shows the slump flow of CVC and SCC. The parameter most used to indicate the consistency and workability of SCC is the measurement of the slump flow (Thrane *et al.*, 2008).

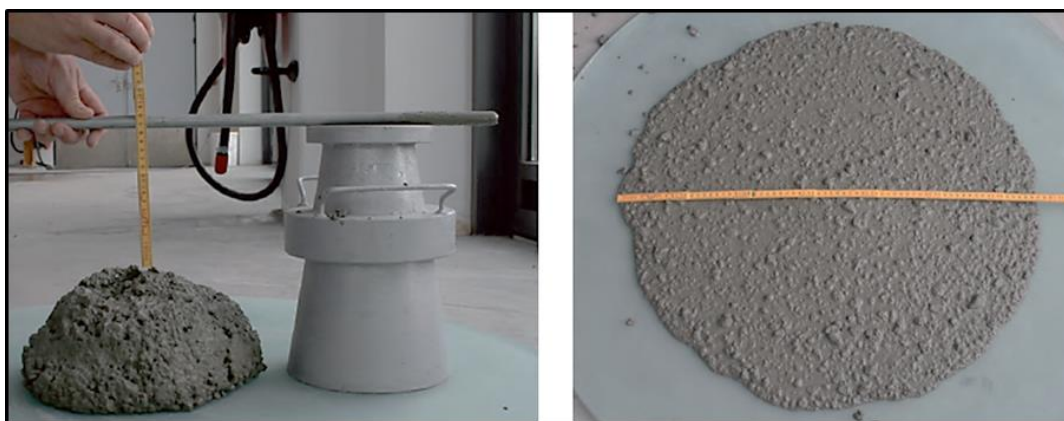


Figure 2-2: The slump flow of CVC (left) and the slump flow of SCC (right) (Thrane *et al.*, 2008).

The characteristics and rheological properties of fresh SCC are also different from CVC, mainly in terms of its ability to compact itself and flow under its own weight without the requirement of compaction. In SCC the fresh concrete easily flows around dense reinforcement and into all corners of the formwork. SCC is a highly flow-able concrete and is poured or placed in the same manner as CVC. As it does not require compaction, it saves time, labour and energy. Furthermore, the surface finish produced by SCC is very good, and patching is eliminated.

The main purpose of the development of SCC was to obtain flow properties that would allow concrete to pass through dense reinforcement (Geel *et al.*, 2007). It was developed with the purpose of improving the quality of concrete structures and increasing the rate of the casting process far above the rate at which CVC can be cast. Casting can occur faster, as there is no need to stop the placement or pouring of the fresh concrete to vibrate the concrete. However, increasing the casting rate leads to higher lateral pressure on the formwork, which can lead to formwork failure or deformation of the concrete elements.

SCC requires the addition of a superplasticiser (SP), which allows it to become workable without the addition of excessive water to the mixture (Haddadou *et al.*, 2015). Substances such as fly ash, silica fume, calcined clay, ground-granulated blast furnace slag (GGBFS), and pulverised limestone may be added to the mixture to combat segregation. On the other hand, to enhance resistance of segregation, a viscosity modifying agent (VMA) can be added to the concrete (Lange *et al.*, 2008).

2.2.3 Hydration

Hydration of cement occurs instantly after mixing. During the hydration process, the cement particles are able to react with water to form various hydration products. With the hydration progress, the products tend to grow and connect the unreacted cement grains to form the microstructure of cement paste. The formed paste microstructure directly determines the strength and durability of concrete (Liu, 2014).

Kim (2010) defined hydration as:

“A series of chemical reactions and physical processes of cement after water is added to form the binding material to determine the setting and hardening properties of concrete”.

2.2.4 Thixotropy

Thixotropy is the increase in viscosity of the concrete at rest due to the build-up of the material structure, and the decrease in viscosity of the concrete when subjected to shear stress due to the breakdown of the material structure (Ferron *et al.*, 2007).

Feys (2008) states that:

“Thixotropy is a time-dependent effect which increases the internal structure of the material during rest and decreases the internal structure of the material during flow. The lower the materials internal structure the more fluid the material”.

2.2.5 Viscosity

Badman *et al.*, (2003) states that:

“Viscosity is one of the rheological constants of fresh concrete, fresh mortar, and fresh paste when they are regarded as Bingham fluids. The magnitude of the change in the applied stress required for changing the unit flow velocity”.

2.2.6 Yield Stress

Badman *et al.*, (2003) states that:

“Yield stress is one of the rheological constants of fresh concrete, fresh mortar, and fresh paste when they are regarded as Bingham fluids. The minimum stress required to make the concrete flow”.

2.2.7 Formwork Systems

Formwork shown in Figure 2-3, is the temporary structural systems that are constructed quickly to provide support and mould the fresh concrete to the required size and shape while it hardens.

For the designed shaped of the concrete to be maintained, the form must be firm under the load of construction to maintain the designed shape of the concrete. It is important that for a few hours during the placement of the fresh concrete the formwork should be able to support its own weight, as well as that of the fresh concrete and the live loads of construction workers, their supplies and tools (Nemati, 2005).

The load bearing capacity and the tightness of the formwork must be designed based on the impacts that are normally calculated for the casting of concrete. The weight of SCC is no different to that of CVC, yet, because of its high flow capacity, there are some differences that must be taken into account when constructing the formwork (Thrane *et al.*, 2008).

There are three types of formwork: vertical formwork, in the form of either a wall or a column, shown in Figure 2-3; horizontal formwork, in the form of either a floor or a slab and beam formwork. The design and use of these formwork in South Africa, is governed by the British

Standard BS 5975 2008: 2011 “Code of Practice for Formwork” (BS 5975 2008+A1: 2011). The Formwork Code of Practice is a guideline on how to manage the formwork in the process of selecting materials, and designing formwork, and procedures for building, and dismantling.

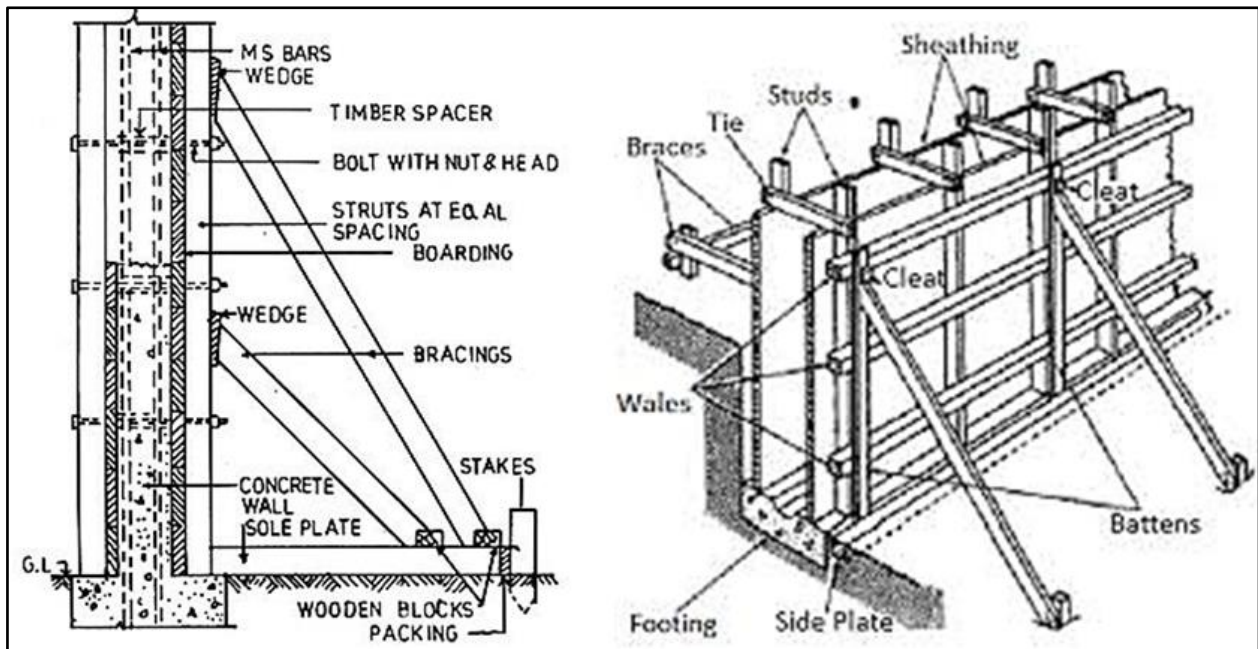


Figure 2-3: A typical formwork set-up for a concrete wall (The Constructor).

Formwork systems consist of five basic parts: plywood and board sheathing, to mould and hold the fresh concrete until it hardens; studs, to shape the framework and support the sheathing; single or double wales, to keep the form aligned and support the studs; bracings, to retain the forms upright under lateral pressure; and snap and screw ties and wood spreaders, to keep the sides of the forms at the correct spacing (Smith and Andres, 1993 as cited by Senouci and Al-Ansari, 1996 (French). It is necessary to use highly durable materials to manufacture formwork systems used today, because the hardware and accessories are used multiple times (Nemati, 2005). Traditionally, formwork was discarded after only one usage.

2.3 Overview of Lateral Formwork Pressure

From the studies covered in the literature review it was found that lateral formwork pressure is a function of different variables. These variables can be divided into three groups namely: placement characteristics; material characteristics and formwork characteristics.

Several researchers have performed a number of field and laboratory tests to investigate the lateral pressure exerted by SCC. The studies performed by the researchers took into consideration the placement of the concrete from either the top or from the base of the formwork system, the formwork geometry, the presence of reinforcement, setting time of the SCC, temperature of the

SCC, the casting rate, chemical and mineral admixtures, coarse aggregate, water-cement ratio (w/c), composition and content of the cement, concrete density, concrete consistency and concrete flow characteristics.

Because a large percentage of the total cost of a concrete structure is formwork costs, the knowledge of lateral concrete pressure becomes essential for the economical design of formwork. A concern exists that during the casting of the SCC the lateral pressure could reach hydrostatic pressure. This leads to an increase in the formwork design costs when using SCC and thus directly increase overall construction costs (Billberg, 2012).

Brameshuber and Uebachs (2003), Assaad (2006), and Tejeda-Dominguez (2005) suggest that the greatest factor influencing lateral pressure is time, the faster the concrete is pumped the greater the pressure exerted will be. Hurd (2005) reported that an assessment of the lateral formwork pressure is needed for the design of formwork systems. He further states that SCC can be regarded as a fluid, exerting equal pressures in all directions at any measurable point, thus essentially assuming a hydrostatic pressure effect (Hurd, 2005).

In recent years, because of the interest in reducing or eliminating vibrations during the placement of concrete, SCC has grown in popularity. However, design recommendations for Conventional Vibrated Concrete (CVC) cannot entirely be applied to SCC applications. This is due to the high fluidity level of SCC which is a main factor in the assumption that the lateral pressure may potentially reach full hydrostatic pressure. Research studies so far have revealed limited information about the scale of lateral pressure exerted by SCC (Brameshuber and Uebachs, 2003; Assaad 2004).

As reported by Giammatteo *et al.* (2007), adoption of the cast-in-place applications of SCC have been retarded by the technical issues associated with the use of SCC. These technical problems cannot be solved because of the lack of knowledge with regard to the lateral pressure that SCC exerts on formwork systems.

Gardner (1985) reports two ways to tackle the problem with regard to the lateral pressure. The first way proposed is a practical approach: to measure and record the lateral pressure either on site or under laboratory conditions and then formulate an empirical equation from the data obtained. The second proposal is to create a theoretical model based on the rheological and mechanical properties of SCC.

Most design codes and procedures available for estimating lateral pressure have been established for CVC (Construction Industry Research and Information Association, (CIRA) CIRA Report 108, 1985 and American Concrete Institute, (ACI) ACI Committee 347, 2004) but there are currently no

accepted standards or guidelines in South Africa that can be used to facilitate the design of formwork systems by predicting the lateral pressure exerted by fresh SCC. Appropriate determination of the initial lateral pressure is vital to ensure the safe and economic design of formwork systems (Nemati, 2005).

2.4 Placement Characteristics

2.4.1 Method of Placement

There are usually two types of placement methods that are used when casting SCC into wall elements, shown in Figure 2-4 namely: placement from the top of the formwork system, and pumping from the base of the formwork system (Khrapko, 2007).



Figure 2-4: Pumping from the top (left) and bottom (right) of the formwork (Khrapko, 2007).

The most commonly used method of placing concrete is from the top of the formwork system. This is often done by guiding a vertically hanging pump pipe into the top of the formwork system. Billberg (2003), has reported from his studies that casting from the top of the formwork system resulted in the values of the induced lateral pressure of below hydrostatic level.

The alternative method involves pumping the fresh concrete from the base of the formwork system through an inlet connection fitted on the formwork system with a shut-off valve. This method is often used when placing fresh concrete into wall and column elements with a difficult geometry, dense reinforcement schedules and when there is limited access to the top of the formwork system (Thrane *et al.*, 2008). According to Tichko *et al.* (2014), research done in terms of pumping fresh SCC from the base of the formwork is limited.

From studies conducted by Assaad *et al.* (2003), it was suggested that when pumping fresh SCC from the base of the element, pauses during the casting procedure should be avoided. The authors further state that if this is not avoided then high pumping pressures would be necessary to break down the mass that SCC built up because of its thixotropic behaviour.

When being placed, fresh SCC acts like a fluid; however, if it is cast gradually, or if it is left to rest, it will start to flocculate and build up an internal structure which can withstand the load of the fresh concrete cast from above without increasing the lateral pressure being exerted on the formwork system (Roussel *et al.*, 2007).

Generally, fresh SCC has a very low yield stress, which would be expectedly to result in the lateral pressure exerted reaching full hydrostatic pressure. However, due to its thixotropic nature, the lateral pressures exerted can result in lower than hydrostatic pressure values; this is most notably true when casting from the top of the element. Conversely, pumping from the base of the element could cause the lateral pressure to reach, or even exceed, full hydrostatic pressure because of the constant pump pressure and non-thixotropic behavior, shown in Figure 2-5 (Billberg, 2006).

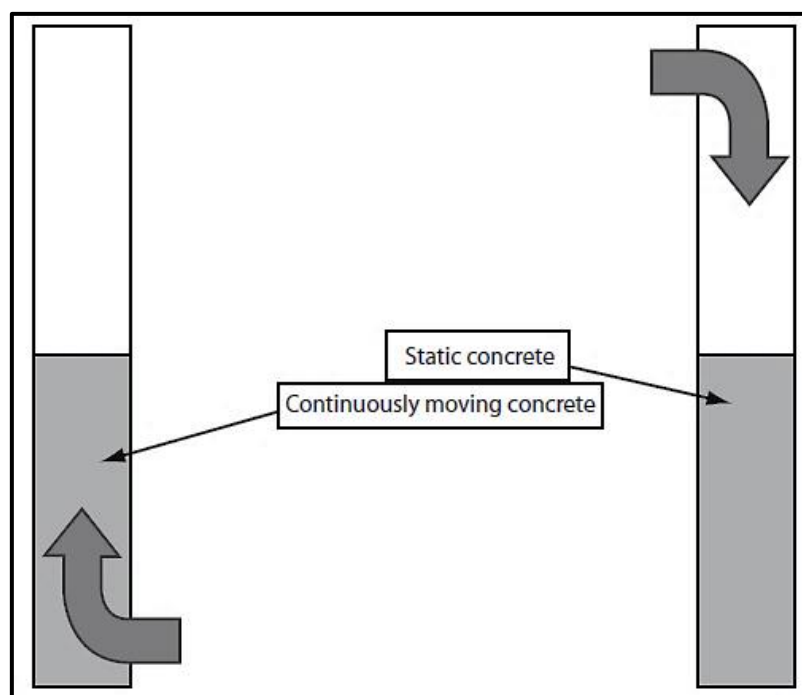


Figure 2-5: Base and top placement locations influence thixotropic behaviour (Szecsy & Mohler, 2009).

Assaad *et al.* (2003b) reported that, with regard to the 12.5 m high walls investigated, the lateral pressure exerted by the SCC showed a 30% reduction from hydrostatic value when pumped from the base, at a casting rate of 25 m/h, and a 35% reduction when filling from the top of the formwork system using buckets at a casting rate of 18 m/h.

Tichko *et al.* (2015) performed experiments to investigate the lateral pressure exerted by SCC when pumped from the base of the element. They also carried out numerical simulations in order to validate the experiments. The lateral pressure was measured at three different locations on the formwork system. The authors concluded from their investigation, that when pumping fresh SCC from the base of the formwork system hydrostatic pressures can be anticipated.

Brameshuber and Uebachs (2003) conducted a study in which five wall elements were investigated; as shown in Figure 2-6 for the experimental setup used. Of the five walls investigated, four were tested using SCC and the last one was tested using CVC. With regard to the tests that involved the SCC, two of the walls were filled from the top, using buckets, and the remaining two were pumped from the base of the formwork system at casting rates of 2 and 10 m/hr. The last wall using CVC was filled from the top using buckets at a casting rate of 7.5 m/hr.

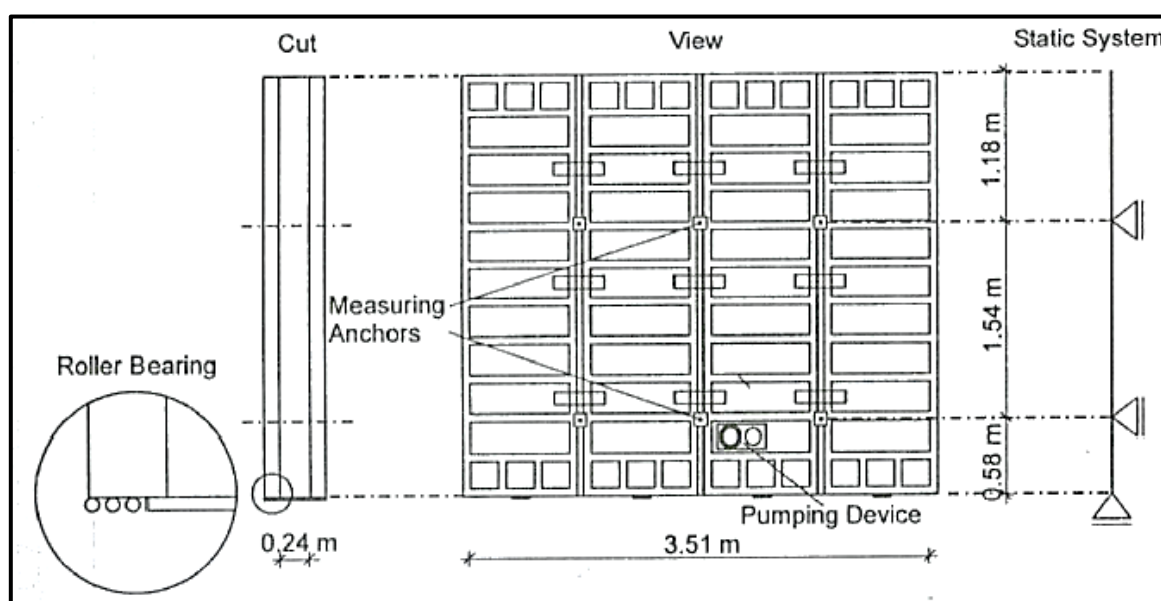


Figure 2-6: Test set-up and position of the measuring anchors (Brameshuber & Uebachs, 2003).

From the investigation the authors found that much lower lateral formwork pressures resulted from SCC cast from the top of the formwork system by using buckets. Conversely, it was found that lateral formwork pressure reached hydrostatic pressure after pumping the SCC from the base of the element. The authors reported that the lateral formwork pressure when SCC was pumped from the base of the formwork was twice as great as that resulting when filling the element from the top, shown in Figure 2-7. The authors concluded that when pumping from the base of the formwork system the designer should design the system to withstand full hydrostatic pressure.

Leeman *et al.* (2006) reported from their investigation that when pumping SCC from the base of the formwork system the resultant lateral pressures were 10% above hydrostatic pressure, shown in Figure 2-8.

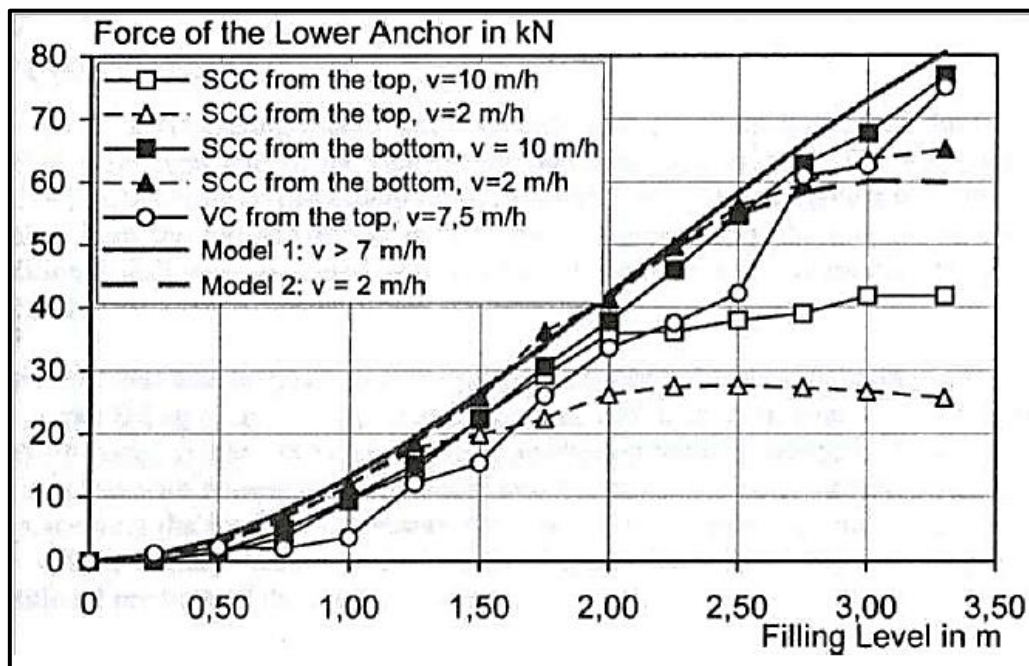


Figure 2-7: Force of the lower anchor (Brameshuber & Uebachs, 2003).

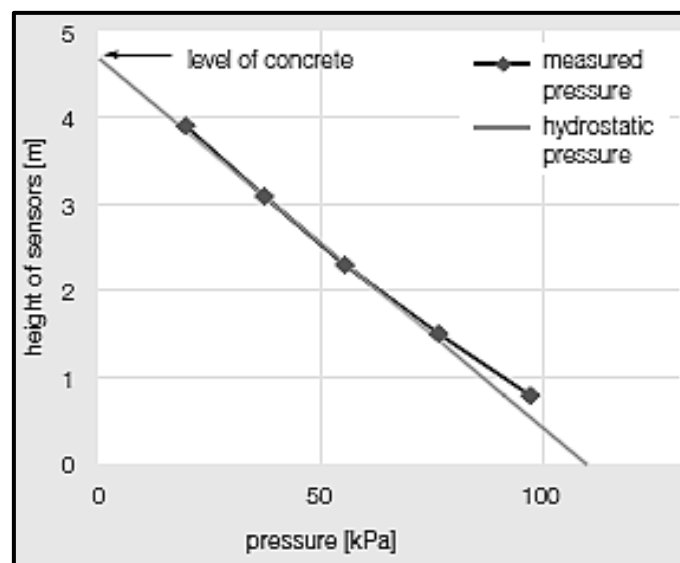


Figure 2-8: Lateral Pressure of SCC at the end of the casting (Leeman et al., 2006).

Billberg (2006) also reported that when designing formwork systems where the SCC is cast from the base, the formwork system ought to be designed to withstand hydrostatic pressure plus the pump pressure. Billberg's reasoning is that the fresh concrete is in motion during the pumping procedure, therefore allowing no time for the concrete shear strength to develop.

Both placement methods have their advantages as well as disadvantages (De Schutter *et al.*, 2010). These are briefly summarised in Tables 2-2 and 2-3.

Table 2-2: Advantages of Top and Bottom placement methods (De Schutter *et al.*, 2010).

Advantages	
Top placement method	Bottom placement method
The thixotropic property of SCC can benefit from this type of filling method if performed properly.	Tall concrete elements can be cast at high casting rates without any disruption of the filling process, thereby significantly reducing the time needed for casting.
The surface finish quality is not reduced by the presence of an inlet duct.	The risk of air getting entrapped during this filling method is prevented or reduced, thus leading to an improved quality of the cast.
Easy and simple	This filling method improves the final strength of the concrete element because the occurrence of segregation is counteracted by the continuous upward movement of the concrete.
Good visual control of the concrete surface is often possible.	There are no weak interfaces in the final cast, as a result of the continuous pumping of SCC from the base of the formwork.
Well suited for practically every type of task.	Long supply ducts are not needed.
	The pumping and concrete do all the work.
	Best for complex castings where there is limited access to the formwork from above, e.g. top side shutting.

Table 2-3: Disadvantages of Top and Bottom placement methods (De Schutter *et al.*, 2010).

Disadvantages	
Top placement method	Bottom placement method
There is a probability of more air becoming entrapped during this filling method, which negatively influences the strength development and durability of the concrete.	This filling method requires the use of a shut-off valve, which increases the complexity of the formwork. The formwork system must be prepared with connection pieces at the correct locations.
Pauses in the filling process leads to weak interfaces between the cast concrete layers.	A good surface finish might be compromised by the cast element near the inlet valve when the formwork is stripped, leaving surface marks.
The height of the cast elements must be reduced because of the necessity for long supply ducts.	When casting at high wall rates, very strong and stiff formworks are required, which are considerably more expensive. This might limit the casting height.
The fact that the concrete is falling down inside the formwork, increases the risk of segregation.	Long flow distances for the concrete increase the risk of dynamic segregation.
It may be difficult to get deep enough down into the vertical formwork.	Visual monitoring of the result is difficult.
The inlet location must be planned taking into account the flow properties and the formwork geometry.	

2.4.1 Casting Rate

A critical parameter which affects the pressure exerted on the lateral formwork is the rate at which the fresh concrete is cast. Higher casting rates result in higher lateral pressures being exerted that could even surpass the hydrostatic pressure levels. However, the lateral pressures exerted would reduce if the casting rate were to be reduced to such a degree that fresh SCC was able to undergo structural build-up, because of its thixotropic properties (Deb, 2013).

Khayat and Omran (2007) reported that if the casting rate is high enough, to prevent the SCC from hardening, then the resultant lateral pressure could reach full hydrostatic pressure. Yet, with regard to larger structures, where lower casing rates were implemented, it was noted that the maximum lateral pressure exerted was significantly less than hydrostatic pressure.

Billberg (2003) performed an investigation in order to evaluate the effect of low casting rates (1 to 2.5 m/h) on the exerted lateral formwork pressure. Billberg used a 1500 mm high stainless steel tube and two different SCC mix designs in which the water-cement ratio (w/cm) was 0.40 and 0.45 respectively, and the slump flow was 730 ± 50 mm and 700 ± 50 mm. They also investigated one conventional vibrated concrete (CVC) mix design. The results of the investigation are shown in Figure 2-9 and show a linear relationship between the relative formwork pressure and the low casting rates.

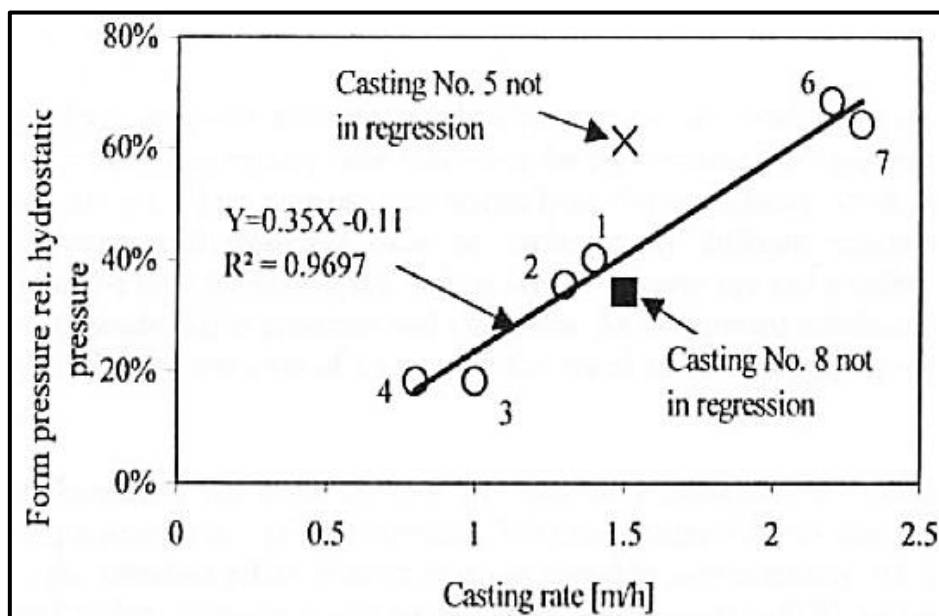


Figure 2-9: Relative formwork pressure for low casting rates (Billberg, 2003).

Assaad and Khayat (2006) embarked on an investigation to assess the effect of the casting rate on the lateral pressure on the formwork. They used a 2.8 m high PVC column with a diameter of 200 mm to perform their experiments. From their investigation it was found that if the casting rate

is decreased from 25 to 5 m/hr the resultant lateral pressure reduced by approximately 15%, shown in Figure 2-10.

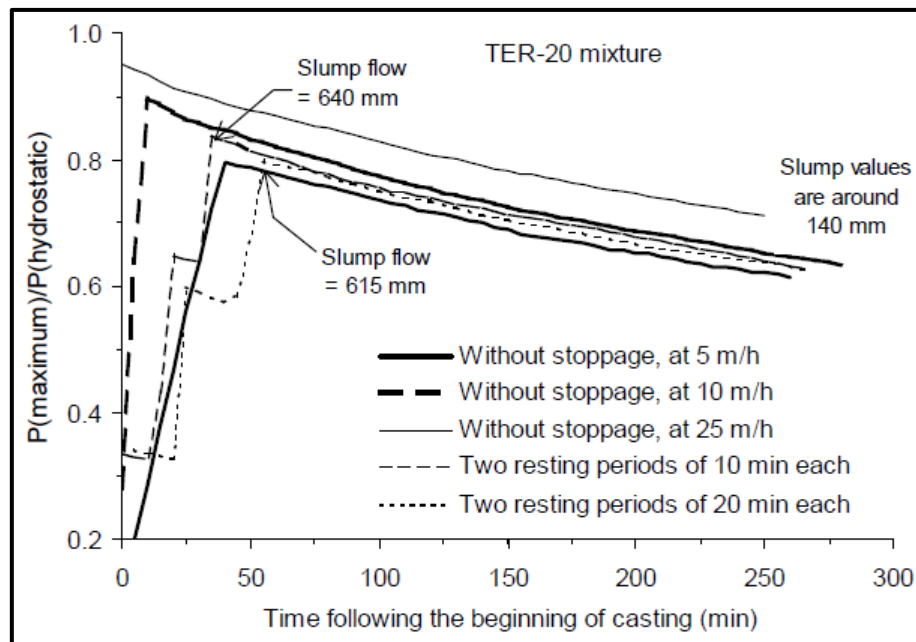


Figure 2-10: Influence of casting rate on the lateral pressure (Assaad and Khayat, 2006).

Omran *et al.* (2014) investigated the effect of casting rates ranging from 2 to 30 m/h on the lateral pressure exerted by fresh SCC. They cast the fresh SCC at six different casting rates namely: 2, 5, 10, 17, 24 and 30 m/h. It was noted by the authors that as the casting rate increased so did the resultant lateral pressure. During the investigation it was found that the lateral pressure significantly increased when casting at 10 m/h, when compared to previous lower casting rates. However, when the casting rate was increased from 10 to 30 m/h the resultant lateral pressures increased only slightly. The authors reported that at the casting rate of 30 m/h, the measured lateral pressure approached full hydrostatic pressure.

2.4.2 Concrete Temperature

Khayat and Assaad (2006) performed a series of experiments in order to investigate the effect of the temperature of the fresh concrete on the lateral pressure exerted on the formwork system. From the investigation the authors concluded that the temperature of the fresh SCC, namely 10°C, 20°C, and 30°C had no significant effect on the lateral pressure at the end of the casting process. However, the authors found that the change in the initial concrete temperature had a significant effect on the pressure decay. The author found the time needed to reduce the percentage of hydrostatic ratio (K_o) by 25% at the temperatures of 10°C, 20°C, and 30°C were 400, 250, and 160 min respectively, shown in Figure 2-11.

Omran *et al.* (2014) investigated the effect of the temperature of the SCC, ranging between 10 and 32°C on the exerted lateral pressure. The author used the Sherbrook pressure column to monitor and simulate the initial lateral pressure up to casting depths of 13 meters. From the tests, the authors found that an increase in the concrete's temperature had an effect on the acceleration of the concrete's hardening rate thus resulting in a reduction in the lateral pressure. The authors concluded that at a temperature of 12°C the lateral pressure reached 71% of the hydrostatic pressure.

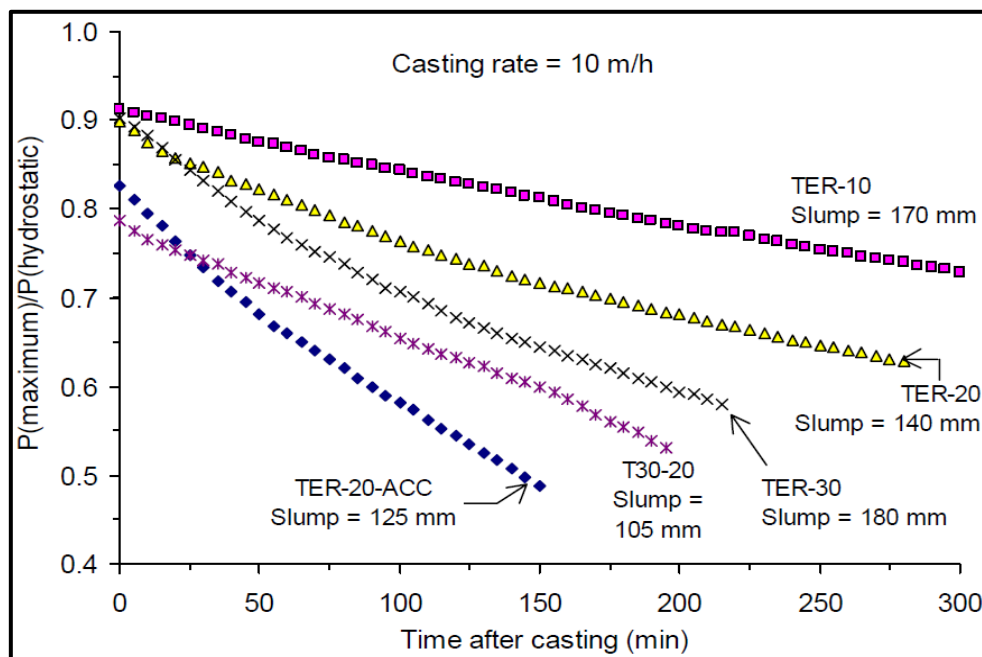


Figure 2-11: Effect of the SCC temperature on the lateral pressure (Khayat & Assaad, 2006).

2.4.3 Waiting Period between casting

Omran *et al.* (2014) performed a study to evaluate the influence of one or two pauses between sequential lifts on lateral pressure. The authors performed their experiments on two SCC mixtures with different thixotropic levels. The two mixes were classified as having low and medium thixotropic levels and were placed cast at 10 m/h at a temperature of $\pm 22^\circ\text{C}$ in a pressure column. The first casting procedure was performed with no interruptions. In the second casting procedure one Waiting Period (WP) of 30 minutes was introduced at a height of 6m. Lastly, in the third casting procedure two waiting periods of 30 minutes each were introduced at heights of 4m and 8m, shown in Figure 2-12.

The authors reported that from their investigation it was clear that the lateral pressure could be reduced by 10% for a medium thixotropic level concrete and a reduction of 15% could be expected for a medium-to-high thixotropic level concrete. The authors further stated that for high or very high thixotropic concrete the lateral pressure can be reduced even further.

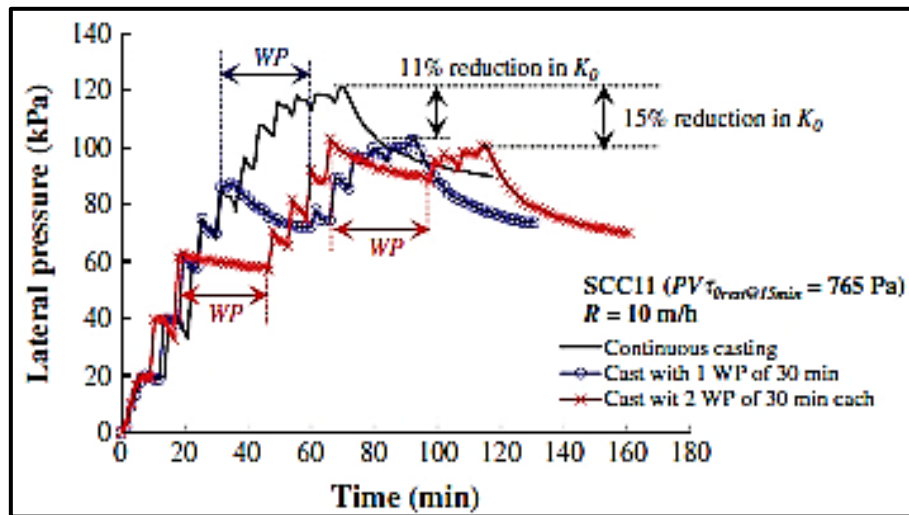


Figure 2-12: Variations of lateral pressure with time for casting constantly, and after one and two Waiting Periods (Omran, et al., 2014).

2.4.4 Consistency Level (Slump Flow)

Assaad and Khayat (2006b) performed an investigation to determine how the lateral pressure could be affected by various levels of consistency, namely 550, 650, and $750 \pm 15 \text{ mm}$. The authors used a 2.8 m PVC column with a diameter of 200 mm. The SCC mix designs used in the investigation contained 450 kg/m^3 of binder and a water-cement ratio (w/cm) of 0.40. The viscosity-modifying admixture (VMA) was set as 2, 2.6, and 3.5 mL/kg , and the sand-to-total aggregate (S/A) ratio was set as 0.46 for all the mixtures. From the results shown in Figure 2-13, it can be seen that the drop in pressure is significantly affected by the consistency level where lower consistency levels result in a faster pressure drop. The author subjects this is due to the higher particle interlocking within the cement paste, and greater build-up of cohesion after the casting period.

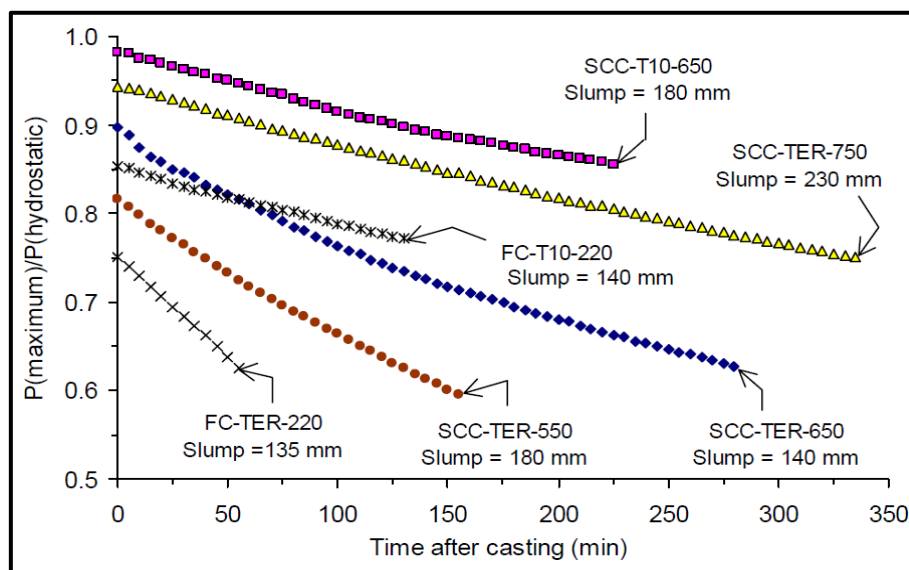


Figure 2-13: Effect of consistency on the lateral pressure (Assaad& Khayat, 2006).

2.5 Material Properties

2.5.1 SCC Binder Composition

Assaad and Khayat in 2005 (2005a and 2005b) conducted a series of experiments with a 2.8 m PVC column with a diameter of 200 mm to investigate the effect of different binder contents on the lateral pressure exerted by SCC. The experiment used Type HE (T HE) and Type GU (T GU) CSA Canadian cements, as well as three blended cements. These blended cements contained (i) a ternary cement (TER) made up of 22% Class F fly ash, 6% silica fume, and 72% Type GU (T GU) cement, (ii) a quaternary cement (QUA) made up of a combination silica fume, Class F fly ash, and granulated blast-furnace slag and 50% Type GU (T GU) cement, and, finally, (iii) a binary cement (BIN) containing 8% silica fume and 92% Type GU (T GU) cement. For the investigation the binder content of the SCC mix designs varied between 400 and 550 kg/ m³. The water-cementitious material ratio (w/cm) was set at 0.40 and the S/A ratio at 0.46. The viscosity-modifying admixture (VMA) was set at 2.6 mL/ kg and the high-range water reducing admixture (HRWRA) and Air-Entraining Agent (AEA) were adjusted to get a slump flow of 650 mm and an air content of 6%.

The results of the investigation shown in Figure 2-14 indicate that Type GU (T GU) cement showed the greatest initial lateral pressure and the Type HE (T HE) cement showed the smallest initial lateral pressure. The authors concluded from their investigation that higher initial lateral pressures could be expected for SCC mixtures containing greater binder contents.

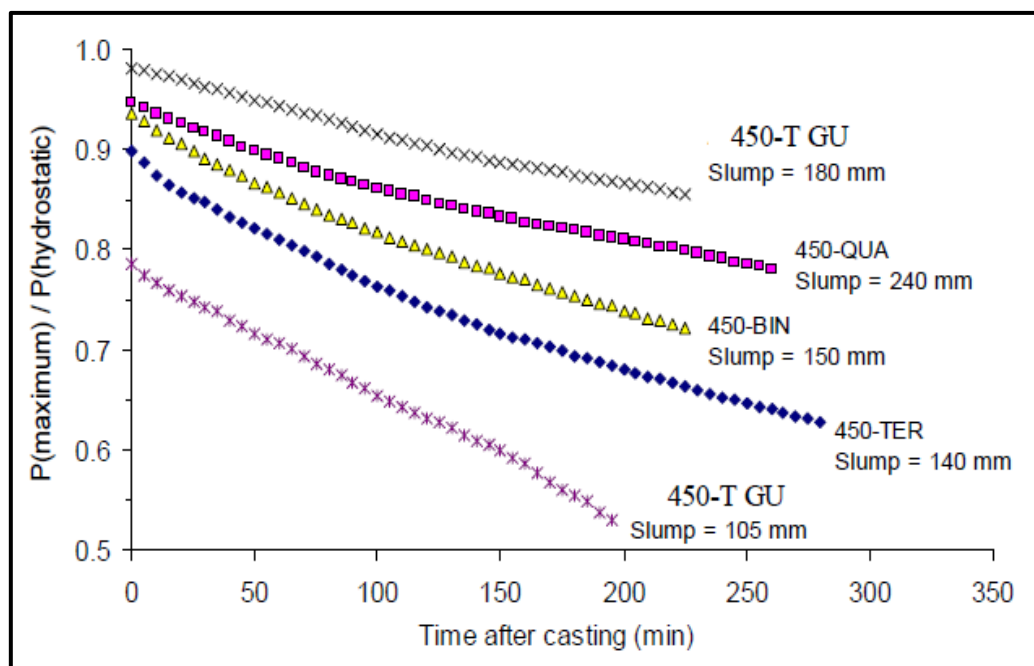


Figure 2-14: Lateral pressure for SCC made with of various binders (Assaad & Khayat, 2005a).

2.5.2 Concrete Aggregate Characteristics

Assaad and Khayat (2005c) performed an investigation on how coarse aggregate can affect the lateral pressure. The authors used a 2.8 m high pressure column and cast the SCC at a rate of 10 m/h. From the results obtained the authors found that increasing the coarse aggregate volume reduced the lateral pressure exerted, shown in Figure 2-15.

This reduction can be attributed to the increases in the internal friction present between the particles in the fresh concrete, as a result of the greater coarse aggregate content. The authors also determined that the maximum size of the aggregate (MSA) has an effect on reducing the initial lateral pressure.

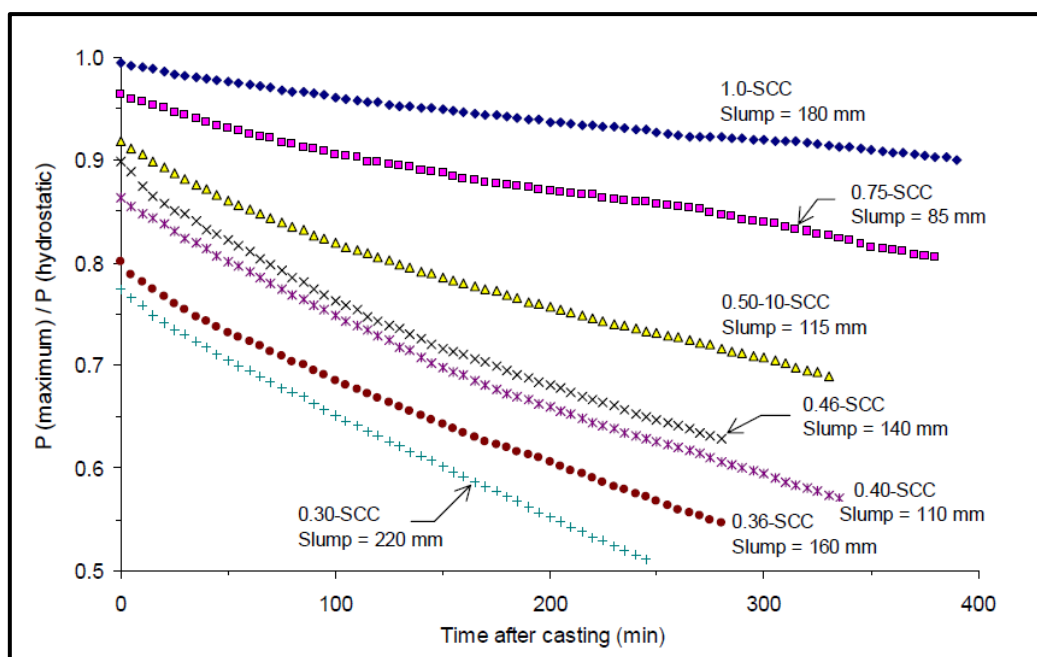


Figure 2-15: Variations of lateral pressure with regard to mixtures made with 10 mm MSA (Assaad & Khayat, 2005c).

2.5.3 Water-Cementitious Material Ratio (w/cm)

From the investigations to test various water-cementitious material ratios (w/cm) and two different based HRWRA (PC and PNS), which were performed by Khayat and Assaad, 2006 it was found that changes in w/cm had an effect on the lateral pressure of the SCC. For a SCC mixture with a w/cm of 0.46 a greater initial lateral pressure was exerted than that of a SCC mixture with a w/cm of 0.40 or 0.36, shown in Figures 2-16 and 2-17. The authors explain that this was linked to the increased paste and water contents of the SCC mixture.

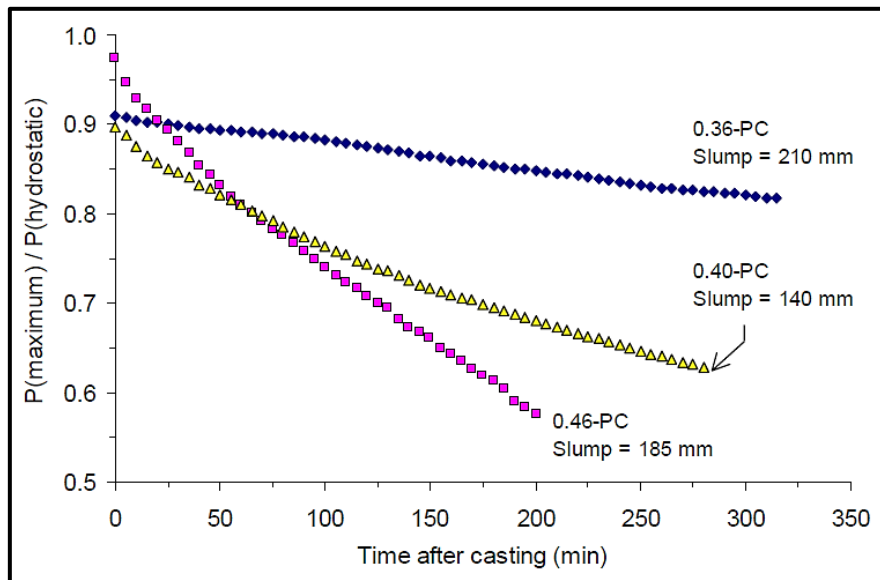


Figure 2-16: w/cm effect on the lateral pressure (PC-based HRWRA) (Khayat & Assaad, 2006).

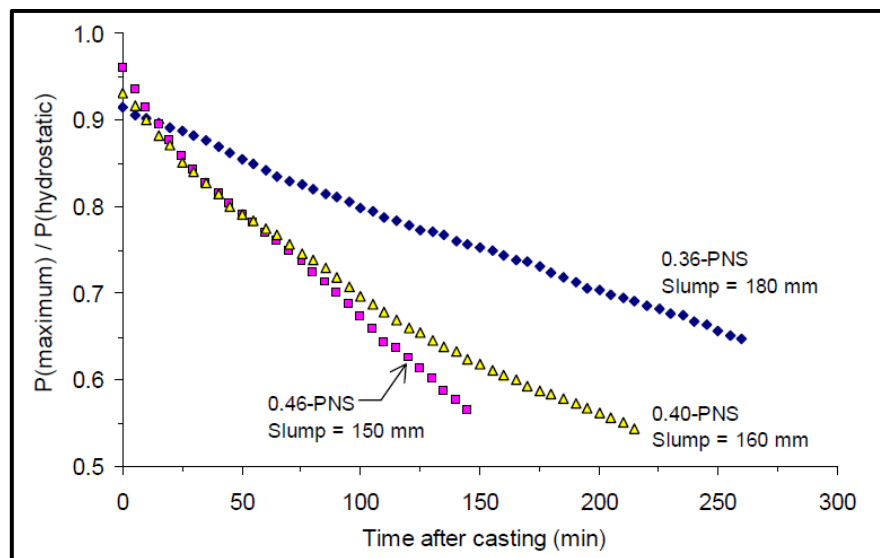


Figure 2-17: w/cm effect on relative pressure (PNS-based HRWRA) (Khayat & Assaad, 2006).

2.5.4 Yield stress and Viscosity

As reported by Szwaboski (1991), Billberg (2005 and 2006), Koehler (2009), Khayat *et al.* (2010) and Khayat *et al.* (2012 a & b) rheological behaviour of fresh concrete can be expressed through the yield stress and plastic viscosity. The yield stress and plastic viscosity are two critical parameters that govern the flowability and segregation resistance of fresh concrete (Tregger *et al.*, 2008; Schwartzenruber *et al.*, 2006).

From both a workability and practical point of view, yield stress may be associated to filling capacity and more generally to whether or not concrete will flow or stop flowing under an applied stress whereas, plastic viscosity may be associated to the velocity at which a given concrete will

flow once flow is initiated. According to Tattersall and Banfill (1983), yield stress is the most important parameter for formwork filling.

To determine the yield stress, different strain rates are used depending on the type of rheometer, mixture composition and what properties are sought after (Barnes and Nguyen, 2001). Shaughnessy and Clark (1988) describe yield stress as a unique material property and may, in the case of cement pastes, be measured using conventional rheological tools such as Couette Viscometer or parallel plates rheometer. Nehdi and Rhaman (2004), and Billberg (2005) developed a method to measure the increase in the yield stress at rest. The author did this by using a concrete rheometer, and showed that yield stress increased linearly with resting time. Drewnoik *et al.* (2017) performed an investigation into the correlations between static and dynamic yield stress, and lateral pressure. After casting, a reduction in the lateral pressure was observed (shown in Figure 2-18).

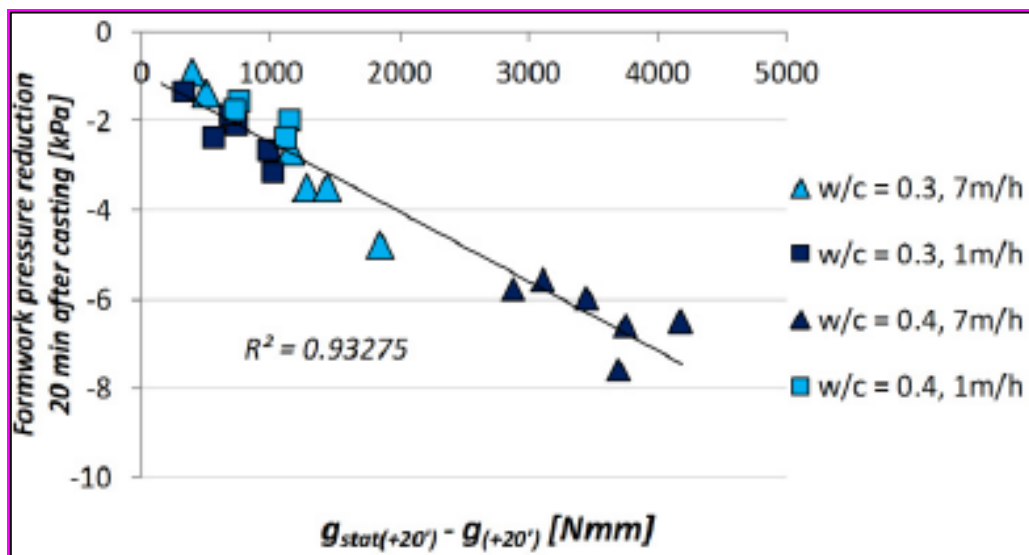


Figure 2-18: Lateral formwork pressure reduction 20 minutes after casting according to static and dynamic yield stress changes.

2.5.5 Thixotropy

Assaad and Khayat (2004) stated:

“Almost all of the relationships established between thixotropic indices and $P_{(maximum)}/P_{(hydrostatic)}$ values indicate that the greater the degree of thixotropy, the lower magnitude of initial lateral pressure that can develop after casting, and faster such pressure can decrease with time. This is attributed to the reversible effect of thixotropy (restructuring), which enables the material to re-gain its shear strength when left at rest with any shearing action. Such increase in shear strength is the result of combined increase in internal friction and cohesion of the concrete”.

Khayat *et al.* (2005) showed that the lateral pressure exerted by SCC could be directly related to the magnitude of thixotropy. The greater the degree of thixotropy, the lower the initial lateral pressure and the faster is the rate of pressure decay with time. The authors attributed it to the stiffening effect, which enables the material to regain its shear strength when left at rest without any shearing action.

According to Lapasin *et al.* (1983) and Barnes (1997) there are no standard methods to measure thixotropy, but typical thixotropic experiments often consist of either rheological tests conducted at a constant shear rate (equilibrium flow curves) or using varied sheared rates (hysteresis curves). Billberg (2005), Khayat *et al.*, 2010 and Khayat *et al.*, 2012 developed field-oriented test methods by using a portable van and inclined plane tests to evaluate structural behaviour of the fresh concrete at rest.

Assaad *et al.* (2003a) carried out experimental investigations to determine the influence of thixotropy, on the lateral pressure exerted on an experimental column measuring 2100 mm in height and 200 mm in diameter. The author reported that the lateral pressure exerted by fresh SCC is directly related to thixotropy and with the increase in thixotropy, the initial lateral pressure decreases.

2.6 Formwork Characteristics

2.6.1 Formwork Dimension and Shape

Omran (2009) stated that limited data exists regarding the effect of size and shape of the formwork system on the lateral pressure. Billberg (2006) reported that dimension and shape of the formwork system is an important characteristic due to the shear forces present at the surface of the formwork panels. The author explains the larger the formwork system's dimension and shape becomes, the smaller the shear forces become small in relation to the concrete mass.

2.6.2 Presence of reinforcing bars

Tichko *et al.* (2015) stated that the reinforcement present in the formwork system can reduce the flow cross-section therefore leading to greater losses in flow as a function of the casting rate. The authors highlighted studies performed by Perrot *et al.* (2009), in which they state that when filling from the top of the formwork system, the reinforcement present can create a new friction area that could reduce the lateral pressure. Conversely though the author stated that when pumping fresh concrete from the base of the formwork system, the reinforcement present could increase the lateral pressure as the reinforcing bars make additional surfaces of friction dissipation.

2.6.3 Formwork System Material Type

Tejeda-Dominguez (2005) investigated the effect of the formwork material on the exerted lateral pressure exerted on the formwork system. The author performed four tests in which the lateral pressure was recorded to be close to hydrostatic pressure immediately after casting. However, the author stated that after casting the decrease in the lateral pressure was dependent on the formwork material.

Vanhove *et al.* (2000) showed in their investigation that the roughness of the formwork material had a considerable influence on friction experienced during the casting procedure. The authors explain that the lateral stresses experienced can decrease with an increase in the friction experience during the casting of the fresh concrete.

2.7 Lateral Pressure Measuring Systems

Several approaches have been employed to monitor the lateral pressures exerted on formwork systems. Roby (1935) monitored the lateral pressure by using a steel plate which extended the full length of the formwork system. The author determined the lateral pressure by observing the deflections in the steel plate.

Stanton (1937), as cited by Khayat *et al.* 2007), implemented a makeshift metal disk like gauge pressure transducers to measure the lateral pressure. Rubber diaphragms were attached to one side of the pressure transducers and the space between the diaphragm and the metal disk was filled with a liquid. Stanton inserted the makeshift transducers into the formwork panels so that the diaphragms would be flush with the concrete surface.

Macklin (1946), as cited by (Omran and Khayat, 2013), measured the lateral pressure of the fresh concrete on the formwork system by determining the deflection of the formwork panel relative to the supporting studs, by using a dial-type micro meter.

Assaad *et al.* (2003) implemented flush diaphragm millivolt output type pressure transducers to measure lateral pressure. Before conducting the experiments the authors set the pressure transducers flush with the inner side of the formwork system and connected each transducer to a data acquisition system.

Billberg (2003) determined the lateral formwork pressure by calculating the stresses in the tie rods of the formwork system. This method required that the base of the formwork should be able to move freely on its foundation to prevent inaccurate results due to friction.

Leeman *et al.* (2005) used five pressure transducers to measure the lateral pressure by positioning each of the five transducers flush with the inner surface of the formwork system. The principle of the transducers used is based on the change in electrical resistance of thin-film metal wire strain gauges when they are deformed as a result of the lateral pressure.

Giammatteo, *et al.* (2007) used two different types of pressure transducers namely, dilatometer cells and common diaphragm pressure transducers. The dilatometer cell, as shown in Figure 2-19 (left), consists of a 0.2 mm thick circular steel membrane with a diameter of 60 mm. The lateral pressure is measured by the expansion of an internal gas, due to the pressure applied to the diaphragm from the fresh concrete. The authors attached dilatometer cells to the formwork, with their membrane flush to the concrete surface. The test layout used by Giammatteo is shown in Figure 2.19 (right).

The principle of the dilatometer pressure cell as used by the author is shown in Figure 2-20. During the experimental procedure the dilatometer cell would work as an electric switch, having an on/off functionality. When the pressure inside the dilatometer cell counterbalances the lateral pressure exerted, the diaphragm of the cell would lose contact with its support, thus causing an interruption in the signal, and prompting the operator to read the exerted pressure (Giammatteo, *et al.*, 2007).

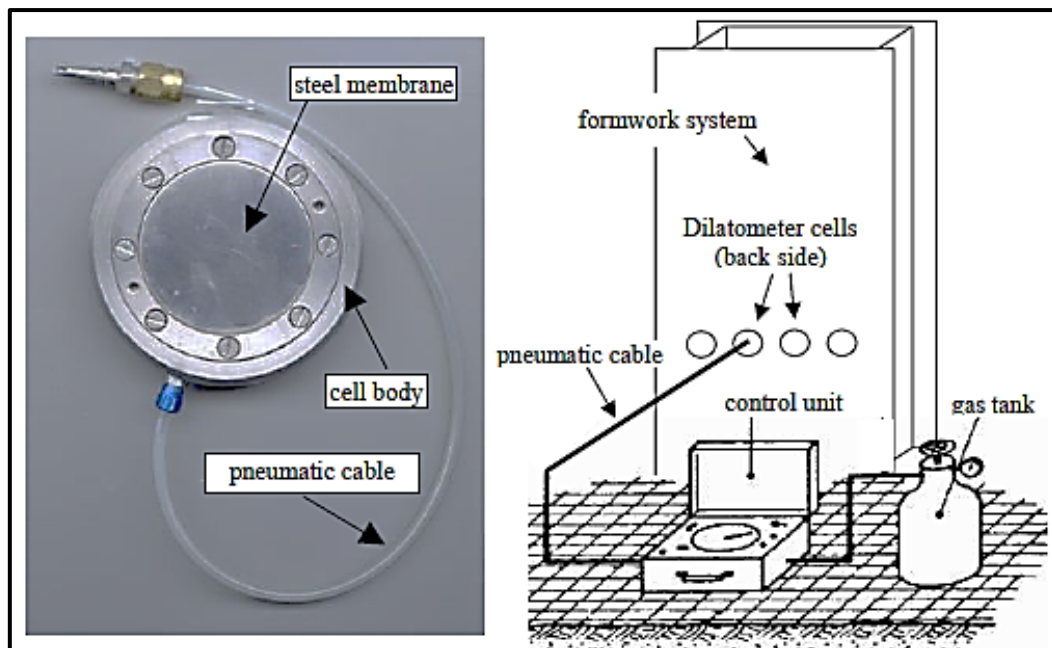


Figure 2-19: Dilatometer pressure cell (left) and test layout implemented (right) (Giammatteo, *et al.*, 2007).

Khayat and Assaad (2008) recommended test set-ups and measurement systems that could be used in both laboratory evaluations and in field tests. The authors used flush diaphragm millivolt output type pressure transducers, in the experiments to measure the lateral pressure exerted by the fresh concrete, as shown in Figure 2-21.

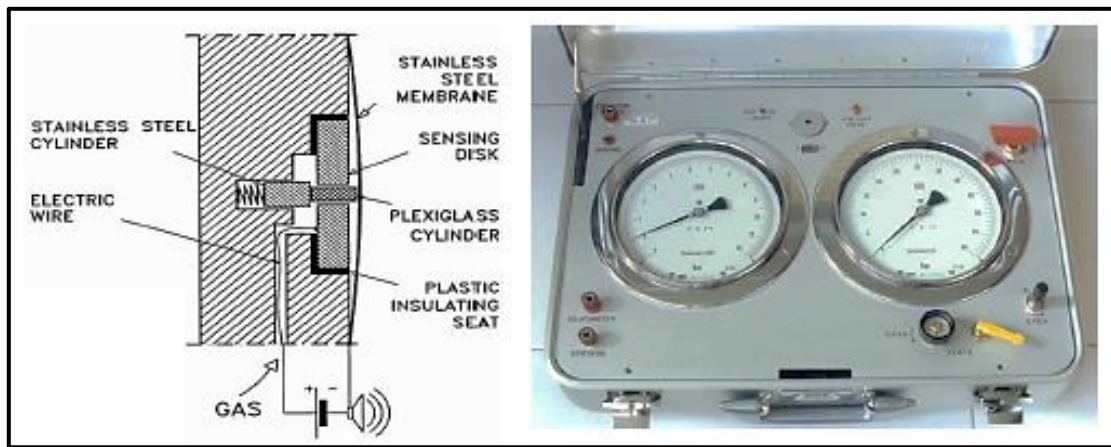


Figure 2-20: Dilatometer cell diagram (left) and control unit (right). (Giammatteo, et al., 2007).

The flush diaphragm transducers using semi-conductor gauges with bending beams that are operable over a temperature range of -50 to $+100^{\circ}\text{C}$. The transducers are connected to a data logger system of relatively low scanning voltage. Pressure transducers with maximum capacities of 50 to more than 500 kPa can be used, depending on the expected lateral pressure developed by the concrete. According to the authors, the diameters of these transducers can range from 20 to 100 mm.



Figure 2-21: Lateral pressure transducer (left) and pore-water pressure transducer (right). (Khayat & Assaad, 2008).

Khayat and Assaad (2008) used two systems for measuring lateral pressure exerted by SCC, to evaluate the reliability of using the pressure transducers to monitor formwork pressure in the repair of retaining walls. In their experimental programme, the diameter of the pressure transducer was 20 mm compared to a 10 mm maximum aggregate size. The transducers were set flush with the inner side of the formwork. The authors compared the performance of the transducers to the stresses determined from the measurement of deformations using strain gauges, welded onto steel bars anchored to the concrete substrate, shown in Figure 2-22.

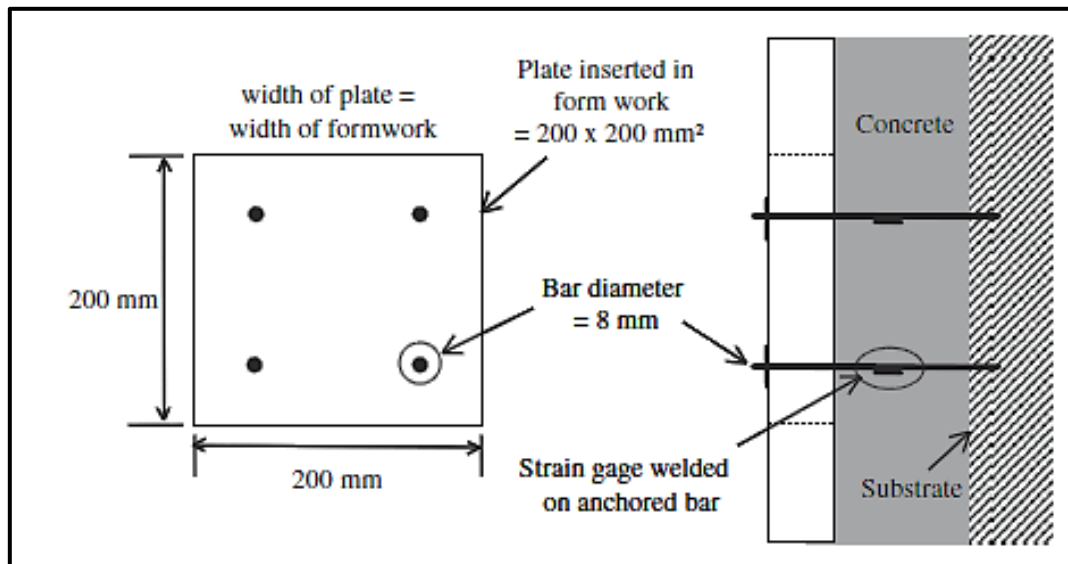


Figure 2-22: Schematic diagram showing the strain gauge system used for measuring lateral pressure. (Khayat & Assaad, 2008).

Comparison of the lateral pressures determined by using the strain gauge and pressure transducers is shown in Figure 2-23 for SCC mixture with a slump flow of 640 mm. The authors obtained a maximum difference of 5% lateral pressure with a similar pressure drop in both cases during the first 4 hours following casting. The authors found that the pressure measured from the anchored bars did not show any further decrease, while that determined from the transducers continued to decrease, until the cancellation of the lateral pressure after 18 hours.

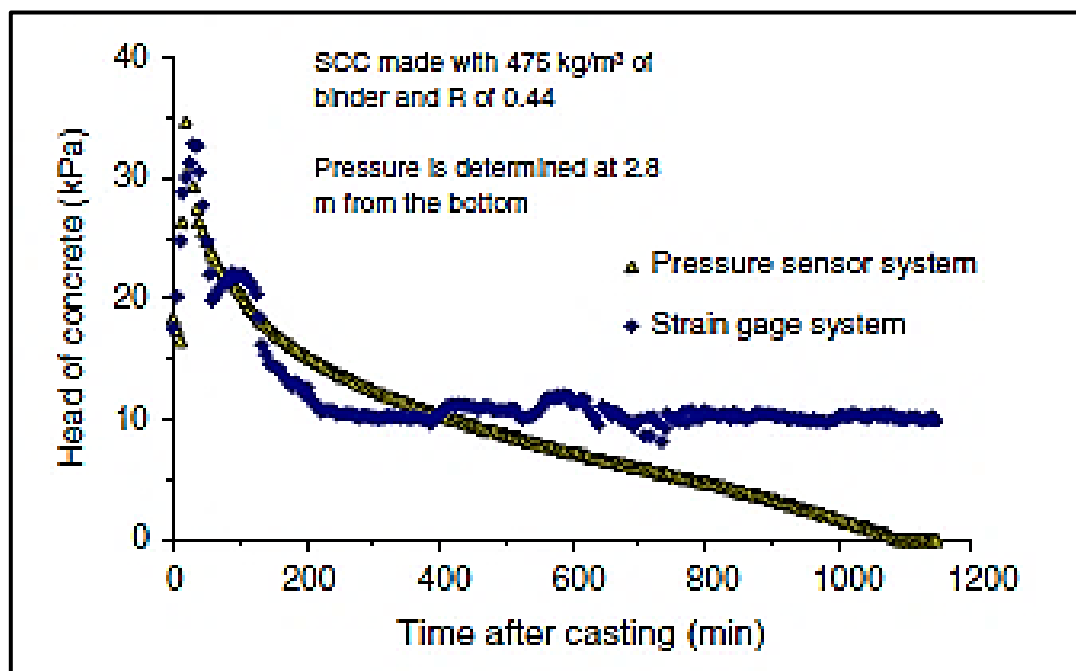


Figure 2-23: Comparison of lateral pressure determined using the pressure sensor and strain gauge systems until cancellation in the hardened state (R: sand-to-total coarse aggregate ratio) (Khayat & Assaad, 2008).

Gregori *et al.* (2008) used a deflecting membrane device to measure the lateral pressure in a concrete column. The authors reported that the measured lateral pressures recorded by the deflecting membrane device reduced slowly to a constant non-zero level and remained unchanged after the concrete hardened. It was noted by the authors that this was because the hardening of the concrete meant that it remained in touch with the deflected membrane thus preventing the membrane from recovering to its un-deflected state.

Khayat and Omran (2009) reported on a portable pressure device, referred to a UodS2 pressure column, which was developed and effectively used by the authors to evaluate the lateral pressure exerted by SCC. The UodS2 column, shown in Figure 2-24, has a diameter of 200 mm, a height of 700 mm, and a wall thickness of 10 mm. The tube was filled to a height of 500 mm with concrete and the top of the pressure column was sealed tightly. Air was steadily pumped from the top of the column to simulate the lateral pressure up to 13 m. An AB-high-performance pressure transducer was installed at 63 mm from the base of the pressure column and was set flush to the surface of the concrete surface to measure the lateral pressure.

McCarthy and Silfwerbrand (2011) compared three approaches to measuring lateral pressure, namely by means of: tensile load in the form ties, deflecting membrane pressure transducers, and strain in the formwork framing. The authors found that all three approaches produced the same result when recording the lateral pressure.

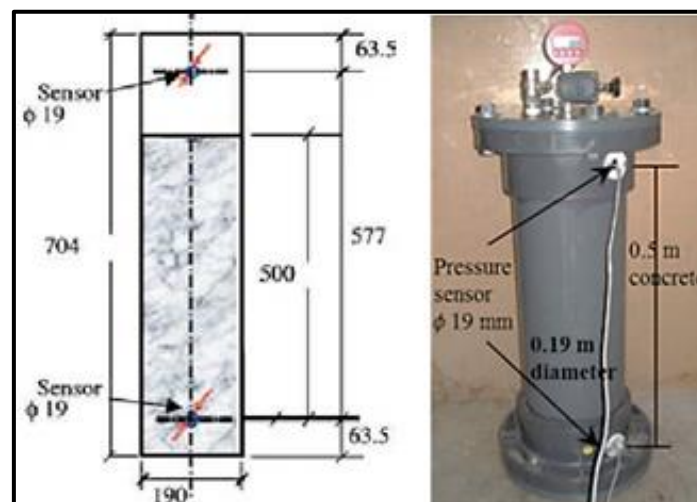


Figure 2-24: Schematic of UodS2 portable pressure column (left), and of UodS2 portable pressure column (right) (Khayat & Omran, 2009).

2.8 Existing Models

At present there is no widely accepted model for predicting the lateral formwork pressure exerted by SCC. The design recommendations for CVC cannot be used for SCC because the greater fluidity

of SCC that could produce lateral pressures reaching the level of hydrostatic pressures. Various models have been proposed by previous researchers to predict the exerted lateral pressure of SCC against formwork, and a summary of these which considers different parameters is shown in Tables 2- 4 and 2-5.

The researchers' approaches took into consideration a great number of parameters: the temperature and material properties of the concrete, the casting rate, casting depth, the formwork dimensions, the age of the concrete, and the initial setting time of the concrete, concrete density, yield shear stress, friction, and pumping of the concrete from either the top or the base of the formwork form geometry, the gravitational acceleration, and the waiting periods between castings. From various forms and combinations of these parameters, different models have been developed for calculating the lateral pressure exerted by SCC.

These models are briefly discussed in the following paragraphs and the reader is advised to consult the original source of the published work for an in-depth study and a better description of each model. Construction Industry Research and Information Association (CIRIA) Report 108, (1985) proposed a model where the value of $P_{(maximum)}$ is calculated from Equation 1, in which the lateral pressure is never larger than the hydrostatic pressure.

$$P_{max} = \left(C_1 \sqrt{R} + C_2 K \sqrt{H_1 - C_1 \sqrt{R}} \right) \gamma \quad (\text{Eq.1})$$

Where:

P_{max}	: Maximum lateral pressure against formwork (kPa)
R	: Rate of placement (m/h)
C_1	: Coefficient for the size and shape of the formwork (1 for walls).
C_2	: Coefficient for the constituent materials of the concrete (0.3 - 0.6).
γ	: Specific weight of concrete (kN/m^3).
H_1	: Vertical form height (m).
K	: Temperature coefficient $K = (36/T + 16)^2$.

Vanhove *et al.* (2004) obtained estimations of the lateral pressures exerted on formwork by using the Janssen's Model (Janssen, 1895). The authors considered the concrete to be a constant material and assumed that the horizontal pressure is proportional to the vertical one, where the proportional

factor (K) is constant throughout the entire height and depends on the material's internal friction angle (Φ). This study determined the correlation between friction coefficient and lateral pressure. The authors proposed Equation 2 to determine the pressure exerted by the fresh concrete on the lateral formwork.

$$P_{max} = \frac{\gamma g A - \alpha \tau_0 (2e + 2d)}{\alpha (2e + 2d) \mu K_1} \left(1 - e^{\frac{\alpha (2e + 2d) \mu K_1 H}{A}} \right) \quad (\text{Eq.2})$$

Where:

- γ : Unit weight of concrete (kN/m^3).
- e : Formwork element thickness (m).
- τ_0 : Yield shear stress (Pa).
- K_1 : Reduction factor of the hydrostatic pressure.
- g : Gravitational acceleration, $9.81 \text{ m}/\text{s}^2$.
- d : Formwork width (m).
- H : Formwork height (m).
- μ : Friction coefficient.
- A : Area of the formwork pressure (m^2).
- α : Top-bottom casting (0.15) and bottom-up casting (0.34).

Tejeda-Dominguez (2005) characterised the SCC behaviour at rest by the characteristic pressure decay that occurred after casting the concrete at the base of the formwork. The author developed Equations 3 and 4 for predicting the lateral pressure from continuous casting.

$$C(t) = \frac{C_0}{(at^2 + 1)^\alpha} \quad (\text{Eq. 3})$$

Where:

- $C(t)$: Characteristic pressure decay as a function of time.
- C_0 : Initial pressure (kPa).
- a, α : Time-dependent variables.
- t : Time (h).

$$P_h = \gamma R t \frac{c_0}{(at^2+1)^\alpha} \quad (\text{Eq.4})$$

Where:

- P_h : Lateral pressure (kPa).
 γ : Unit weight of concrete (kN/m^3).
 R : Casting rate (m/h).
 α, a : Time-dependent variables.
 t : Time (h).

Roussel and Ovarlez (2006) used Janssen's silo theory (Janssen, 1895) to propose a theoretical model that characterises SCC by its static yield stress (τ_o) at rest. It assumes that there are yield stresses and frictional contacts on the walls, and that the maximum stress in the material reaches the material's static yield stress. The lateral pressure may be determined from Equation 5 for rectangular formwork.

$$P_{max} = \left(1 - \frac{HA_{thix}}{\rho g e R}\right) * \rho g H \quad (\text{Eq.5})$$

Where:

- P_{max} : Maximum formwork pressure (kPa).
 H : Wall height (m).
 A_{thix} : Static yield stress at rest (Pa\|s).
 ρ : Unit weight of concrete (kN/m^3).
 g : Gravitational acceleration, $9.81 \text{ m}/\text{s}^2$.
 e : Wall thickness (m).
 R : Casting rate (m/h).

The German guidelines Deutsche Institut für Normung (DIN) (DIN 18218-10 (2010)), are based on the study of Proske and Graubner Group (Brameshuber *et al.* (2011); Graubner *et al.* (2012); Proske and Graubner, (2002 a & b) who recommended a bilinear distribution of the lateral pressure exerted by SCC against the formwork, with a hydrostatic distribution that increases up to the maximum

pressure and then stays constant down to the base of the formwork. The maximum value of the lateral pressure is determined by Equations 6 and 7.

Considering that $P_{max} \leq P_{hyd}$.

$$P_{max} = (0.8[m] + 0.16 \cdot R \cdot t_E) \cdot \gamma_c \quad (\text{Eq.6})$$

Considering that $P_{max} \leq 30$ and $P_{max} \leq P_{hyd}$.

$$P_{max} = (1.0[m] + 0.26 \cdot R \cdot t_E) \cdot \gamma_c \quad (\text{Eq.7})$$

Where:

P_{max} : Maximum formwork pressure (kPa).

γ_c : Specific weight of concrete (kN/m³).

t_E : Setting time (h).

Khayat and Omran (2011) carried out laboratory investigations at the Université de Sherbrooke to develop prediction models Equations 8, 9, and 10 for estimating SCC maximum formwork pressure.

$$K_0 (\%) = \frac{P_{max}}{P_{hyd}} \times 100 \quad (\text{Eq.8})$$

$$P_{max}(kPa) = \frac{pgH}{100,000} (112.5 - 3.80H + 0.6R - 0.6T + 10D_{min} - 0.021PV_{\tau_{0rest@15minT=22\pm2^\circ C}}) \cdot f_{MSA} \cdot f_{WP} \quad (\text{Eq.9})$$

$$P_{max}(kPa) = \frac{pgH}{100,000} (112 - 3.83H + 0.6R - 0.6T + 10D_{min} - 0.023IP_{\tau_{0rest@15minT=22\pm2^\circ C}}) \cdot f_{MSA} \cdot f_{WP} \quad (\text{Eq.10})$$

Where:

P_{max} : Maximum formwork pressure (kPa).

P_{hyd} : Maximum formwork pressure (kPa).

p : Unit weight of concrete (kN/m³).

g : Gravitational acceleration, 9.81 m/s².

H : Concrete wall height (m), $1 \leq H \leq 13$.

R : Casting rate (m/h), $2 \leq R \leq 30$.

- D_{min} : Minimum lateral dimension of formwork (m).
- $PV_{\tau_{0rest@15minTi}}$: The static yield stress measured at 15 min of rest using the PV test (Pa).
- $IP_{\tau_{0rest@15minTi}}$: The static yield stress measured at 15 min of rest using the IP test (Pa).
- f_{MSA} : Modification factor (maximum size of aggregate).
- f_{WP} : Modification factor (Waiting period between lifts).

Gardner (2014) developed a model based on the time required for the slump flow of the SCC to reach zero (t_0). Since it is not measurable in practice, the authors estimate t_0 as the time required for the initial slump flow decays to 400 mm. Thus, the author defines t_0 according to Equations 11, 12 and 13.

For $t < t_E/2$:

$$p = w_c R \left(t - \frac{t^2}{t_E} \right) \quad (\text{Eq.11})$$

For $t > t_E/2$:

$$p_{max} = w_c R t_E / 4 \quad (\text{Eq.12})$$

If $t_H = H/R < t_E/2$ Substituting t_H for t in (Eq.A.13)

$$p_H = w_c R \left(t_H - \frac{t_H^2}{t_E} \right) = w H \left(1 - \frac{t_H}{t_E} \right) \quad (\text{Eq.13})$$

Where:

- w_c : Unit weight of concrete (kN/m^3).
- R : Casting rate (m/h).
- t_E : Setting time (h).
- t_H : Time to fill a form to height H (h).
- P_H : Lateral pressure at head H (kPa).

In the case of SCC, The American Concrete Institute (ACI) Committee 347, (2014) suggested using a hydrostatic distribution until the effect on lateral formwork pressure is comprehended by measurement. The maximum pressure is determined by Equations 14 and 15.

When $R < 2.1$ m/h and $H < 4.2$ m

$$P_{max} = C_W C_C (7.2 + \frac{785R}{T+17.8}) \quad (\text{Eq.14})$$

When $R < 2.1$ m/h and $H > 4.2$ m and for all walls with $2.1 \text{ m} = h < R < 4.5 \text{ m} = h$

$$P_{max} = C_W C_C (7.2 + \frac{1156}{T+17.8} + \frac{244R}{T+17.8}) \quad (\text{Eq.15})$$

Where:

P_{max} : Maximum lateral pressure against formwork (kPa).

R : Rate of placement (m/h).

C_W : Unit weight coefficient.

C_C : Chemistry coefficient.

γ : Specific weight of concrete (kN/m^3).

H : Concrete depth (m).

T : Concrete temperature ($^{\circ}\text{C}$).

2.1 Conclusion

This chapter presents aspects of the lateral pressure that is exerted by SCC on formwork systems. The lateral formwork pressure is discussed, and the known characteristics that affect the lateral pressure are highlighted, as well as the reason for performing investigations into lateral formwork pressure. These known characteristics are discussed and divided into placement characteristics, material properties and formwork characteristics. Each of these sections is further addressed. The lateral pressure measuring systems used by other investigators are briefly discussed. Finally, calculation models recommended by various authors for the prediction of lateral formwork pressures exerted by SCC are briefly mentioned.

The majority of the knowledge regarding lateral formwork pressure has come from laboratory investigations and most of the parameters studied were those involving material properties and low

to medium casting rates (2-30 m/h). It was found that when casting from the top of the formwork system induced lateral pressure could be below hydrostatic level, it was further stated that this was due to SCC flocculating and it then building up an internal structure (thixotropic behavior) which can withstand the load of the fresh concrete cast from above without increasing the lateral pressure being exerted on the formwork system.

Conversely, pumping from the base of the element could cause the lateral pressure to reach, or even exceed, full hydrostatic pressure because of the constant pump pressure and non-thixotropic behavior. It was suggested that when pumping fresh SCC from the base of the element, pauses during the casting procedure should be avoided else high pumping pressures would be necessary to break down the mass that SCC built up because of its thixotropic behavior. Thus it was suggested that when designing formwork systems where the SCC is cast from the base, the formwork system ought to be designed to withstand hydrostatic pressure plus the pump pressure.

It was highlighted that higher casting rates (high enough to prevent the SCC from setting) could result in higher lateral pressures being exerted which even surpassed hydrostatic pressure levels. However, the lateral pressures exerted would reduce if the casting rate were to be reduced to such a degree that fresh SCC was able to undergo structural build-up. However, regarding larger structures when lower casting rates were implemented, it was noted that the maximum lateral pressure exerted was significantly less than hydrostatic pressure.

From the literature it was found that the temperature of the fresh SCC had no significant effect on the lateral pressure at the end of the casting process. It was found that if the casting process was interrupted and waiting periods were implemented the lateral pressure could be reduced. It was found that the slump flow, binder composition, type of aggregate and water-cementitious material ratio (w/cm) had notable influences to the lateral pressure. However, it was found that the formwork characteristics had less effect on decreasing the lateral pressure.

Therefore, since most of the investigations were performed in the laboratory using low casting rates, this study concentrates on performing experiments under site conditions and studies the placement characteristics that can be controlled on-site. Namely, placement method (top-down and bottom-up pumping), casting rate and the interruption of the casting process by implementing waiting periods. The study also compares the recorded pressure data from the experiments with the existing models presented in this chapter. The equipment used to investigate are discussed in Chapter 3.

Table 2-4: Parameters of the models to predict lateral pressure on formwork.

Lateral Pressure Models	Waiting period between casts	Gravity	Placement Method	Friction	Yield shear stress	Concrete density	Setting Time	Concrete age	Formwork geometry	Casting depth	Material properties	Concrete temperature	Casting rate
CIRIA Report 108 (1985)													
Vanhove <i>et al.</i> , (2004)													
Tejeda-Dominquez (2005)													
Ovarlez and Roussel (2006)													
DIN 18 218 (2010)													

Table 2-5: Parameters of the models to predict lateral pressure on formwork (cont.).

Waiting period between casts	Gravity	Placement Method	Friction	Yield shear stress	Concrete density	Setting Time	Concrete age	Formwork geometry	Casting depth	Material properties	Concrete temperature	Casting rate	Lateral Pressure Models
													Khayat and Omran (2011)
													Gardner (2014)
													ACI Committee 347 (2014)

Chapter 3 : Research Equipment

3.1 Introduction

This chapter covers the research equipment which was used in the investigation. The experimental equipment used to monitor and record the lateral pressure exerted by the self-compacting concrete on the formwork system is discussed. Specifications regarding the flush diaphragm pressure transducers used to record the necessary lateral pressure the data are documented. The method of mounting the pressure transducers and the specifications of data logger used are covered. Information and specifications regarding the on-site equipment (boom and static pumps) are discussed. See Figure 3-1 for an overview of Chapter 3.

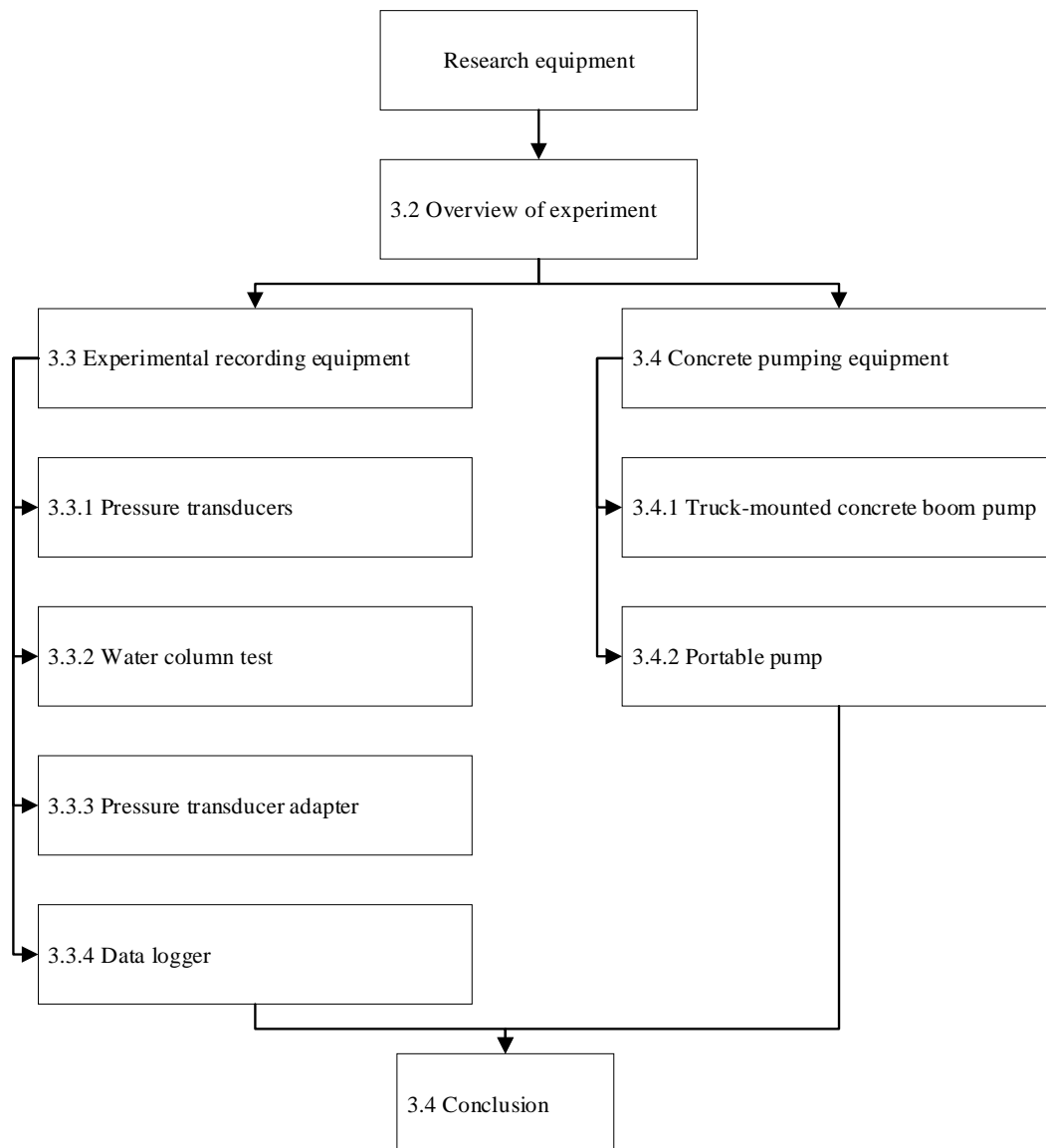


Figure 3-1: Layout and overview of Chapter 3.

3.2 Overview of Experiment

An important objective of the investigation was to perform field tests on large-scale walls elements under site conditions by simulating a construction project's environment. This was achieved by using project labour and site equipment. Six large scale wall elements were constructed with a height of 5.4 meters, a width of 2 meters, and a thickness of 0.2 meters. The walls were divided into two sets of three, the first set dealt with pumping the SCC from the top of the wall element (top-down casting) and the second set dealt with pumping the fresh concrete from the base (bottom-up casting). This was accomplished by using truck-mounted concrete boom pumps and a portable pump.

The top-down casting experiments were divided into three walls, Wall 1 cast the SCC at a constant 80 m/h, Wall 2 and Wall 3 were cast at an average of 27 m/h and waiting periods of 10 and 15 minutes were implemented. The bottom-up castings were also divided into three walls where the SCC was cast at 65 m/h for Wall 4, 80 m/h for Wall 5 and 55 m/h for Wall 6. In order to obtain the lateral pressure from each of the six wall elements eight flush diaphragm pressure transducers were mounted to the formwork panels at predetermined locations. A detailed explanation of the experimental procedure is given in Chapter 4 of this report.

3.3 Experimental Recording Equipment

3.3.1 Pressure Transducers

For the purpose of measuring the lateral pressure exerted by the SCC, eight flush diaphragm pressure transducers were used. Flush diaphragm pressure transducers were chosen because the set-up of the transducers was simpler when compared to other methods, and these types of transducers are mainly implemented to measure the pressure from slurry in factories thus the transducers would be able to withstand the pressures exerted by the SCC.

The Gems 1701 BGA25F210F320 pressure transducers, shown in Figure 3-2, were chosen because of its designed pressure range and shape which allowed for the easy fabrication of an adaptor necessary to mount the pressure transducer to the formwork system. According to the manufacturer's information, a maximum gauge pressure of 2.5 bar (250 kPa), with an accuracy of $\pm 0.25\%$ can be obtained. A summary of the pressure transducers' specifications and dimensions is shown in Table 3-1.

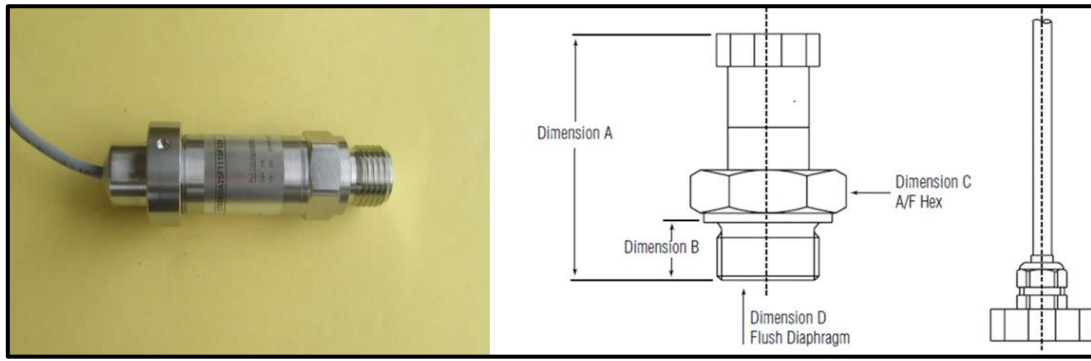


Figure 3-2: Stainless steel flush diaphragm pressure transducer – Series 1701.

Table 3-1: Summary of the pressure transducer specifications.

Thread	Dim A	Dim B	Dim C	Dim D
G 3/4"	78.5 mm	16.0 mm	34.0 mm	22.0 mm
Electrical Connection	Cable Gland including 2m Cable			
Accuracy	$\pm 0.25\%$			
Filling Fluid	Silicon Oil			
Output	4-20mA			
Datum	Gauge			
Pressure Range	0-2.5 bar			
Seal	Viton			
Diaphragm Material	Stainless Steel			

3.3.2 Water Column Test

In order to test the accuracy of the pressure transducer a one meter long Polyvinyl Chloride (PVC) water column was set up. Figure 3-3 shows the test setup for the water column. Pressures were recorded and logged at both the beginning and the end of the filling process in order to compare the pressure transducer reading with the theoretical calculations, as well as to compare the pressure transducer reading to each of the others. An average reading was documented at both the start and the end of the filling process for each of the pressure transducers. These average values were used to create suitable equations to more accurately identify and document the pressures exerted on the

flush diaphragm pressure transducers. The pressure transducers exhibited acceptable pressure values and performance. See Table 3-2 for the results of the test.

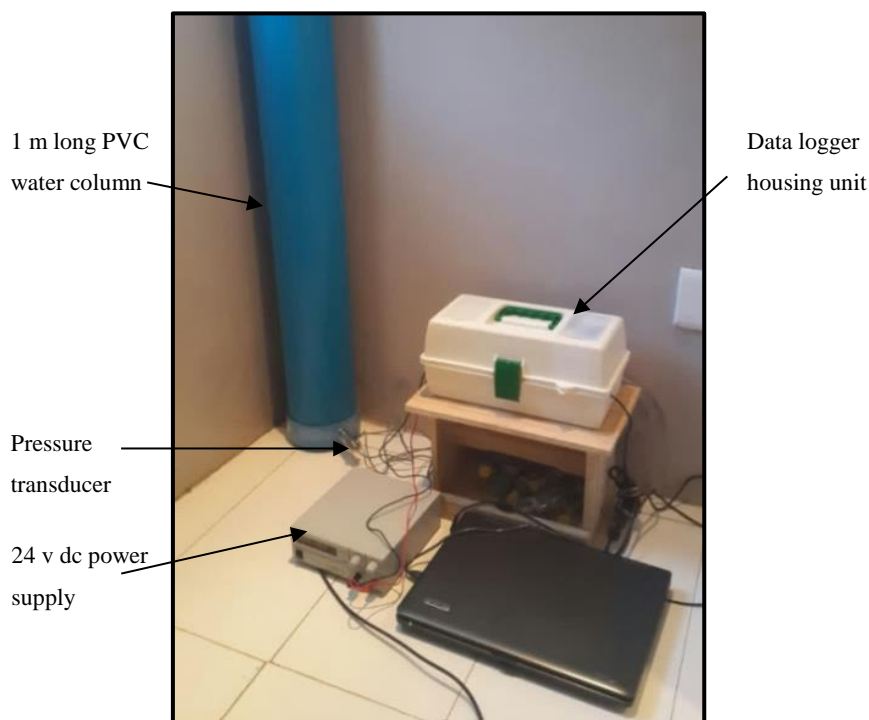


Figure 3-3: Water column testing equipment.

Table 3-2: Water column readings and transducer accuracy (v: voltage).

Transducers	Average Gauge Pressure (Empty Reading)		Average Gauge Pressure (Filled Reading)		Theoretical Hydrostatic Pressure	Variation
	v	kPa	v	kPa	kPa	%
# 1	0.4878	0	0.5657	9.98	9.81	1.7
# 2	0.5958	0	0.5707	9.46	9.81	3.7
# 3	0.4908	0	0.5726	10.4	9.81	5.9
# 4	0.4737	0	0.5458	9.52	9.81	3.1
# 5	0.493	0	0.5714	9.95	9.81	1.4
# 6	0.5083	0	0.5892	9.98	9.81	1.8
# 7	0.5082	0	0.5902	10.1	9.81	3.2
# 8	0.4731	0	0.5501	10.2	9.81	3.6

3.3.3 Pressure Transducer Adaptor

To mount the eight flush diaphragm pressure transducers to the Domino formwork system panels, an adaptor was designed and then machined in the Stellenbosch University Civil Engineering workshop, from a solid one meter long PVC rod. The PVC rod was cut to specification into eight disks and then machined into the adaptors required to mount the flush diaphragm pressure transducers to the formwork panels. The adaptors were designed to withstand the maximum lateral pressures which the pressure transducers were capable of measuring (250 kPa).

The flanges of the adaptor were designed to have a thickness of 6 mm so that the flanges could withstand the moment and the punching shear that could potentially be induced by the maximum lateral pressure. The location of the holes where the bolts are inserted was chosen to limit the magnitude of the induced moment by creating the smallest possible moment arm from the point where the pressure is applied to the centroid of the hole where the bolts are situated, shown in Figure 3-4.

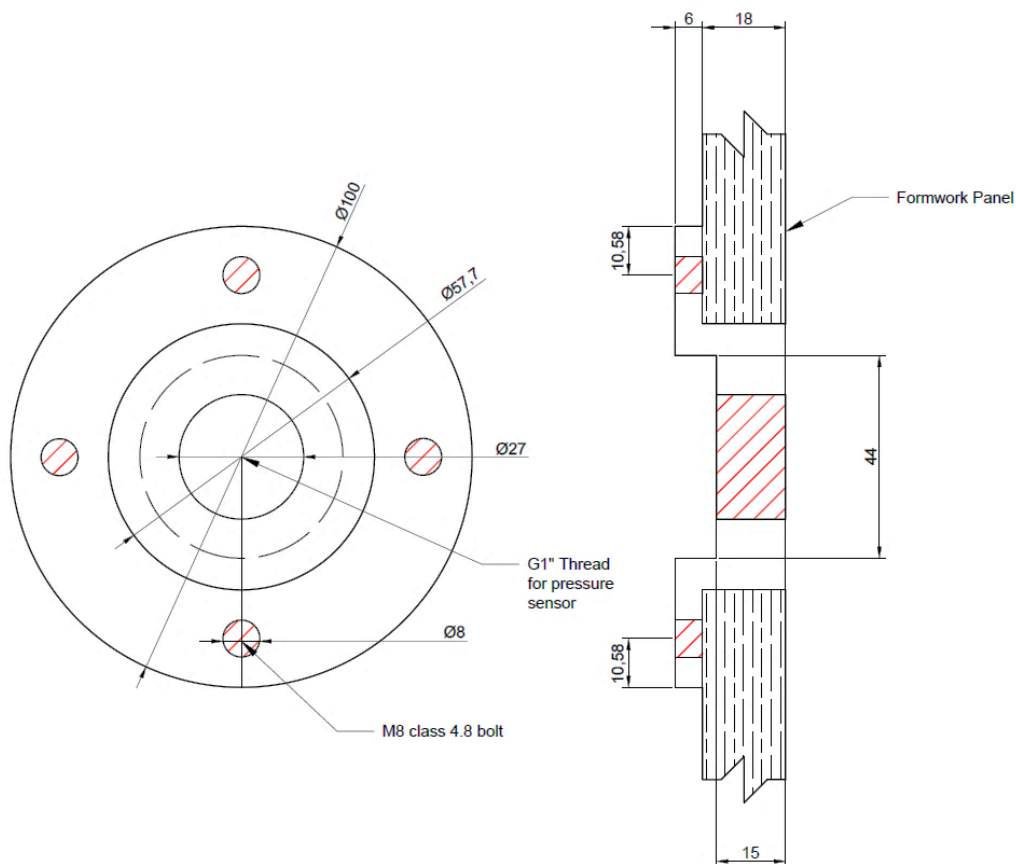


Figure 3-4: Drawing of the PVC adaptor with dimensions (mm).

The adaptor's centre was tapered to the specification of the pressure transducers threading of G 3/4" so that the pressure transducers could be mounted flush and securely to the formwork system panels, shown in Figure 3-5.

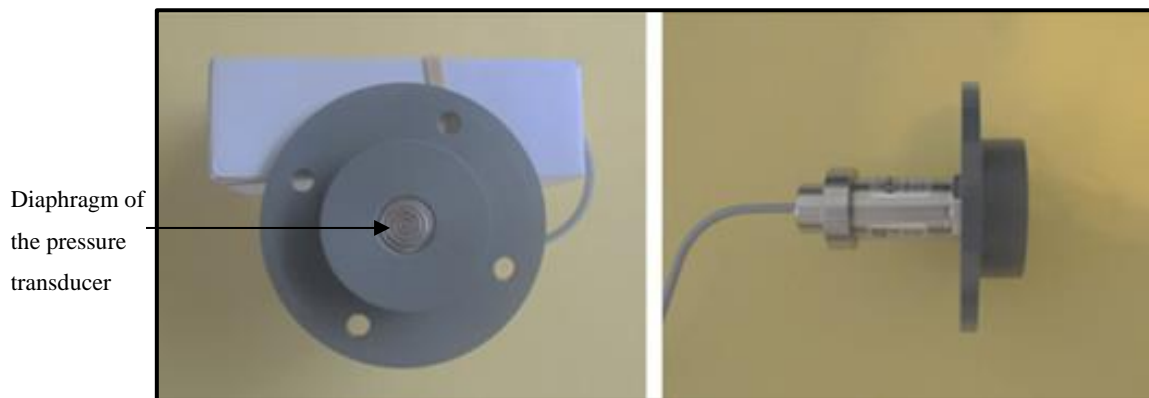


Figure 3-5: Pressure transducer in the PVC Adaptor.

Eight holes were cut into the wooden formwork panels at the specific locations chosen to place the machined jackets into the formwork panels, shown in Figure 3-6 (left). Once the PVC jackets had been placed into the formwork panels, each individual jacket was fastened into place, using four M8 Class 4.8 bolts and washers, shown in Figure 3-6 (right). The class of bolt was chosen, after following the design calculations according to South African National Standards (SANS) SANS 10162-1:2011, to withstand the tensile force created by the induced lateral pressures throughout the casting period.



Figure 3-6: Drilled hole in the formwork panel (left) and PVC adaptor mounted in the formwork panel (right).

3.3.4 Data Logger

During this test lateral pressure data was logged by using the XR5-SE Compact Data Logger. The data logger was powered internally with the aid of two AA 3.6V lithium batteries. These two batteries powered only the data logger's internal systems and software. These lithium batteries did not power the accompanying Gems 1701 BGA25F210F320 pressure transducers.

An external 24 v dc power supply, as shown in Figure 3-7, was used to provide power to the eight pressure transducers.

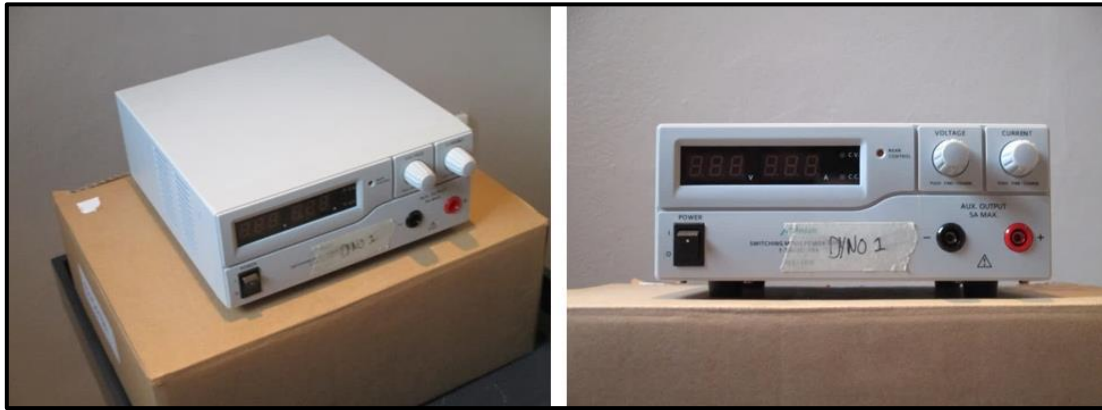


Figure 3-7: 24 v dc power supply.

To power the eight pressure transducers effectively, each transducer was connected to the XR5-SE Compact Data Logger and the 24 v dc power supply by using multiple current loops, shown in Figure 3-8. The positive terminal (+) of the power supply and the white wires (+) of eight transducers were connected together to power each individual transducer.

Each one of pressure transducers' brown wires (-) and the negative terminal (-) from the power supply were connected to a machined motherboard, which contained eight 120 Ohm resistors (one resistor for each transducer). From the motherboard eight copper wires (corresponding to the combination of the positive terminal of the power supply and the white wires of the transducers) were used to connect each of the eight transducers to one of eight input channels available and a wire (corresponding to the combination of the negative terminal of the power supply and the brown wires of the transducers) was connected to the C terminal (Ground) on the XR5-SE Compact Data Logger.

The motherboard used to create the required current loops was assembled in the machine laboratory of the Electrical and Engineering department at Stellenbosch University. The design and machining of the motherboard was performed with the aid of Stefan Erasmus, the machine laboratory manager.

The current loops constructed, as well as XR5-SE Compact Data Logger were placed in a modified toolbox, eight holes were drilled into the toolbox and marked one to eight, to mark which of the input channels each of the transducers were connected to. Two holes were drilled on the side of the toolbox and marked to identify the positive and negative terminals which connected the power supply to the data logger; lastly a hole was drilled to allow for a connection between the data logger and the computer used to monitor the lateral pressures, as shown in Figure 3-9.

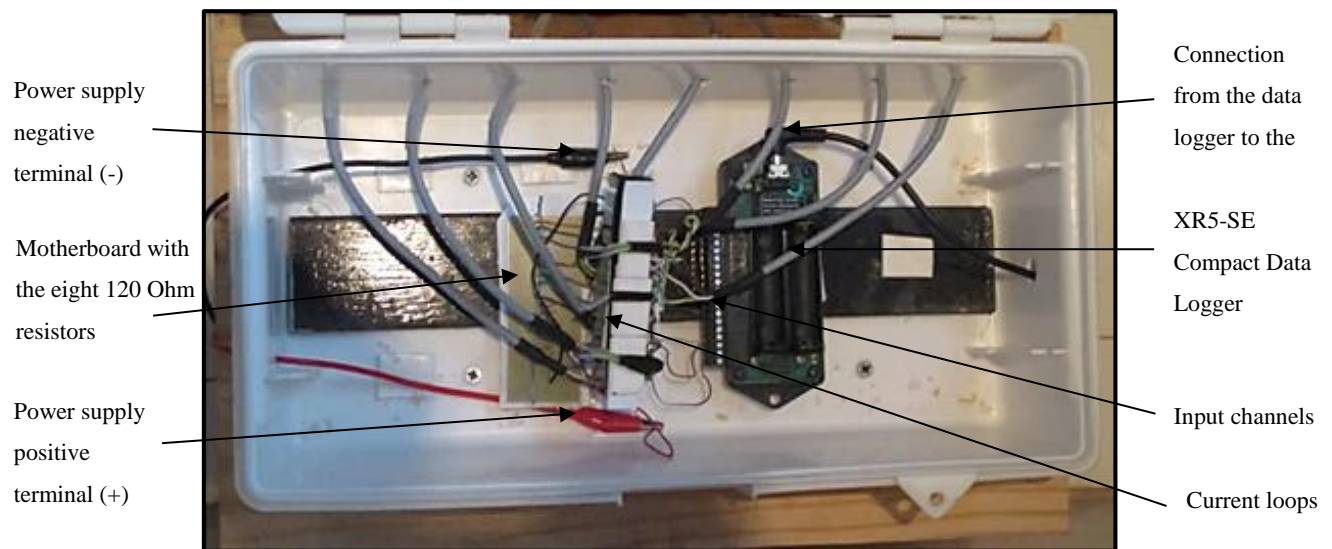


Figure 3-8: The current loop between the transducers and the XR5-SE Data Logger.

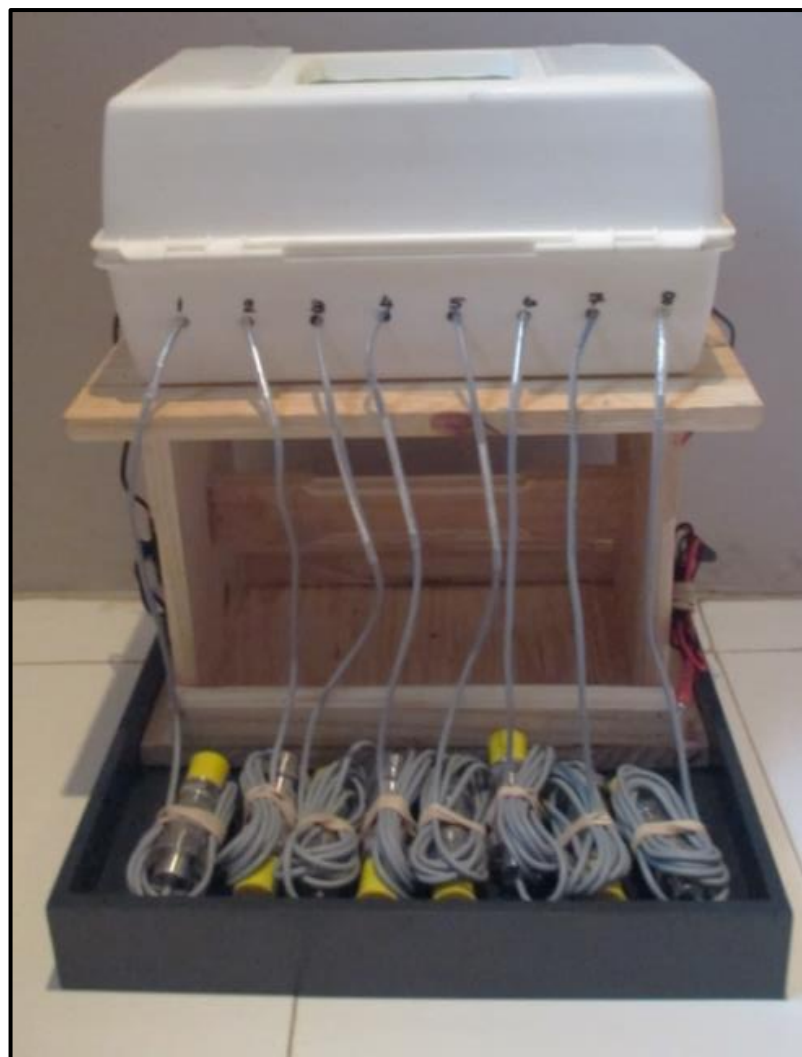


Figure 3-9: XR5-SE data logger housing unit and pressure transducers

3.4 Concrete Pumping Equipment

Concrete pumping equipment was used to pump the SCC from the top and base of the wall element. The CIFA K31L and Putzmeister 36Z-Meter truck-mounted concrete boom pumps were used for Walls 1-3 where the fresh concrete was cast from the top of the wall element, and the CIFA S8 Series PC 907 portable pump was used for Walls 4-6 where the SCC was pumped from the base of the wall element.

3.4.1 Truck-Mounted Concrete Boom Pump

A truck-mounted concrete boom pump's operation involves both hydraulic and electrical systems. The boom pump is designed to pump fresh concrete through a delivery system of pipes and hoses attached to a boom. Stability is provided to the truck-mounted boom pump during operation by four hydraulic outriggers located on the side of the truck. The boom is mounted on a pedestal directly behind the chassis cab and is equipped with a rotational mechanism which allows the boom arm to move 360° around the truck. Each boom section on the arm operates independently of the other sections. A steel pipe delivery line is installed from the hopper discharge outlet, along the deck, through the pedestal and attached alongside of the boom sections; a heavy duty end hose is provided to facilitate concrete placement.

The CIFA K31L truck-mounted concrete boom pump (shown in Figure 3-10) was one of two truck-mounted boom pumps used to pump the SCC from the top of the formwork wall element in the investigation of how the lateral formwork pressure is affected by casting SCC from the top of the formwork system. A summary of the technical information on the CIFA K31L is given in Table 3-3. A diagram of the CIFA K31L's dimensions and the ways in which each boom arm section can be deployed are shown in Appendix A.



Figure 3-10: CIFA K31L Truck-Mounted Concrete Boom Pump.

Table 3-3: CIFA K31L - HP1606H Technical data sheet.

Model		HP1606H
Max. theoretical output	m^3/h	160
Max. pressure on concrete	bar	53
Max. numbers of cycles per min	nr	30
Conc. cylinders (diam. X stroke)	mm	230x2100
Concrete hopper capacity	l	550
Hydraulic circuit		open

The second truck-mounted boom pump used in the investigation was the Putzmeister 36Z-Meter truck-mounted concrete boom pump, shown in Figure 3-11. The Putzmeister was larger than the CIFA K31L but operated in the same manner. A summary of the technical information of the Putzmeister 36Z-Meter is given in Table 3-4. A diagram of the Putzmeister 36Z-Meter's dimensions and the way each boom arm section can be deployed are shown in Appendix B.

**Figure 3-11:** The Putzmeister 36Z-Meter Truck-Mounted Concrete Boom Pump.

Table 3-4: Putzmeister 36Z.12H - Technical data sheet.

Model		36Z.12H
Output (rod side)	m^3/h	110
Output (piston side) - Exit	m^3/h	74
Pressure (rod side)	bar	85
Pressure (piston side)	bar	130
Maximum stroked per minute (rod side)	nr	21
Maximum stroked per minute (piston side)	nr	14
Hydraulic system		Free flow
Water tank (pedestal)	l	700

3.4.2 Portable Pump

The CIFA S8 Series PC 907 portable pump, shown in Figure 3-12, was used to pump the SCC from the base of the wall element to investigate how the lateral formwork pressure is affected by casting the SCC from the base of the formwork. A summary of the technical information on the CIFA S8 Series PC 907 is given in Table 3-5.

**Figure 3-12:** CIFA S8 Series PC 907 Portable Pump.

Table 3-5: The CIFA S8 Series PC 907 - Technical data sheet.

Model		PC 907
Max. theoretical output	m^3/h	87
Max. pressure on concrete	bar	66
Max. numbers of cycles per min	nr	26
Concrete cylinders diameter	mm	200
Stroke length	mm	1800
Concrete hopper capacity	l	400
side drive		rod

3.5 Conclusion

This chapter presents the equipment which was used in the investigation to get the lateral pressure readings. The description of the research equipment can be classified as either experimental equipment or pumping equipment. The experimental equipment discussed was the pressure transducers used to measure the lateral pressure, the PVC adaptor used to mount the transducers to the formwork panels, and the data logger implemented to document and store the lateral pressure readings. The various pumps that were used in the experiment are discussed and a summary of the specifications of each pump are given. The experimental methodology and how the equipment was setup are discussed in Chapter 4.

Chapter 4 : Experimental Methodology

4.1 Introduction

The following chapter discusses the experimental procedures and parameters measured. Namely, the lateral pressure exerted on the experimental wall by the Self-Compacting Concrete (SCC) using two different placement methods (top-down and bottom-up casting), three waiting periods (WP) for Wall 1 and two waiting periods for Wall 2, and three different casting rates when pumping the SCC from the base of the wall element.

The lateral pressure was measured and documented for six vertical walls with the same dimensions (5.4m x 2m x 0.2m). The material and design information is presented, and the concrete properties such as slump, temperature and filling ability were measured and recorded. Using flush diaphragm pressure transducers the lateral pressure exerted on the formwork was monitored and recorded, and the rate and method of placement were monitored throughout the duration of the casting operation. See Figure 4-1 for an overview of Chapter 4.

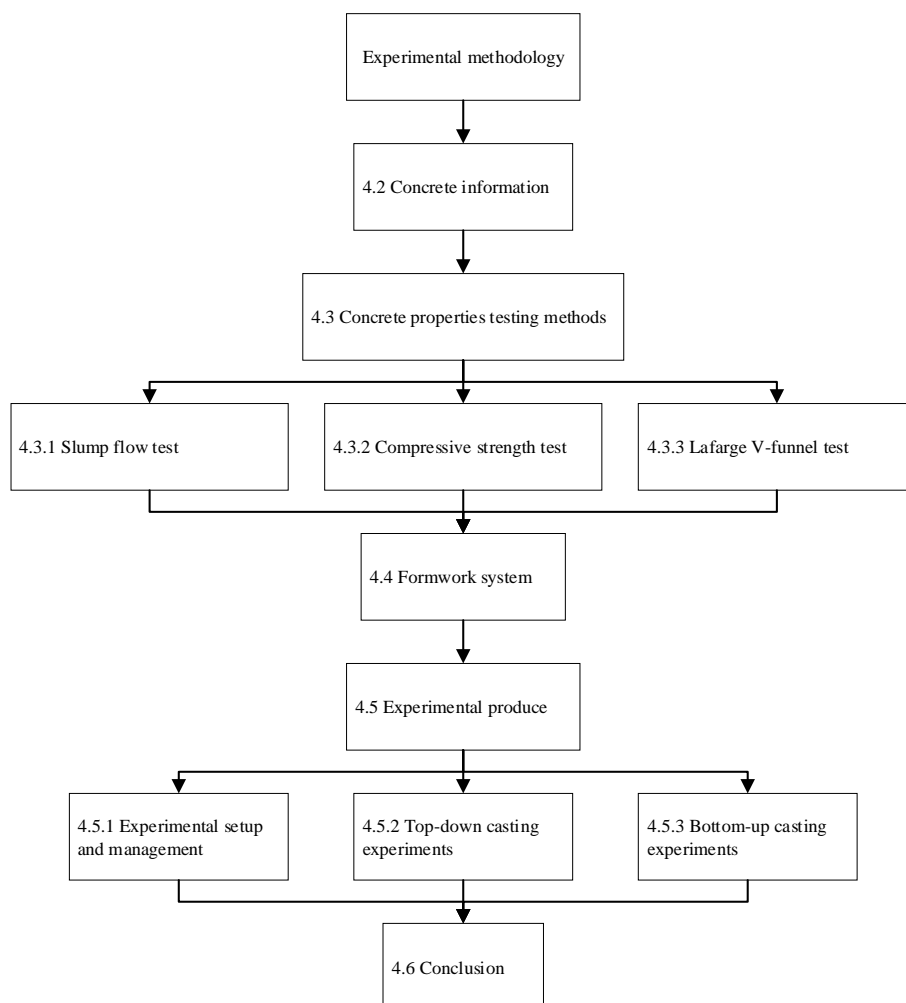


Figure 4-1: Layout and overview of Chapter 4.

4.2 Concrete Information

The SCC used in the experiments was the Agilia Vertical, supplied by Lafarge. Agilia is a SCC designed to flow under its own weight and is able to completely fill all spaces within the formwork while remaining homogenous. The Agilia is specifically designed for vertical elements (Agilia Vertical) and was implemented in the experiment, as the investigation concerned around wall elements. Agilia Vertical is designed with improved viscosity to ensure better off-shutter finishes and better flowability between reinforcement making it ideal for use in all vertical applications. It is commercially available and is the SCC mixture supplied by Lafarge when ordered for vertical elements.

See Table 4-1 for a summary of the materials of which the Agilia Vertical is composed, and also see Table 4-2 for a summary of the information regarding the mix design. For confidential reasons, it is not possible to give either the exact concrete mix design or the exact mix proportions used in this investigation. However, the concrete used is widely commercially available in the South African construction industry.

4.3 Concrete Properties Testing Methods

Due to the objective of the investigation being to determine the effect of placement methods under site conditions on the exerted lateral pressure, the material properties were kept constant. In order to make sure that the material properties do not vary to such a degree as to affect the lateral pressure three tests were performed.

4.3.1 Slump Flow Test

The slump flow of the Agilia Vertical concrete was obtained before each test, in accordance with American Society for Testing Materials (ASTM) ASTM C1611, shown in Figure 4-2, by taking a sample of freshly mixed concrete and then placing it in a mould in an upright position. The concrete was placed in the mould in one lift without tamping or vibration. The mould was raised, and then the concrete was allowed to spread. After the spreading stopped, two diameters of the concrete mass were measured in approximately orthogonal directions, after which the slump flow was calculated shown in Equation 16.

Table 4-1: Agilia Vertical: Composition Materials.

Materials	Standard Codes	Origin of Supply
Sand (Atlantic Sand)	SANS 1083	Vaatjie Farm
Stone	SANS 1083	Lafarge peak quarry
OPC (CEM II 52.5 A-L)	SANS 50197	PPC De Hoek
Slag (Correx)	SANS 1491	PPC Saldanha
Admixtures	ASTM C 494	Chryso

Table 4-2: Agilia Vertical: Information on Mix Design.

Coarse aggregate size	14 mm
Coarse aggregate type	Hornfels
Coarse aggregate quantity	Between 600 kg/ m ³ and 800 kg/ m ³
Fine aggregate type	Hornfels crusher sand / Silica dune sand
Cementitious	50% OPC / 50% SLAG
Minimum cement content	± 500 kg/m ³
C/W	2.2 - 2.5
Workability (Slump flow)	650 - 700 mm
Design strength (28 days)	40 MPa

$$S = \frac{d_1 + d_2}{2} \quad (\text{Eq. 16})$$

Where:

S : Slump Flow (mm)

d_1 : The largest diameter of the circular spread of the concrete

d_2 : The circular spread of the concrete at an angle approximately perpendicular to d_1

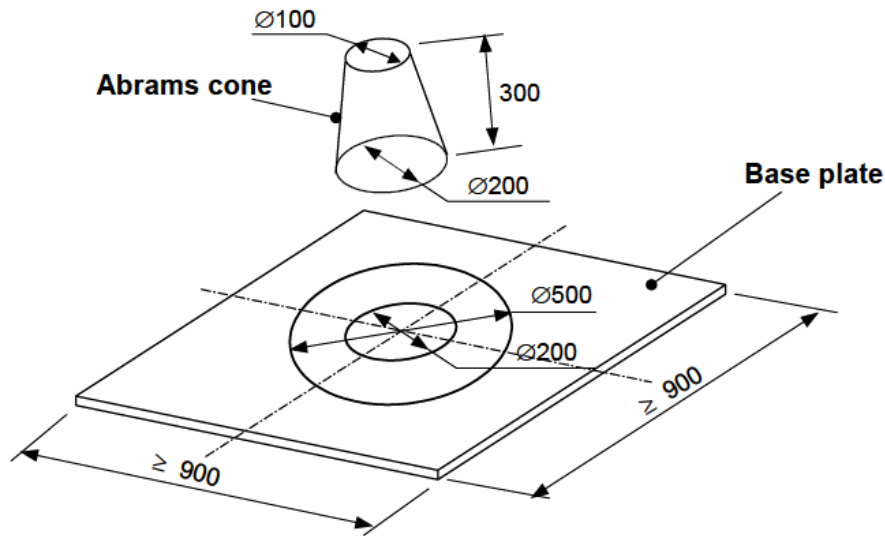


Figure 4-2: Base plate and Abrams cone used to measure the slump flow (De Schutter 2005).

4.3.2 Compressive Strength Test

The 7 day and 28 day compressive strength of the Agilia Vertical concrete was obtained, in accordance with SANS 5863: 2006. All the tests were performed at Lafarge's laboratory, in which samples were taken from each batch so that the compressive strength of the SCC of the six walls could be obtained. The compressive strength of the SCC was determined by Equation 17.

$$f_{cc} = \frac{F}{A_c} \quad (\text{Eq. 17})$$

Where:

f_{cc} : Compressive strength (MPa)

F : Maximum load at failure (N)

A_c : Cross-sectional area of the specimen (m^2)

4.3.3 Lafarge V-Funnel Test

The V-Funnel test is used to measure, the flow rate of fresh SCC through the opening under self-weight, and the flow time is an indication of its plastic viscosity. The filling ability of the SCC was determined by using Lafarge's version of the V-funnel test, shown in Figure 4-3. The V-funnel flow time is the period a defined volume of SCC needs to pass through a narrow opening and it gives an indication of the filling ability of the SCC, provided that no blocking or segregation takes place. (De Schutter, (2005) and Domone, 2009). The flow time of the V-Funnel test is to some degree related to the plastic viscosity (De Schutter, 2005, Turk, 2012 and Gambhir, 2013). Felekoğlu *et al* (2006) used a programmable DV model viscometer in a study on the viscosity of SCC, that V-Funnel time correlate in certain cases with the viscosity.

Before each casting session the V-funnel test was performed on Lafarge's SCC Agilia Vertical brand; this was done by taking a sample of the freshly mixed SCC and placing it in a large metal V-funnel mounted on a metal tripod in an upright position over an open container. The concrete was poured into the top of the large metal funnel. Once completely filled, a latch at the bottom of the funnel was opened allowing the concrete to flow freely into the open container below and the stopwatch was simultaneously started. As the SCC flowed into the container, the time was stopped and recorded the instant daylight could be seen through the opening. The flow-time for all of the fresh concrete to exit the funnel is recorded as a measure of filling ability. Koehler and Fowler (2003) recommend that for SCC, the flow time should be less than 10 seconds.

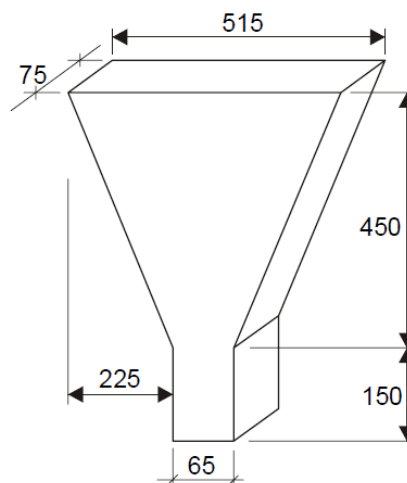


Figure 4-3: Typical image and dimensions of the V-funnel (De Schutter 2005).

4.4 Formwork System

A modified Domino formwork system was used in the experiments. The standard Domino is designed to withstand a maximum pressures of 60 kPa, however due to the investigation involving

high casting rates the system was reinforced to withstand maximum pressures of 100 KPa. The formwork system consisted of a lightweight panel formwork made of red-coated steel and 21 mm thick plywood with form lining (steel components are red powder-coated and aluminium elements are yellow, as shown in Figure 4-4. The configuration of the formwork for the vertical wall element was 5.4 m high, the width of the wall was 2.0 m and the wall thickness was 0.25 m, as shown in Figure 4-5.

The formwork system was designed and constructed by PERI formwork systems. Because South Africa does not have any nationally accepted guidelines and standards for the design of formwork systems involving the lateral pressures exerted by SCC, international standards were used to design the formwork of the wall element that was tested. The international design codes implemented to predict the exerted lateral pressure were the CIRIA Report 108, (1985), DIN 18218: 2010-01, (2010), Section 8.2.3.2 concrete pressure of the BS EN 12812, (2008) and imposed loads of section 17.4.2 of the BS 5975 (2008). See Appendix C for the technical drawing of the experimental wall element, with all the dimensions and associated views.



Figure 4-4: Lightweight steel formwork panels.



Figure 4-5: The 5.4 m high experimental wall element.



Figure 4-6: The DRS alignment coupler (left) and rigid tie (right).

The basic equipment includes the panels, corner and stop-end formwork elements as well as length compensations and scaffold brackets. The DRS alignment couplers were used for standard joints, external and internal corners, obtuse and acute-angled corners, and all connections. Because of their integrated inset tie points, the panels can be used in both a vertical and horizontal positions. The construction process of the experimental wall is shown in Figure 4-7.



Figure 4-7: The construction process of the modified Domino formwork system.

The formwork panels used to construct the experimental wall consisted of plywood with a film-faced coating of about 200 g/m^2 on both sides of the panel, shown in Figure 4-7. The formwork lining is placed in the metal frames to protect the edges and is riveted to the frames, and the joint between the lining and form is elastically sealed. Smooth film-coated non-absorbent formwork panels were used for the lining. A wall inlet and shut-off valve, as shown in Figures 4-8 and 4-9 was

designed and constructed by PERI formwork systems, so that the SCC could be pumped from the base of the experimental wall element by using the CIFA S8 Series PC 907 portable pump.



Figure 4-8: The wall inlet and shut-off valve.

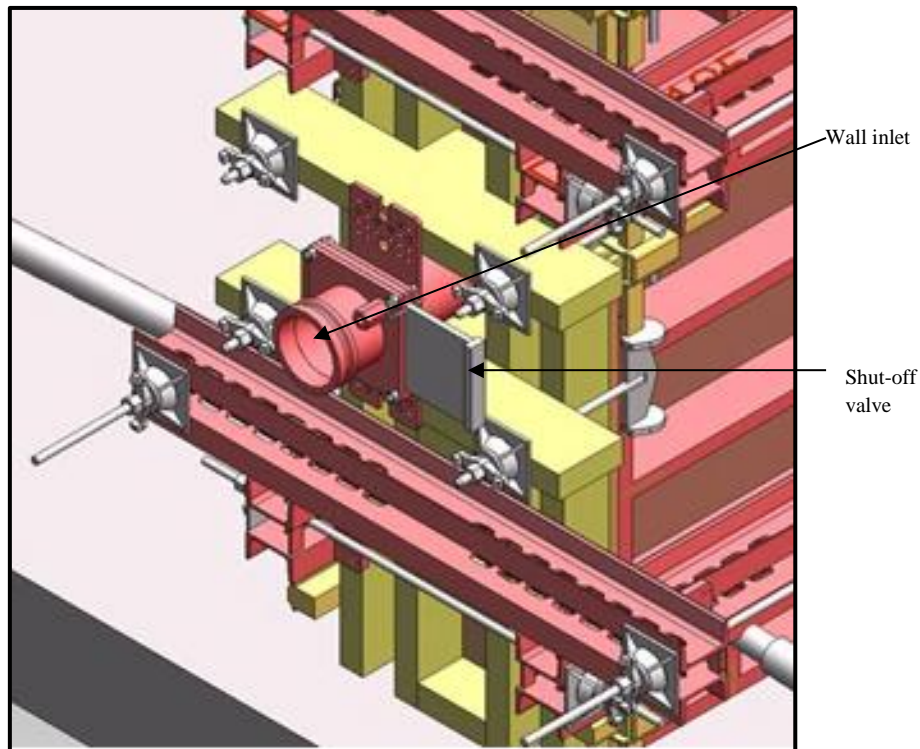


Figure 4-9: A 3D Autocad design drawing of the wall inlet and shut-off value.

4.5 Experimental Procedure

4.5.1 Experimental Set-up and Management

Due to the scope of the investigation various parties were involved; therefore it was necessary that various management procedures were implemented so that the investigation could be performed. During the early stages of the investigation communication strategies were outlined. Co-ordination,

management, and delegation of responsibility were implemented so that each of the stakeholders knew what needed to be done in order to move the project forward. The different parties included the formwork designer, the construction site manager, and the concrete supplier and pump subcontractor.

Before the experiments could be performed on site to gather the data on the lateral pressure exerted by the SCC (Agilia Vertical), the eight flush diaphragm pressure transducers described in Section 3.2.1 were greased to protect the transducers' diaphragm from the fresh concrete. After the transducers had been greased, they were inserted into PVC adaptors mounted into the formwork panels, as shown in Figure 4-10.



Figure 4-10: Flush diaphragm transducer mounted in the PVC jacket.

Each of the eight flush diaphragm pressure transducers was inserted into one of the eight PVC adaptors which were mounted at predetermined heights and in a specific layout, shown in Figure 4-11. The heights were chosen specifically so that the best possible lateral pressure profile could be provided when measured and monitored. The layout of the pressure transducers was selected so that pressure transducers could be placed as close as possible to the centre of the formwork system, as well as placing two transducers at the base of the formwork system.

This pressure transducer arrangement was chosen so that an accurate lateral pressure exerted could be monitored and documented. The reason for the two pressure transducers at the base was to act as a failsafe in the event of one pressure transducer malfunctioning as a result of the high lateral pressures predicted.

Once the pressure transducers were inserted into their appropriate locations the XR5-SE data logger was set-up and connected to the external 24 v dc power supply. The LogXR software which accompanied the data logger was used in the investigation. Each of the eight pressure transducers

was connected to one of the eight communication ports located on the data logger and each communication channel was set up to monitor the exerted lateral pressure.

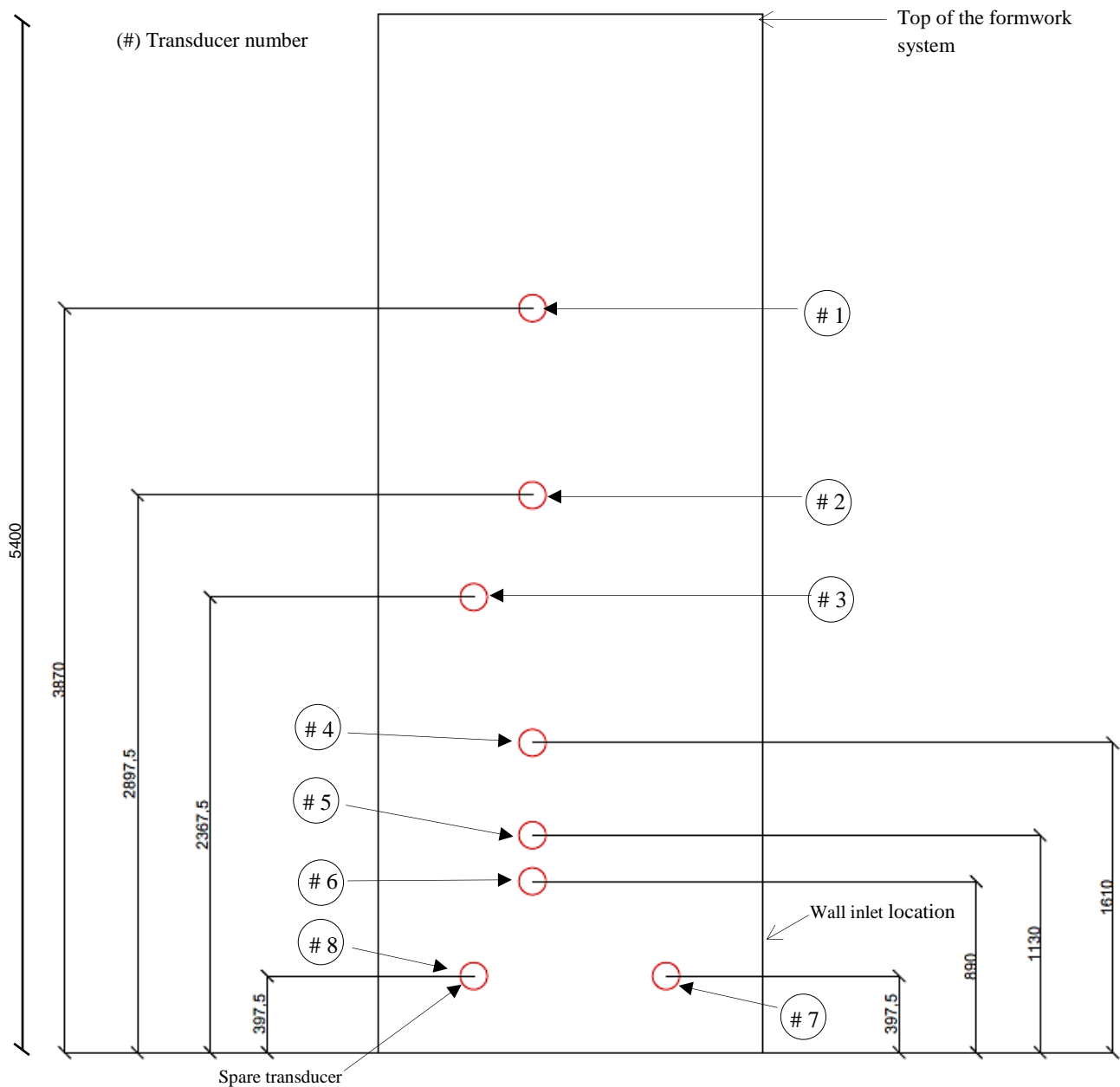


Figure 4-11 Drawing of the pressure transducer heights and layout (mm)

Due to the high cost of the formwork system, only one wall was constructed for the experiment. Once the experiment had been completed, the concrete was expelled from the formwork system by using an outlet located on the side of the experimental wall element. Once most of the concrete had been removed from the wall element, the formwork panels located on the side of the wall were removed and the remaining concrete was scooped out. After all the concrete had been removed, the inside of the formwork system was cleaned and the side panels replaced and fixed into their original

locations. PERI formwork systems then checked that the panels were sealed and that the wall element was safe.

4.5.2 Top-down Casting Experiments

Two different experimental setups were executed to measure the lateral pressure. The first set of tests was set up to pump the SCC (Agilia Vertical) from the top of the formwork system and implement two different casting procedures (continuous casting and interrupting casting with two different predetermined waiting periods) were implemented.

The SCC was pumped with the use of truck-mounted concrete boom pumps, as discussed in Sections 3.3.1 and 3.3.2. For the experiment performed on the first wall element, the CIFA K31L concrete boom pump was used, and for the second and third wall elements the Putzmeister 36Z-Meter concrete boom pump was used. The truck-mounted concrete boom pump was placed near the wall element and the boom pump arm was extended to reach the top of the formwork system, as shown in Figure 4-12. The reason for the change in the pump was, because the pumping equipment was the available equipment from the pumping contractor. Refer to Table 4-3 for the summary of the experimental casting for Walls 1 to 3.

Table 4-3: Summary of the experimental casting for Walls 1 to 3.

Wall	Casting Rate (m/h)	Pump type	Pump setting (rpms)
1	80	CIFA K31L	700
2	27	Putzmeister 36Z-Meter	1000
3	27	Putzmeister 36Z-Meter	1000

After the boom pump arm was extended to reach the top of the formwork system, the vertically hanging delivery pipe was placed within the wall element to pump the SCC into the wall element, shown in Figure 4-13 (left). Once the boom pump had been completely setup, the concrete truck was positioned to feed the SCC into the hopper of the boom pump, shown in Figure 4-13 (right).



Figure 4-12: Extended CIFA K31L boom pump arm.

Before the start of each of the three experiments, samples of the SCC were taken for the purpose of making cubes to test the compressive strength of the SCC, and the ambient temperature was recorded. The temperature, slump flow and filling ability of the SCC were measured, with the aid of a technician provided by Lafarge. A theoretical wet density of 2114 kg/m^3 was measured in Lafarge's laboratory. See Table 4-4 for a summary of all the concrete properties recorded throughout the duration of the top-down experiments.



Figure 4-13: The end hose placed within the wall element (left), Agilia Vertical concrete being placed into the wall element (right).

Wall 1

The first wall element was tested in late May, 2017 in the morning at 10:00 am (test ID: SCC-TP-R80). The SCC used in the experiment arrived at 10:45 am from the concrete plant located nearby. Before the start of the test at 10:50 am an ambient temperature of 22°C and a concrete temperature of 25°C were documented. A slump flow of 615 mm and from the V-funnel test, a time of 9 seconds were measured and recorded by the laboratory technician. Samples were also collected and placed into moulds, and from these samples the average 7 day and 28 day compressive strengths namely, 63 MPa and 73 MPa, were determined.

The casting session started at 11:15 am and the SCC was cast at a constant rate of 80 m/h into the wall element. This was done by the pump operator, who set the CIFA K31L concrete boom pump to cast at 700 rpms. As the SCC was pumped into the formwork wall element, a stop watch was used to monitor the time it took to fill the formwork wall element. The time to fill the wall element completely was 4 minutes. At the end of the casting session the wall and boom pump were cleaned and the wall was set up. During casting the Pressure Transducer #1 (see Figure 4- 11) had stopped measuring; it was found that the connection between the data logger and the transducer had been severed. The wire was reattached for Walls 2 and 3. The casting of the second and third wall elements tests were to be done on the same day as the first wall element but, as a result of issues on site and political demonstrations which occurred on the main road leading to the location of the experiment, this could not be done.

The second and third wall elements were cast in the same way as the first wall element; however the casting process was periodically interrupted, and a waiting period was implemented each time the casting was halted. Because the second and the third wall elements were cast on a different day to casting of the first wall element, a different boom pump was available to cast the SCC (Agilia Vertical).

Wall 2

The setting up of the second wall element occurred on the 19th June, 2017 at 11:00 am (test ID: SCC-TP-WP10-R27). The SCC arrived at 11:30 am from the plant and at 11:40 am an ambient temperature of 21.6°C and a concrete temperature of 21.3°C were recorded before testing. A slump flow of 620 mm and a V-funnel test time of 10 seconds were documented at Lafarge's concrete plant. An average 7 day and 28 day compressive strengths of 60.7 MPa and 68 MPa were recorded by the laboratory technician at Lafarge's concrete plant.

The casting session started at 11:55 am and the SCC was cast at an average rate of 27 m/h by setting the Putzmeister 36Z-Meter Truck-Mounted Concrete Boom Pump to cast at 1000 rpms. The casting of the concrete was interrupted three times and a waiting period of 10 minutes was implemented between each of the casting periods. The first interruption of the casting occurred after 1 minute of casting, the second after 2 minutes of casting and the third after 3 minutes of casting. Once the test had been completed the wall and pump were cleaned and set up for the third wall. During the casting, the Pressure Transducer #1 failed once again and was removed from the system and the investigation. The PVC adaptor used to house the transducer was then sealed to prevent the fresh concrete from leaking out of the formwork system.

Wall 3

On the same day as the second wall at 1:00 pm the third wall element was prepared for testing (test ID: SCC-TP-WP15-R27). The SCC arrived at from the plant at 1:30 pm and at 1:40 pm an ambient temperature of 17.8°C and a concrete temperature of 21.8°C were recorded. At the concrete plant, a slump flow of 615 mm and a V-funnel test time of nine seconds were measured and documented. Average 7 day and 28 day compressive strengths of 60.3 MPa and 69.7 MPa were recorded by the laboratory technician at Lafarge's concrete plant.

The casting session started at 2:00 pm and the SCC was pumped at an average casting rate of 27 m/h; this was done by setting the Putzmeister 36Z-Meter Truck-Mounted Concrete Boom Pump to cast at 1000 rpms. The casting of the concrete was interrupted twice and a waiting period of 15 minutes was implemented between the casting periods. The first interruption of the casting occurred after 1 minute of casting and the second after two minutes of casting. At the end of the test the wall and pump were cleaned and set up for the next set of tests.

4.5.3 Bottom-up Casting Experiments

The second set of tests was set up to pump the SCC from the base of the formwork and implement three different casting rates (55, 65 and 80 m/h). This was done with the static pump (portable pump), the concrete pump discussed in Section 3.3.3.

The CIFA S8 Series PC 907 portable pump was placed near the wall element and connected by using a series of pipes, shown in Figure 4-14. The pipes were fastened and sealed to the inlet and the shut-off valve located on the wall element, shown in Figure 4-15. Table 4-5 shows the summary of the experimental casting for Walls 4 to 6.

Table 4-4: Summary of concrete properties recorded for Walls 1 to 3.

	Wall 1 (SCC-TP-R80)	Wall 2 (SCC-TP-WP10-R27)	Wall 3 (SCC-TP-WP15-R27)
Ambient temperature (°C)	22	21.6	17.8
Concrete temperature (°C)	25	21.3	21.8
Slump flow (mm)	615	620	615
Fill ability (Viscosity) (seconds)	9	10	9
Theoretical wet density (kg/m ³)	2114	2114	2114
Compressive strength (7 day) (MPa)	63	60.7	60.3
Compressive strength (28 day) (MPa)	73	68	69.7

Table 4-5: Summary of the experimental casting for Walls 4 to 6.

Wall	Casting Rate (m/h)	Pump type	Pump setting (rpms)
4	65	CIFA S8 Series PC 907	1500
5	80	CIFA S8 Series PC 907	1800
6	55	CIFA S8 Series PC 907	1300



Figure 4-14: The CIFA S8 Series PC 907 Portable Pump set up near the wall.



Figure 4-15: The pipe from the pump connecting the wall element inlet.

Just as with the first set of tests, samples were taken before each of the three casting sessions for the purpose of making cubes to test the compressive strength of the SCC (Agilia Vertical). The ambient temperature was measured and recorded, as well as the temperature, slump flow and filling ability of the SCC. See Table 4-6 for a summary of all the concrete properties recorded throughout the duration of the bottom-up experiments.

Wall 4

On the 21th June, 2017, early in the morning at 9:00 am the fourth wall element was prepared for testing (test ID: SCC-BP-R65). The SCC needed for the experiment arrived at 9:45 am from the nearby concrete plant. At 10 am an ambient temperature of 10.8°C and a concrete temperature of 19.3°C were recorded, before the experiment commenced. A slump flow of 615 mm and a V-funnel

test time of 11 seconds were measured and recorded at the concrete plant, before the SCC was delivered to the location of the experiment. Samples were also collected at the concrete plant and average 7 day and 28 day compressive strengths of 64 MPa and 76.5 MPa were recorded by the laboratory technician at Lafarge's concrete plant.

The casting session started at 10:15 am and the SCC was cast at a constant rate of 65 m/h, which was done with the aid of the pump operator by setting the CIFA S8 Series PC 907 Portable Pump to cast at 1500 rpms. A stop watch was used to record the time it took for the SCC to fill the formwork wall element. The time recorded to fill the wall element completely was recorded to be 5 minutes. Once the casting session had been completed the wall and pump were cleaned and set up for the fifth wall.

Wall 5

On the same day as the fourth wall, at 11:30 am the fifth wall element was prepared for testing (test ID: SCC-BP-R80). The SCC arrived at 12:15 am from the concrete plant and at 12:30 pm an ambient temperature of 27.5°C and a concrete temperature of 19°C were recorded before testing. Before the concrete was delivered to the location of the experiment a slump flow of 620 mm and a time of 9 seconds for the V-funnel test were recorded. Samples were then collected and average 7 day and 28 day compressive strengths of 66 MPa and 78.5 MPa were recorded by the laboratory technician at Lafarge's concrete plant.

The casting session started at 12:45 pm and the SCC was cast at a constant rate of 80 m/h by setting the CIFA S8 Series PC 907 Portable Pump to cast at 1800 rpms. A stop watch was used to record the time it took for the SCC to fill the formwork wall element. The time recorded to fill the wall element completely was recorded to be 4 minutes. At the end of the casting session the wall and pump were cleaned and set up for the final wall.

Wall 6

The final wall element (Wall 6) was prepared for testing in the afternoon at 1:20 pm (test ID: SCC-BP-R55). SCC arrived on site at 1:50 pm. An ambient temperature of 26.5°C and a concrete temperature of 20°C were recorded at about 2:00 pm. The slump flow of 610 mm and a V- funnel test time of 10 seconds were again measured at the concrete plant, and average 7 day and 28 day compressive strengths of 65 MPa and 73.7 MPa were determined by the laboratory technician at Lafarge's concrete plant.

The casting session started at 2:15 pm and the SCC was cast at a constant rate of 55 m/h by setting the CIFA S8 Series PC 907 Portable Pump to cast at 1300 rpms. A stop watch was used to record

the time it took for the SCC to fill the formwork wall element. The time recorded to fill the wall element completely was recorded to be 6 minutes. At the end of the casting session the pump was cleaned and the wall formwork element was disassembled.

Table 4-6: Summary of concrete properties recorded for Walls 4 to 6.

	Wall 4 (SCC-BP-R65)	Wall 5 (SCC-BP-R80)	Wall 6 (SCC-BP-R55)
Ambient temperature (°C)	10.8	27.5	26.5
Concrete temperature (°C)	19.3	19	20
Slump flow (mm)	615	620	610
Fill ability (Viscosity) (seconds)	11	9	10
Theoretical wet density (kg/m ³)	2114	2114	2114
Compressive strength (7 day) (MPa)	64	66	65
Compressive strength (28 day) (MPa)	76.5	78.5	73.7

4.6 Conclusion

This chapter covered the experimental methodology to acquire the lateral pressure exerted by the SCC (Agilia Vertical) on the prepared formwork element. The experimental investigation included a setup to measure the lateral pressure exerted when the SCC is pumped from the top of the formwork system by using the Putzmeister 36Z-Meter and CIFA K31L truck-mounted concrete boom pumps.

A constant casting process and also a process in which the cast was interrupted were covered. The lateral pressure was measured from the SCC pumped from the base of the formwork system at various casting rates. Whilst the lateral pressures in the literature were recorded at much lower casting rates, the minimum casting rates for these walls were determined by the minimum pump setting. The test methods which were used to obtain the concrete properties of the SCC are

highlighted. This included the compressive strength test, slump flow test, and the V-funnel test. The preparation, testing and any issues encountered for each of the walls are documented in this chapter. Chapter 5 discusses and explains the results obtained from results of this experimental methodology.

Chapter 5 : Experimental Results

5.1 Introduction

In this chapter the results obtained from the experiments on six wall elements are discussed. The first section covers the data obtained from the first set of tests by illustrating the lateral pressure profiles for Walls 1 to 3, which were cast from the top of the formwork system. The second section covers the lateral pressure profiles for Walls 4 to 6, in which the Self-Compacting Concrete (SCC) was pumped from the base of the wall elements. The third part of the chapter covers the comparison of the results of the investigation with one another and discusses the observations made. Figure 5-1 shows an overview of Chapter 5.

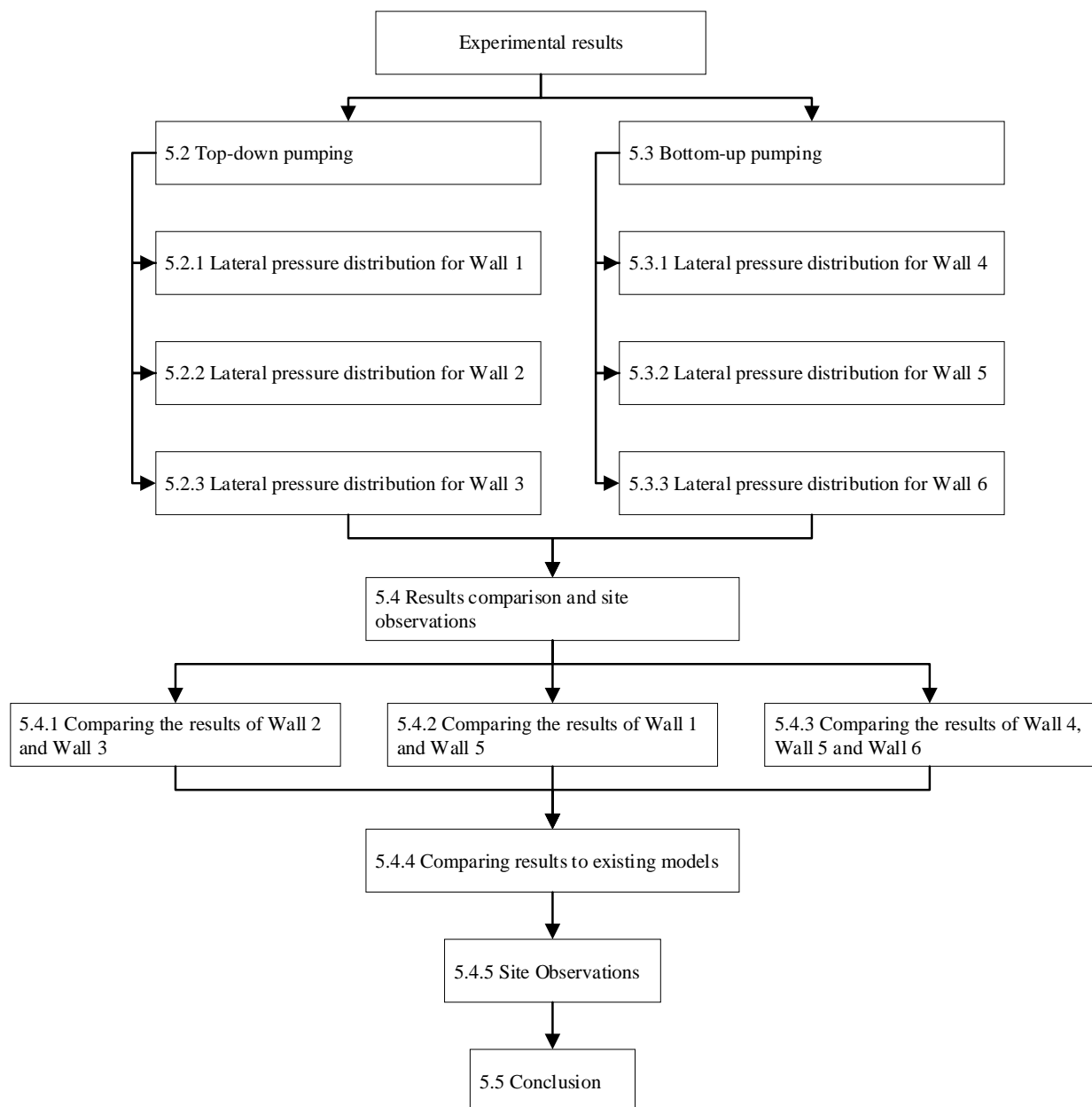


Figure 5-1: Overview and layout of Chapter 5.

5.2 Top-down Pumping

Sections 5.2.1 to 5.2.3, shown in Figure 5-2, cover the lateral pressure obtained when the SCC was pumped from the top (TP) of the formwork system at a constant casting rate (R) of 80 m/h and an interruption of the average casting rate of 27 m/h with 10 and 15 minutes waiting periods (WP). The lateral pressure profiles are shown in Figures 5-2, 5-9, and 5-11. It shows the pressures at various casting heights namely, 2.2, 2.6, 3.0, 3.4, 3.8, 4.2, 4.6, 5.0 and 5.4 m, in order to compare the exerted lateral pressure exerted on the formwork to the hydrostatic pressures at the specified heights.

5.2.1 Lateral Pressure Distribution for Wall 1

This section discusses the results recorded and observations made from the experiment performed on the 21st May, 2017 (SCC-TP-R80). The lateral pressure profile shown in Figure 5-2 was obtained from a casting rate of 80 m/h and using top-down placement method (casting from the top of the formwork system with a boom pump). See Appendix D for a tabulated summary of the results measured.

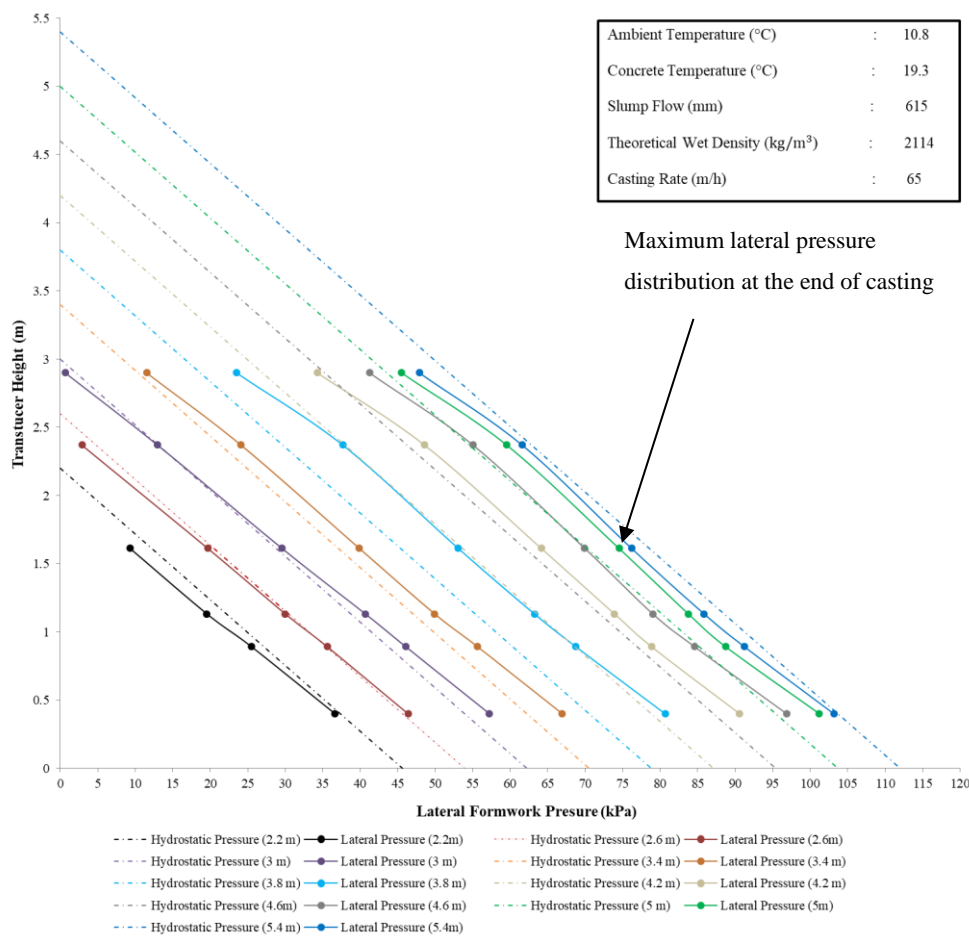


Figure 5-2: Lateral pressure profile at various casting heights during casting for Wall 1 (SCC-TP-R80).

Casting Height of 2.2 Meter

As can be seen in Figure 5-2, when the SCC reached the height of 2.2 m from the base, the lateral formwork pressure was below the theoretical hydrostatic pressure. The maximum lateral formwork pressure measured near the base of the formwork system (0.398 m from the base) by Transducer 7, showed 73.4 % of hydrostatic pressure ($K_0 = P_{(maximum @ 2.2 m)} / P_{(hydrostatic @ 2.2 m)}$) between the maximum measured pressure ($P_{(maximum @ 2.2 m)}$) and the theoretical hydrostatic pressure ($P_{(hydrostatic @ 2.2 m)}$). The pressure measured by Transducer 6 (0.890 m from the base), Transducer 5 (1.13 m from the base) and Transducer 4 (1.61 m from the base) showed a K_0 of 56.1 %, 43.9% and 1% between the measured pressure and the theoretical hydrostatic pressure, as shown in Figure 5-3.

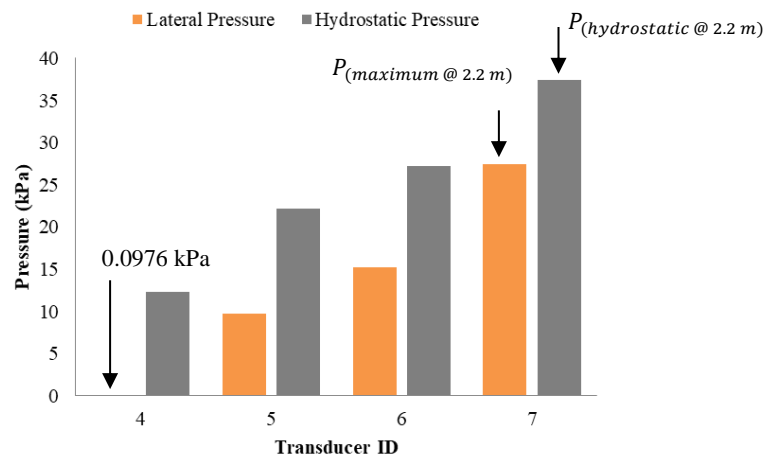


Figure 5-3: Pressure comparison at a casting height of 2.2 m for Wall 1 (SCC-TP-R80).

Casting Height of 2.6 Meter

At the casting height of 2.6 m, the lateral formwork pressure (indicated by the solid red line shown in Figure 5-2) was below the theoretical hydrostatic pressure (indicated by the dashed red line). The maximum lateral pressure measured near the base of the experimental wall element by Transducer 7, showed 82.9 % of hydrostatic pressure ($K_0 = P_{(maximum @ 2.6 m)} / P_{(hydrostatic @ 2.6 m)}$) between the measured pressure ($P_{(maximum @ 2.6 m)}$) and the theoretical hydrostatic pressure ($P_{(hydrostatic @ 2.6 m)}$). The pressure measured by Transducer 6, Transducer 5 and Transducer 4 showed a K_0 of 75.4 %, 71.1 % and 51.1 % between the measured pressure and the theoretical hydrostatic pressure, shown in Figure 5-4.

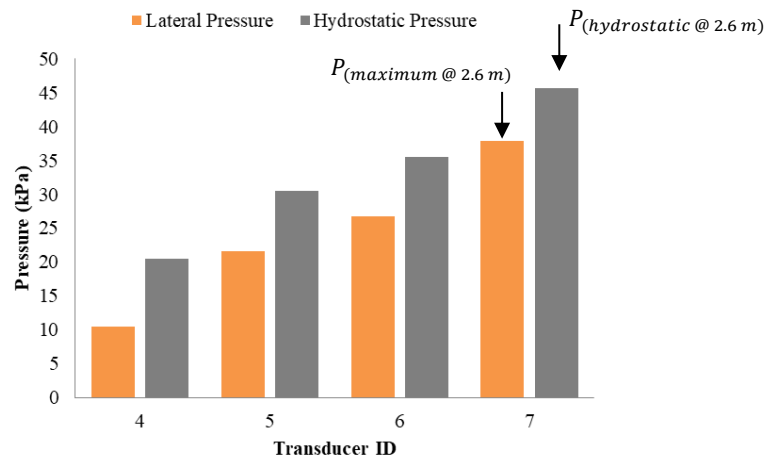


Figure 5-4: Pressure comparison at the casting height of 2.6 m for Wall 1 (SCC-TP-R80).

Casting Height of 3 Meter

The lateral pressure at the casting height of 3 m was below the theoretical hydrostatic pressure. The lateral pressure measured near the base of the experimental wall (0.398 m from the base) by Transducer 7, showed 91 % of hydrostatic pressure ($K_0 = P_{(maximum @ 3 m)} / P_{(hydrostatic @ 3 m)}$) between the measured pressure ($P_{(maximum @ 3 m)}$) and the theoretical hydrostatic pressure ($P_{(hydrostatic @ 3 m)}$). The pressure measured by Transducer 6 (0.890 m from the base), Transducer 5 (1.13 m from the base), Transducer 4 (1.61 meters from the base), Transducer 3 (2.368 m from the base) and Transducer 2 (2.898 meters from the base) showed a K_0 of 86.7 %, 84.8 %, 74.3 %, 36.9 % and 2.9 % between the measured pressure and the theoretical hydrostatic pressure, shown in Figure 5-5.

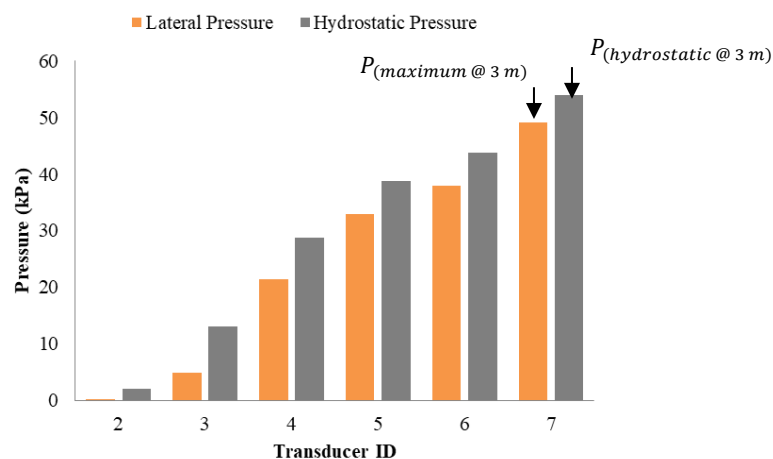


Figure 5-5: Pressure comparison at the casting height of 3 m for Wall 1 (SCC-TP-R80).

Casting Height of 3.4 Meter

At 3.4 m from the base, the lateral formwork pressure was below the theoretical hydrostatic pressure. The maximum lateral pressure measured near the base of the wall by Transducer 7, showed 96.1 % of hydrostatic pressure ($K_0 = P_{(maximum @ 3.4 m)} / P_{(hydrostatic @ 3.4m)}$) between the measured pressure ($P_{(maximum @ 3.4 m)}$) and the theoretical hydrostatic pressure ($P_{(hydrostatic @ 3.4 m)}$). The pressure measured by Transducer 6, Transducer 5, Transducer 4, Transducer 3 and Transducer 2 showed a K_0 of 93 %, 93.4 %, 87.1 %, 73.9% and 33.7 % between the measured pressure and the theoretical hydrostatic pressure, shown in Figure 5-6.

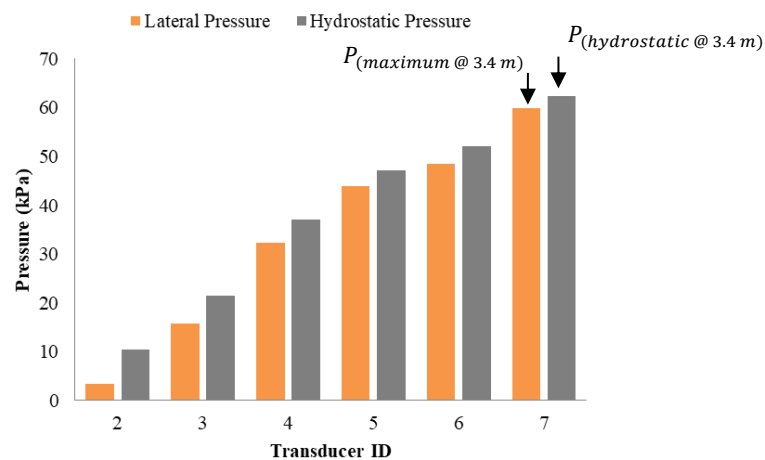


Figure 5-6: Pressure comparison at the casting height of 3.4 m for Wall 1 (SCC-TP-R80).

Casting Height of 3.8 Meter

At the casting height of 3.8 m, the lateral pressure distribution was below the theoretical hydrostatic pressure. The lateral pressure measured near the base of the experimental wall by Transducer 7, showed 97.1 % of hydrostatic pressure ($K_0 = P_{(maximum @ 3.8 m)} / P_{(hydrostatic @ 3.8m)}$) between the measured pressure ($P_{(maximum @ 3.8 m)}$) and the theoretical hydrostatic pressure ($P_{(hydrostatic @ 3.8 m)}$). The pressure measured by Transducer 6, Transducer 5, Transducer 4, Transducer 3 and Transducer 2 showed a K_0 of 93.9 %, 93.1 %, 88.3 %, 77.5 % and 59.5 % between the measured pressure and the theoretical hydrostatic pressure, shown in Figure 5-7.

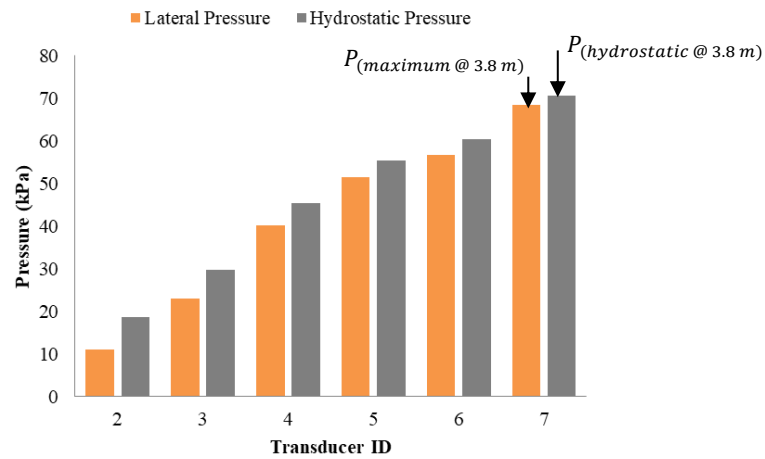


Figure 5-7: Pressure comparison at the casting height of 3.8 m for Wall 1 (SCC-TP-R80).

Casting Height of 4.2 to 5.4 Meter

At 4.2 m, 4.6 m, 5 m and 5.4 m from the base of the wall, the lateral formwork pressures measured were slightly above the theoretical hydrostatic level (indicated by the dashed brown line for 4.2 m, a dashed grey line for 4.6 m, a dashed green line for 5 m and dashed blue line for 5.4 m). The variation of the pressure values for the casting height of 4.2 m are shown in Figure 5-8 (a), for the casting height of 4.6 m the pressures are shown in Figure 5-8 (b), for the casting height of 5 m the pressures are shown in Figure 5-8 (c) and for the casting height of 5.4 m the pressures are shown in Figure 5-8 (d). Refer to Table 5-1 for a summary of the percentage hydrostatic for each transducer at the various casting heights.

Table 5-1: Percentage hydrostatic (K_0) for the casting heights of 4.2 m to 5.4 m for Wall 1 (SCC-TP-R80).

Transducer	Height from the base (m)	Casting Heights (m)			
		4.2	4.6	5	5.4
2	2.898	83.6	91.3	97.3	93.1
3	2.368	89.4	94.6	100	96.5
4	1.61	96.9	97.1	102	98.2
5	1.13	100	100	103	100
6	0.890	100	100	103	100
7	0.398	101	101	102	101

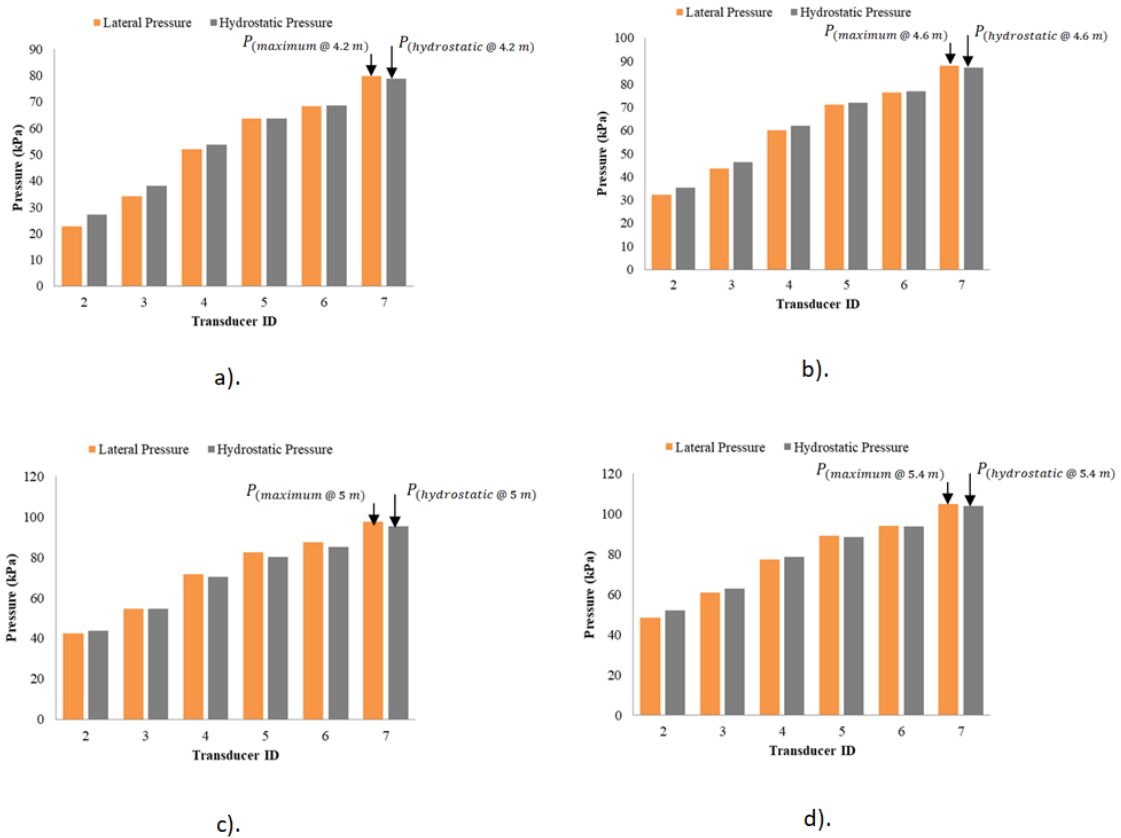


Figure 5-8: Pressure comparison at the casting height of 4.2m to 5.4 m for Wall 1 (SCC-TP-R80).

From the experiment (SCC-TP-R80) it was observed that the maximum lateral pressure ($P_{(maximum @ 5.4 m)}$) at the end of casting is approximately equal to the theoretical hydrostatic pressure ($P_{(hydrostatic @ 5.4 m)}$). From the test it was found that the lateral pressure was below the theoretical hydrostatic pressure up to a casting height of 3.8 m. From Figure 5-2 it can be seen that the lateral pressure distribution steadily approaches and even slightly exceeds hydrostatic pressures as the fresh concrete rises in the wall element.

5.2.2 Lateral Pressure Distribution for Wall 2

The section covers the results recorded from the experiment performed on the 19th June, 2017 (SCC-TP-WP10-R27). The lateral pressure profile as shown in Figure 5-9 was created from the measured lateral formwork pressure exerted by the tested SCC at an average casting rate of 27 m/h, using a top-down placement method, and implementing three waiting periods of 10 minutes each. See Appendix E for a tabulated summary of the results measured.

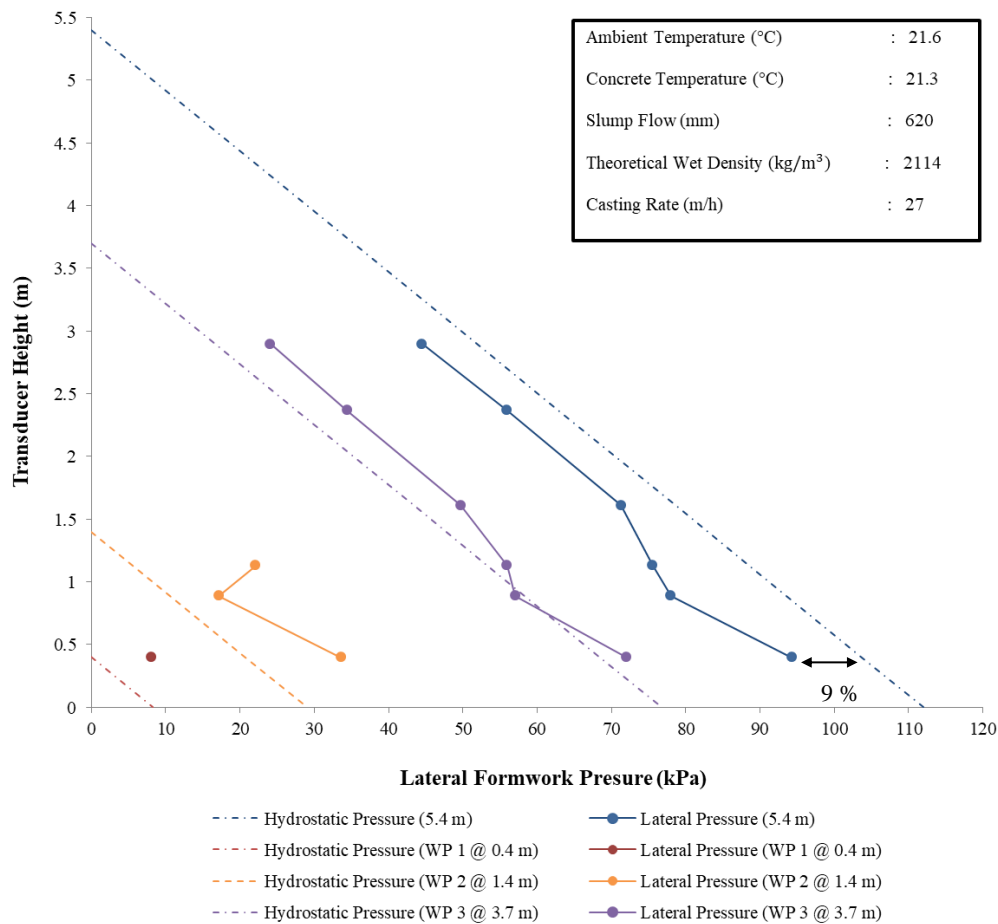


Figure 5-9: Maximum lateral pressure profile at end of casting for Wall 2 (SCC-TP-WP10-R27).

Waiting Period 1 to 3

The lateral pressure when the first, second and third waiting periods was implemented was above the theoretical hydrostatic level. It can be seen in Figure 5-9 that with each successive break in the casting season, the lateral pressure exerted by the SCC would approach the theoretical hydrostatic level. These values shown in Figure 5-9 were recorded at the end of each waiting period. These values were practically the same as the readings recorded at the start of each waiting period.

End of Casting

The lateral pressure at the casting height of 5.4 meters at the end of casting was below the theoretical hydrostatic level. The maximum pressure measured near the base of the experimental wall element by Transducer 7, showed 90.9 % of hydrostatic pressure ($K_0 = P_{(maximum @ 5.4 m)} / P_{(hydrostatic @ 5.4 m)}$) between the measured pressure and the theoretical hydrostatic pressure ($P_{(hydrostatic @ 5 m)}$). The pressure measured by Transducer 6, Transducer 5, Transducer 4, Transducer 3 and Transducer 2 showed a K_0 of 83.4 %, 85.3 %, 90.7 %, 88.9 % and 85.8 % between the measured pressure and the theoretical hydrostatic pressure, shown in Figure 5-10.

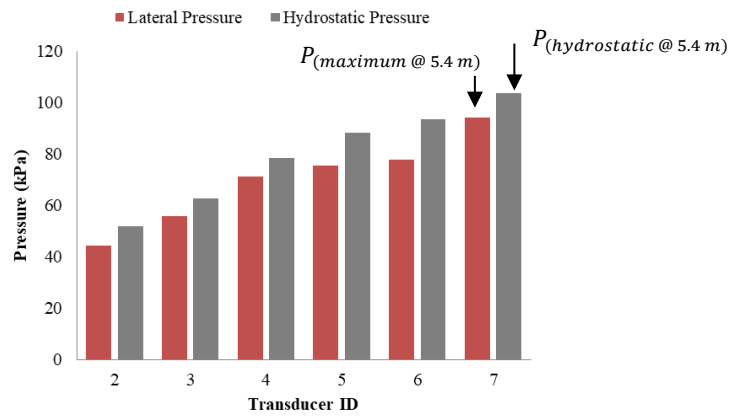


Figure 5-10: Pressure comparison at the end of casting for Wall 2 (SCC-TP-WP10-R27).

Found from the test on Wall 2 (SCC-TP-WP10-R27) it was observed that the maximum lateral pressure ($P_{(maximum @ 5.4 m)}$) at the end of casting was lower than the theoretical hydrostatic pressure ($P_{(hydrostatic @ 5.4 m)}$). However when waiting period 1, 2 and 3 were implemented the maximum lateral pressure was above the theoretical hydrostatic pressure.

5.2.3 Lateral Pressure Distribution for Wall 3

The following section will discuss the results recorded and observations made from the experiment performed on the 19th June, 2017 (SCC-TP-WP15-R27). The lateral pressure profile shown in Figure 5-11 was created from the measured lateral formwork pressure exerted by the tested SCC at a casting rate of 27 m/h, using a top-down placement method, and implementing two waiting periods of 15 minutes each. See Appendix F for a tabulated summary of the results measured.

Waiting Period 1 to 2

The lateral pressure when the first and second waiting periods were implemented was above the theoretical hydrostatic level. Similarly to the previous test it can be seen in Figure 5-11 that with each successive break in the casting session, the lateral pressure would approach the theoretical hydrostatic level. These values shown in Figure 5-9 were recorded at the end of each waiting period. These values were practically the same as the readings recorded at the start of each waiting period.

End of Casting

The lateral pressure at the casting height of 5.4 m at the end of casting was below the theoretical hydrostatic level. The maximum lateral pressure measured near the base of the wall by Transducer 7, showed 85.6 % of hydrostatic pressure ($K_0 = P_{(maximum @ 5.4 m)} / P_{(hydrostatic @ 5.4 m)}$) between the measured pressure ($P_{(maximum @ 5.4 m)}$) and the theoretical hydrostatic pressure

($P_{(hydrostatic @ 5\text{ m})}$). The pressure measured by Transducer 6, Transducer 5, Transducer 4, Transducer 3 and Transducer 2 showed a K_0 of 82.2 %, 82.3 %, 88.7 %, 88.8 % and 86.7 % between the measured pressure and the theoretical hydrostatic pressure, shown in Figure 5-12.

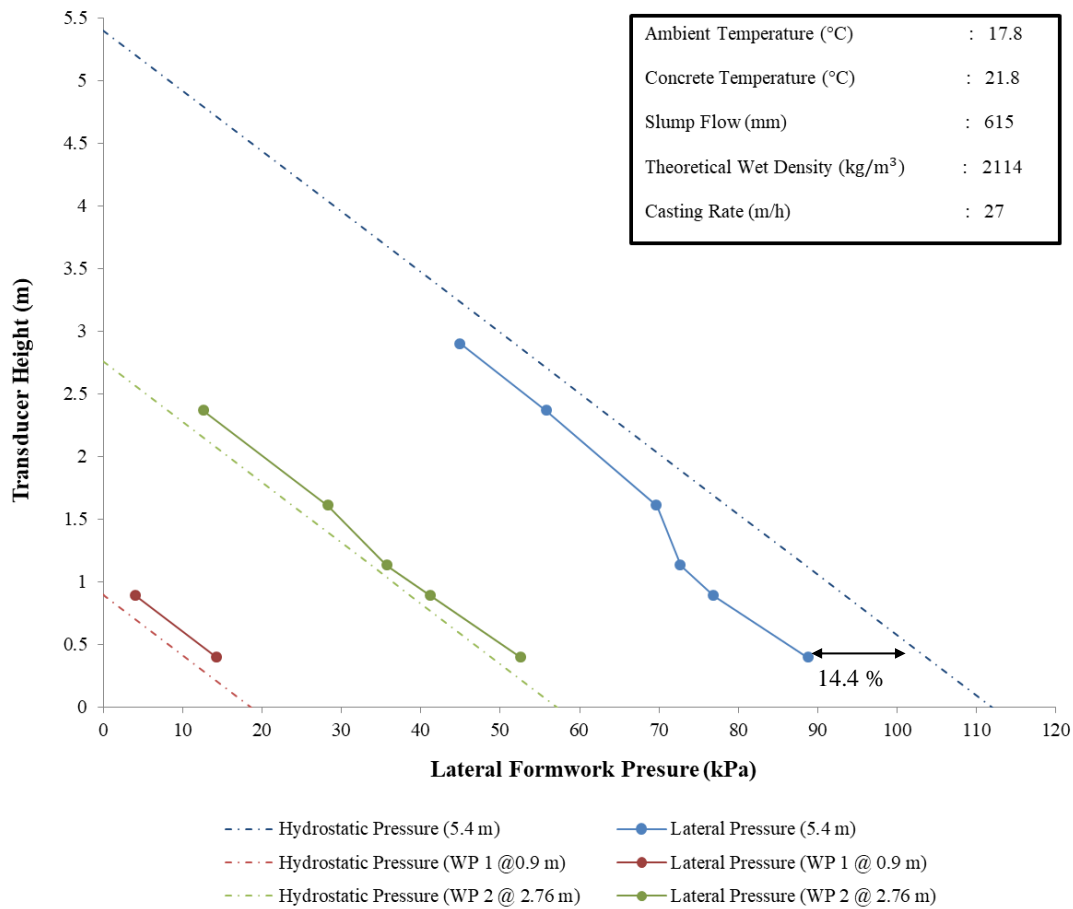


Figure 5-11: Maximum lateral pressure distribution at end of casting for Wall 3 (SCC-TP-WP15-R27).

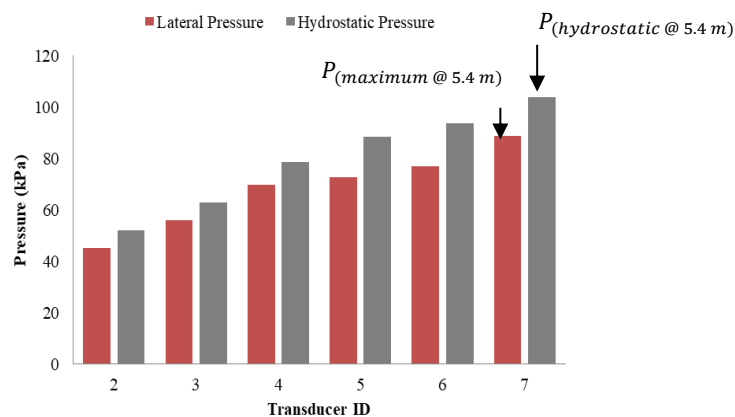


Figure 5-12: Pressure comparison at the end of casting for Wall 3 (SCC-TP-WP15-R27).

Found from the test on Wall 3 (SCC-TP-WP15-R27) it was observed that the maximum lateral pressure ($P_{(maximum @ 5.4\text{ m})}$) at the end of casting was lower than the theoretical hydrostatic

pressure ($P_{(hydrostatic @ 5.4 m)}$). However when waiting period 1 and 2 were implemented the maximum lateral pressure was above the theoretical hydrostatic pressure.

5.3 Bottom-up Pumping

Sections 5.3.1 to 5.3.3, shown in Figure 5-16, covers the results of testing the lateral pressure obtained when the SCC was pumped from the base (BP) of the formwork system at a constant casting rate (R) of 55, 65 and 80 m/h. The lateral pressure profiles are shown in Figures 5-13, 5-20 and 5-27 and show the pressures at various casting heights, namely 2.2, 2.6, 3.0, 3.4, 3.8, 4.2, 4.6, 5.0 and 5.4 m in order to compare the lateral pressure exerted on the formwork to the hydrostatic pressures at the specified heights.

5.3.1 Lateral Pressure Distribution for Wall 4

In the following section the results recorded and observations made from the experiment performed on the 21th June, 2017 will be discussed. The lateral pressure shown in Figure 5-13 was created from the measured lateral formwork pressure exerted by tested SCC at a casting rate of 65 m/h and using the bottom-up placement method (casting from the base of the formwork system by means of a portable pump). See Appendix F for a tabulated summary of the results measured.

Casting Height of 2.2 Meter

As can be seen in Figure 5-13, when the SCC reached the height of 2.2 m from the base, the lateral formwork pressure was slightly below the theoretical hydrostatic pressure. The lateral formwork pressure measured near the base of the wall (0.398 meters from the base) by Transducer 7, showed 98.1 % of hydrostatic pressure ($K_0 = P_{(maximum @ 2.2 m)} / P_{(hydrostatic @ 2.2 m)}$) between the measured pressure ($P_{(maximum @ 2.2 m)}$) and the theoretical hydrostatic pressure ($P_{(hydrostatic @ 2.2 m)}$). The pressure measured by Transducer 6 (0.890 m from the base), Transducer 5 (1.13 m from the base) and Transducer 4 (1.61 m from the base) showed a K_0 of 93.9 %, 88.3 % and 76.4 % between the measured pressure and the theoretical hydrostatic pressure, shown in Figure 5-14.

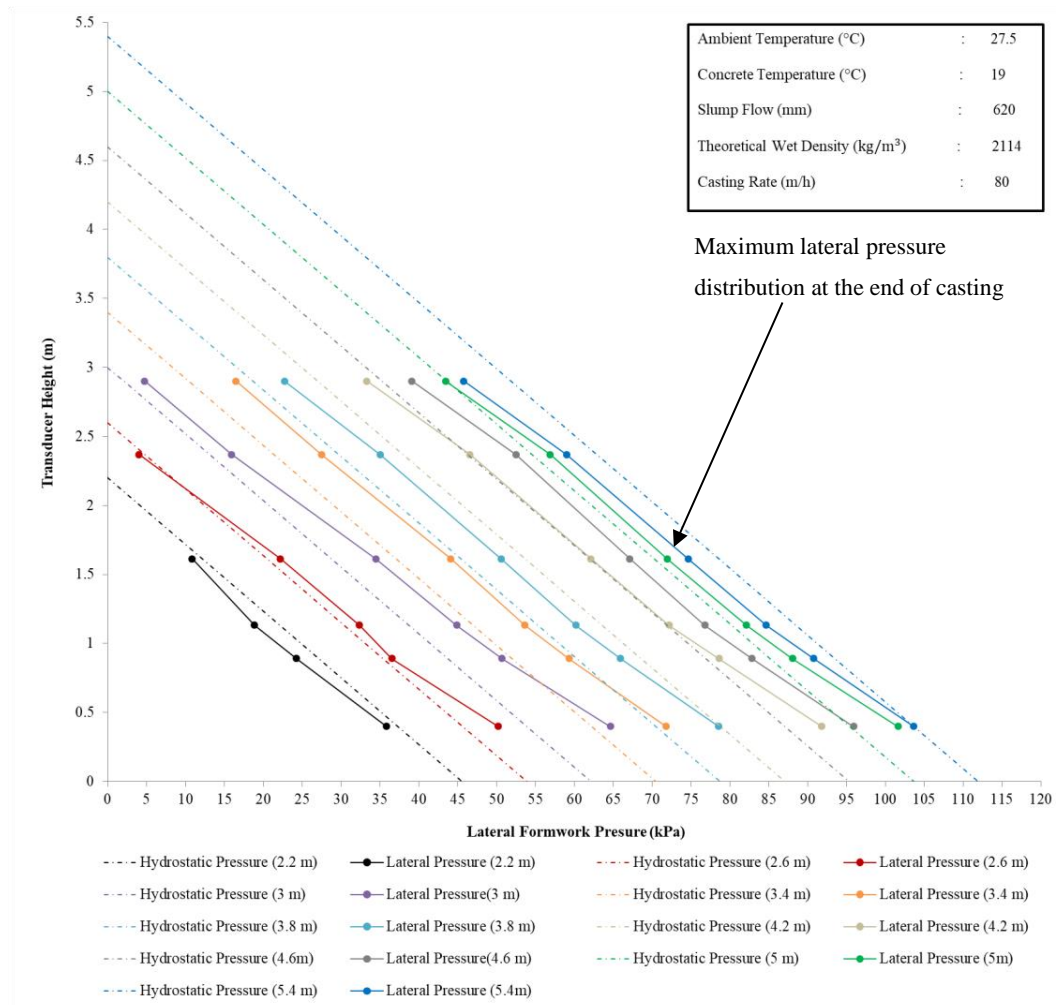


Figure 5-13: Lateral pressure distribution at various heights during casting for Wall 4 (SCC-BP-R65).

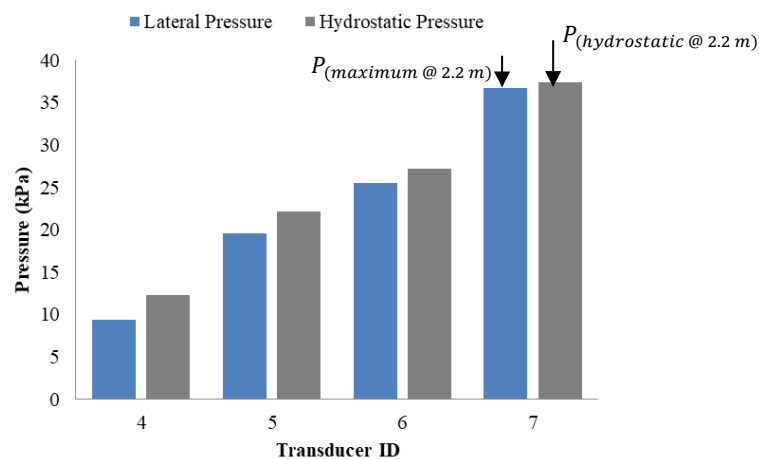


Figure 5-14: Pressure comparison at the casting height of 2.2 m for Wall 4 (SCC-BP-R65).

Casting Height of 2.6 Meter

At the casting height of 2.6 m, the lateral formwork pressure was equal or close to the theoretical hydrostatic pressure. The lateral pressure measured near the base of the wall by Transducer 7,

showed 102 % of hydrostatic pressure ($K_0 = P_{(maximum @ 2.6 m)} / P_{(hydrostatic @ 2.6 m)}$) between the measured pressure ($P_{(maximum @ 2.6 m)}$) and the theoretical hydrostatic pressure ($P_{(hydrostatic @ 2.6 m)}$). The pressure measured by Transducer 6, Transducer 5 and Transducer 4 showed measured pressures equal to the theoretical hydrostatic pressure where Transducer 3 showed a K_0 of 60.5 %, shown in Figure 5-15.

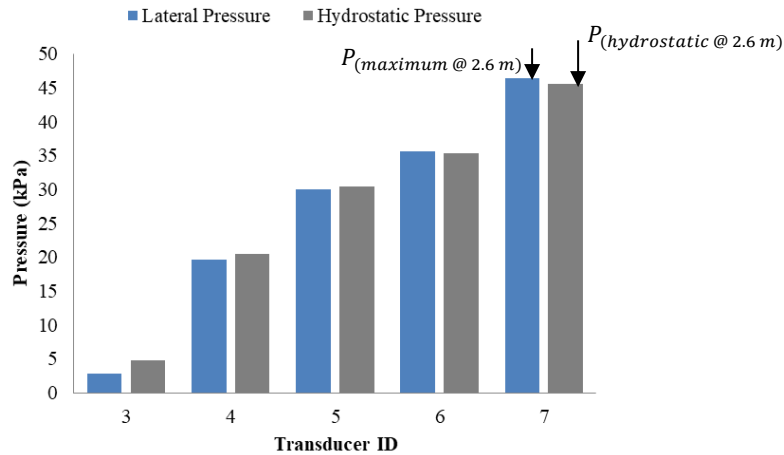


Figure 5-15: Pressure comparison at the casting height of 2.6 m for Wall 4 (SCC-BP-R65).

Casting Height of 3 Meter

The lateral pressure at the casting height of 3 m was above the theoretical hydrostatic pressure. The maximum lateral pressure measured near the base of the wall element (0.398 m from the base) by Transducer 7, showed 106 % of hydrostatic pressure ($K_0 = P_{(maximum @ 3 m)} / P_{(hydrostatic @ 3 m)}$) between the measured pressure ($P_{(maximum @ 3 m)}$) and the theoretical hydrostatic pressure ($P_{(hydrostatic @ 3 m)}$). The pressure measured by Transducer 6 (0.890 m from the base), Transducer 5 (1.13 m from the base) and Transducer 4 (1.61 m from the base) showed a K_0 of 105 %, 105 % and 103 % between the measured pressure and the theoretical hydrostatic pressure. Transducer 3 (2.368 m from the base) showed measured pressures equal to the theoretical hydrostatic pressure, and Transducer 2 (2.898 m from the base) showed a K_0 of 33.4 %, shown in Figure 5-16.

Casting Height of 3.4 Meter

At 3.4 m from the base of the wall, the lateral formwork pressure measured was above to the theoretical hydrostatic pressure. The maximum lateral pressure measured at base of the experimental wall element by Transducer 7, showed 107 % of hydrostatic pressure ($K_0 = P_{(maximum @ 3.4 m)} / P_{(hydrostatic @ 3.4 m)}$) between the measured pressure ($P_{(maximum @ 3.4 m)}$) and the theoretical hydrostatic pressure ($P_{(hydrostatic @ 3.4 m)}$). The pressure measured by

Transducer 6, Transducer 5, Transducer 4, transducer 3 and transducer 2 showed a K_0 of 107 %, 106 %, 108 %, 112 % and 111 % between the measured pressure and the theoretical hydrostatic pressure shown in Figure 5-17.

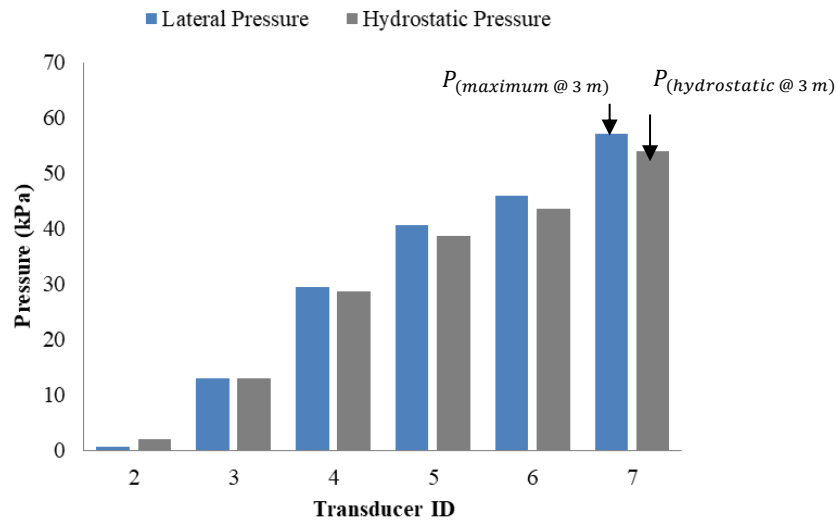


Figure 5-16: Pressure comparison at the casting height of 3 m for Wall 4 (SCC-BP-R65).

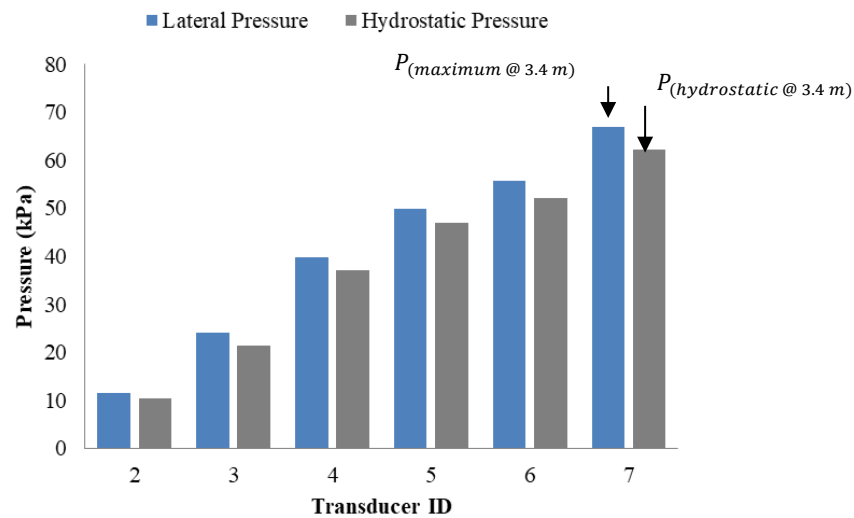


Figure 5-17: Pressure comparison at the casting height of 3.4 m for Wall 4 (SCC-BP-R65).

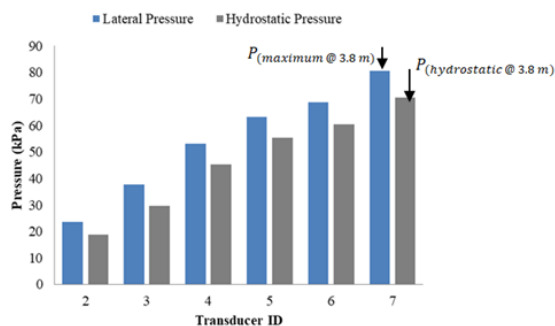
Casting Height of 3.8 to 5.Meter

At 3.8 m, 4.2 m, 4.6 m and 5 m from the base of the wall, the lateral formwork pressures measured were above the theoretical hydrostatic pressure. The variation of the pressure values for the casting height of 3.8 m are shown in Figure 5-18 (a), for the casting height of 4.2 m the pressures are shown in Figure 5-18 (b), for the casting height of 4.6 m the pressures are shown in Figure 5-18 (c) and for

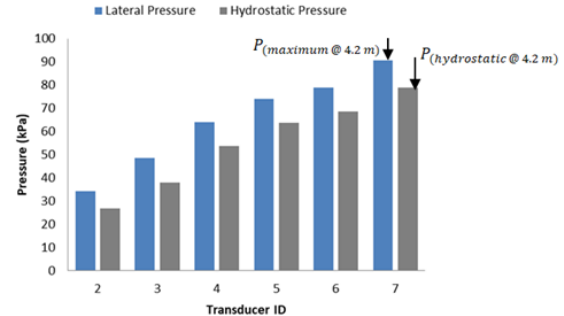
the casting height of 5 m the pressures are shown in Figure 5-18 (d). Refer to Table 5-2 for a summary of the percentage hydrostatic for each transducer at the various casting heights.

Table 5-2: Percentage hydrostatic (K_0) for the casting heights of 3.8 m to 5 m for Wall 4 (SCC-BP-R65).

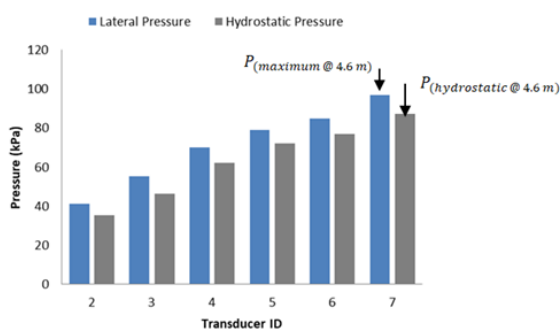
Transducer	Height from the base (m)	Casting Heights (m)			
		3.8	4.2	4.6	5
2	2.898	126	127	117	104
3	2.368	127	128	119	109
4	1.61	117	120	113	106
5	1.13	114	116	110	104
6	0.890	114	115	110	104
7	0.398	114	115	111	106



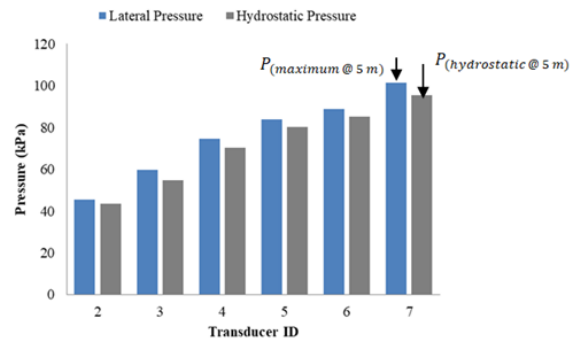
a).



b).



c).



d).

Figure 5-18: Pressure comparison at the casting height of 3.8 m to 5 m for Wall 4 (SCC-BP-R65).

Casting Height of 5.4 Meter

At 5.4 m from the base of the wall, the lateral formwork pressure measured was approximately equal to the theoretical hydrostatic pressure. The maximum lateral pressure measured at base wall by Transducer 7 showed a measured pressure ($P_{(maximum @ 5.4 m)}$) equal to the theoretical hydrostatic pressure ($P_{(hydrostatic @ 5.4 m)}$). The maximum lateral pressure measured by Transducer 6, Transducer 5, Transducer 4, Transducer 3 and Transducer 2 showed a K_0 of 97.6 % 97 %, 97 %, 98 % and 92.3 %, shown in Figure 5-19.

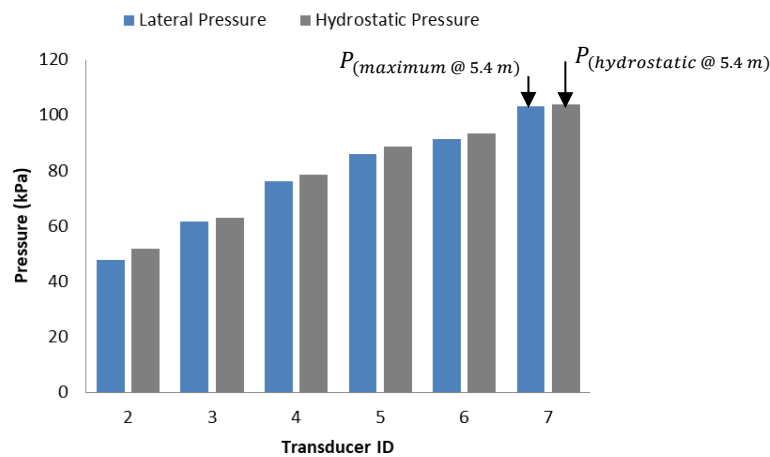


Figure 5-19: Pressure comparison at the casting height of 5.4 m for Wall 4 (SCC-BP-R65).

With the 65 m/h experimental rate pumped from the base (SCC-BP-R65) it was observed the maximum lateral pressure ($P_{(maximum)}$) was greater than the hydrostatic pressure ($P_{(hydrostatic)}$) as the casting process is under way; however, as the casting process completed it was found that the lateral pressures were equal to hydrostatic pressure.

5.3.2 Lateral Pressure Distribution for Wall 5

In the following section the results recorded and observations made from the experiment performed on the 21th June, 2017 will be discussed. The lateral pressure shown in Figure 5-20 was created from the measured lateral formwork pressure exerted by the SCC tested at a casting rate of 80 m/h and using the bottom-up placement method. See Appendix G for a tabulated summary of the results measured.

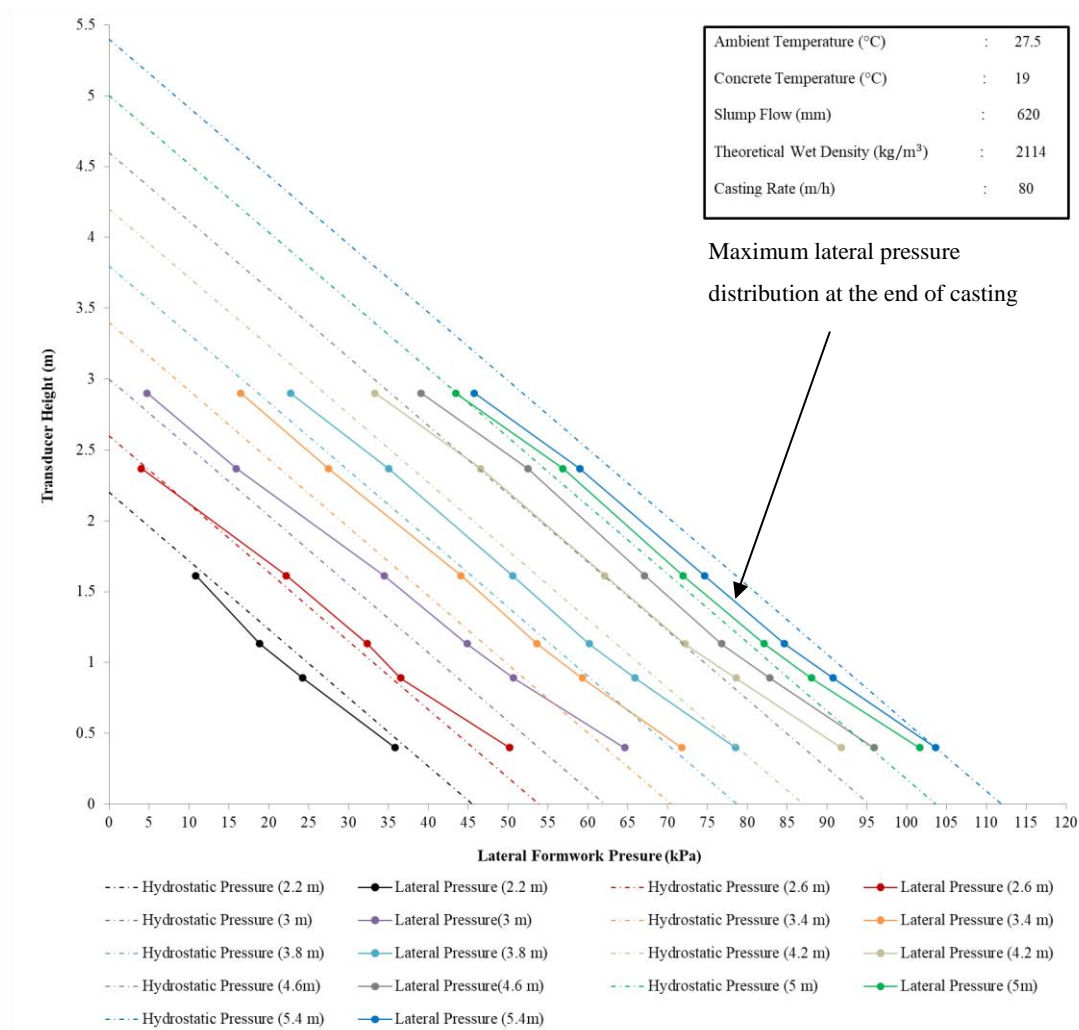


Figure 5-20: Lateral pressure distribution at various heights during casting for Wall 5 (SCC-BP-R80).

Casting Height of 2.2 Meter

As can be seen in Figure 5-20, when the SCC reached the height of 2.2 m from the base, the lateral formwork pressure was slightly below the theoretical hydrostatic pressure. The lateral formwork pressure measured near the base of the formwork system (0.398 m from the base) by Transducer 7, showed 96 % of hydrostatic ($K_0 = P_{(maximum @ 2.2 m)} / P_{(hydrostatic @ 2.2 m)}$) between the measured pressure ($P_{(maximum @ 2.2 m)}$) and the theoretical hydrostatic pressure ($P_{(hydrostatic @ 2.2 m)}$). The pressure measured by Transducer 6 (0.890 m from the base), Transducer 5 (1.13 m from the base) and Transducer 4 (1.61 m from the base) showed a K_0 of 89.5 %, 85.4 % and 89.2 % between the measured pressure and the theoretical hydrostatic pressure, shown in Figure 5-21.

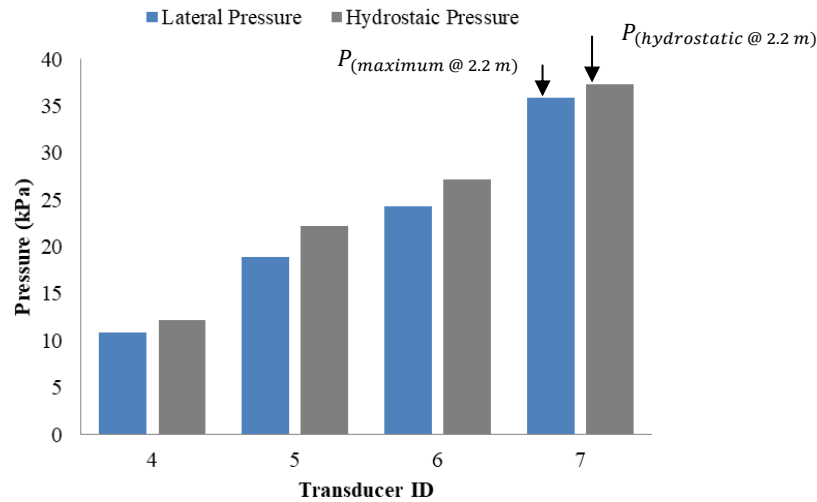


Figure 5-21: Pressure comparison at the casting height of 2.2 m for Wall 5 (SCC-BP-R80).

Casting Height of 2.6 Meter

At the casting height of 2.6 m, the lateral formwork pressure was above to the theoretical hydrostatic pressure. The maximum lateral pressure measured near the base of the experimental wall element by Transducer 7, showed 110 % of hydrostatic pressure ($K_0 = P_{(maximum @ 2.6 m)} / P_{(hydrostatic @ 2.6 m)}$) between the measured pressure ($P_{(maximum @ 2.6 m)}$) and the theoretical hydrostatic pressure ($P_{(hydrostatic @ 2.6 m)}$). The pressure measured by Transducer 6, Transducer 5, Transducer 4 and Transducer 3 showed a K_0 of 103 %, 106 %, 108 % and 85 % between the measured pressure and the theoretical hydrostatic pressure, shown in Figure 5-22.

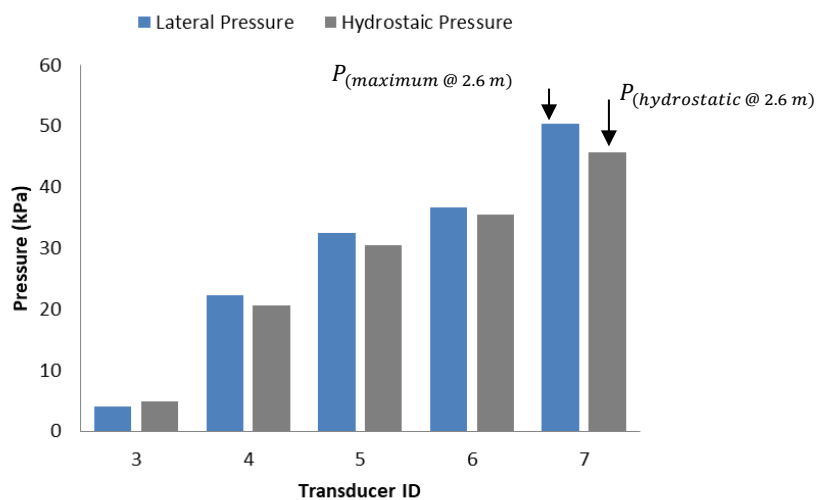


Figure 5-22: Pressure comparison at the casting height of 2.6 m for Wall 5 (SCC-BP-R80).

Casting Height of 3 Meter

The lateral pressure at the casting height of 3 m was above the theoretical hydrostatic pressure. The maximum lateral pressure measured near the base of the wall element (0.398 m from the base) by Transducer 7, showed 119 % of hydrostatic pressure ($K_0 = P_{(maximum @ 3 m)} / P_{(hydrostatic @ 3 m)}$) between the measured pressure ($P_{(maximum @ 3 m)}$) and the theoretical hydrostatic pressure ($P_{(hydrostatic @ 3 m)}$). The pressure measured by Transducer 6 (0.890 m from the base), Transducer 5 (1.13 m from the base), Transducer 4 (1.61 m from the base), Transducer 3 (2.368 m from the base) and Transducer 2 (2.898 m from the base) showed a K_0 of 116 %, 116%, 120 %, 122 % and 226 % between the measured pressure and the theoretical hydrostatic pressure, shown in Figure 5-23.

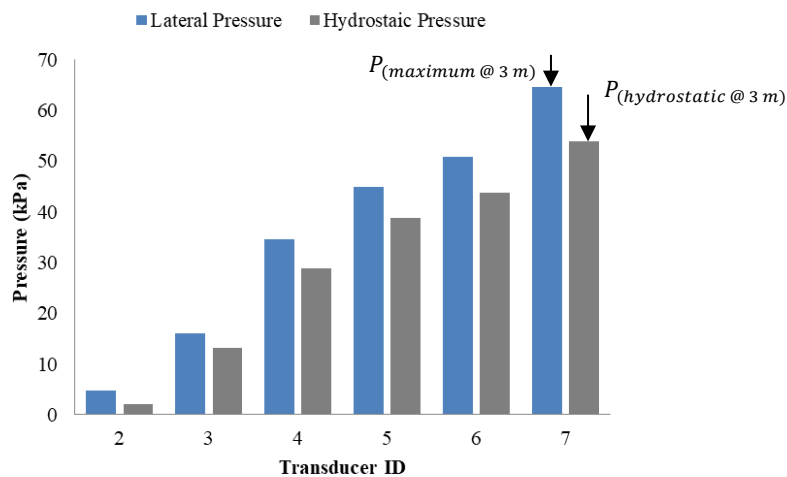


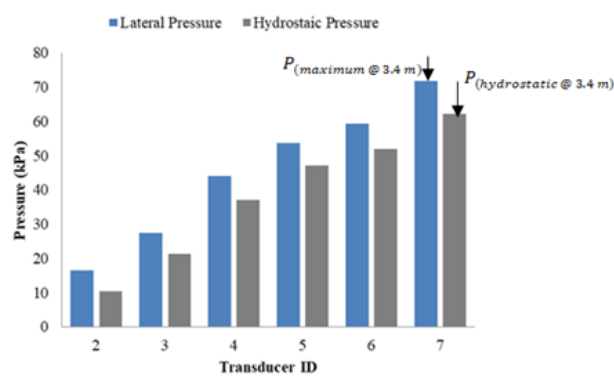
Figure 5-23: Pressure comparison at the casting height of 3 m for Wall 5 (SCC-BP-R80).

Casting Height of 3.4 to 4.6.Meter

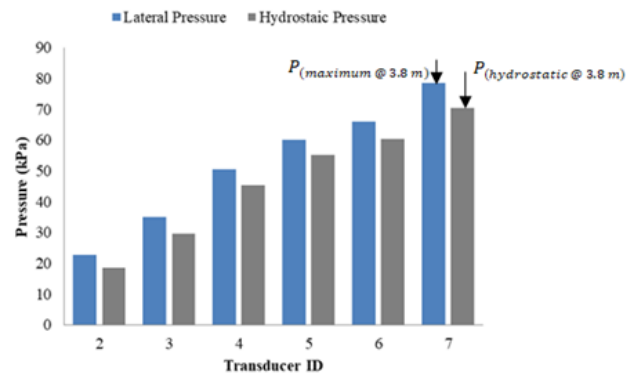
At 3.4 m, 3.8 m, 4.2 m and 4.6 m from the base of the wall, the lateral formwork pressures measured were above the theoretical hydrostatic pressure. The variation of the pressure values for the casting height of 3.4 m are shown in Figure 5-24 (a), for the casting height of 3.8 m the pressures are shown in Figure 5-24 (b), for the casting height of 4.2 m the pressures are shown in Figure 5-24 (c) and for the casting height of 4.6 m the pressures are shown in Figure 5-24 (d). Refer to Table 5-3 for a summary of the percentage hydrostatic for each transducer at the various casting heights.

Table 5-3: Percentage hydrostatic (K_0) for the casting heights of 3.4 m to 4.6 m for Wall 5 (SCC-BP-R80).

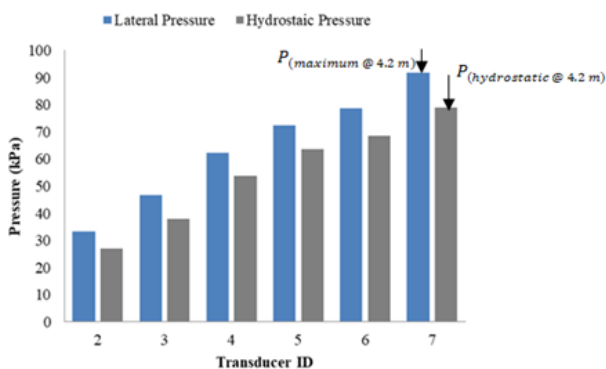
Transducer	Height from the base (m)	Casting Heights (m)			
		3.4	3.8	4.2	4.6
2	2.898	159	122	124	111
3	2.368	129	118	123	113
4	1.61	119	111	116	108
5	1.13	114	109	113	107
6	0.890	114	109	115	108
7	0.398	115	111	117	110



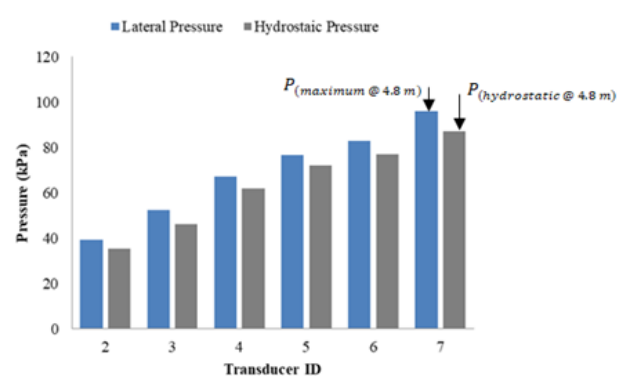
a).



b).



c).



d).

Figure 5-24: Pressure comparison at the casting height of 3.4 m to 4.6 m for Wall 5 (SCC-BP-R80).

Casting Height of 5 Meter

The lateral pressure at the casting height of 5 m was above the theoretical hydrostatic level. The maximum lateral pressure measured near the base of the experimental wall by Transducer 7, showed 107 % of hydrostatic pressure ($K_0 = P_{(maximum @ 5 m)} / P_{(hydrostatic @ 5 m)}$) between the measured pressure ($P_{(maximum @ 5 m)}$) and the theoretical hydrostatic pressure ($P_{(hydrostatic @ 5 m)}$). The pressure measured by Transducer 6, Transducer 5, Transducer 4 and Transducer 3 showed a K_0 of 103 %, 102 %, 102 % and 104 %. Transducer 2 showed measured pressures equal to the theoretical hydrostatic pressure, shown in Figure 5-25.

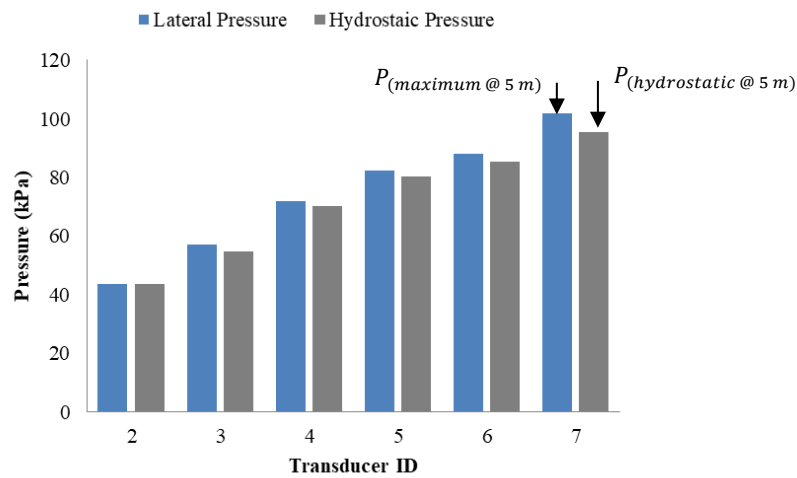


Figure 5-25: Pressure comparison at the casting height of 5 m for Wall 5 (SCC-BP-R80).

Casting Height of 5.4 Meter

At 5.4 m from the base of the wall, the lateral formwork pressure measured was equal or close to the theoretical hydrostatic pressure. The maximum lateral pressure measured at base wall by Transducer 7 showed a measured pressure ($P_{(maximum @ 5.4 m)}$) equal to the theoretical hydrostatic pressure ($P_{(hydrostatic @ 5.4 m)}$). The pressure measured by Transducer 6, Transducer 5, Transducer 4, Transducer 3 and Transducer 2 showed a K_0 of 97 %, 96 %, 95 %, 94 % and 88.3 %, shown in Figure 5-26.

With the 80 m/h experimental rate pumped from the base (SCC-BP-R80) it was observed the maximum lateral pressure ($P_{(maximum)}$) was greater than the hydrostatic pressure ($P_{(hydrostatic)}$) as the casting process is under way; however, as the casting process completed it was found that the lateral pressures were equal to the hydrostatic pressure.

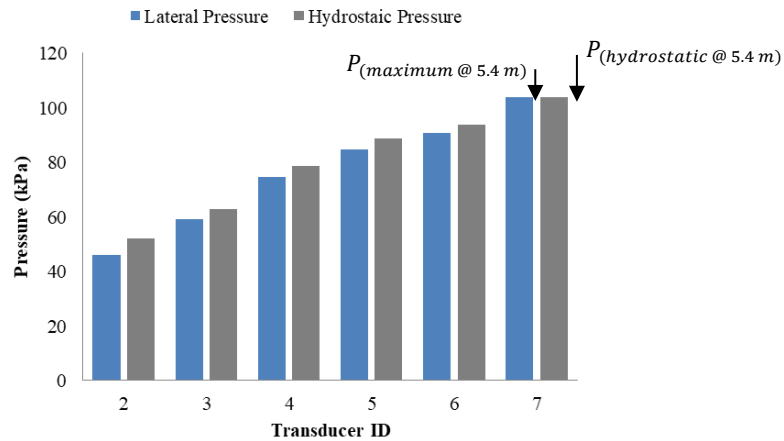


Figure 5-26: Pressure comparison at the casting height of 5.4 m for Wall 5 (SCC-BP-R80).

5.3.3 Lateral Pressure Distribution for Wall 6

In the following section the results recorded and observations made from the experiment performed on the 21th June, 2017 will be discussed. The lateral pressure shown in Figure 5-27 was created from the measured lateral formwork pressure exerted by the SCC tested at a casting rate of 55 m/h and using the bottom-up placement method. See Appendix H for a tabulated summary of the results measured.

Casting Height of 2.2 Meter

As can be seen in Figure 5-27, when the SCC reached the height of 2.2 m from the base, the lateral formwork pressure was below the theoretical hydrostatic pressure. The maximum lateral formwork pressure measured near the base of the formwork system (0.398 m from the base) by Transducer 7, showed 89.5 % of hydrostatic pressure ($K_0 = P_{(maximum @ 2.2 m)} / P_{(hydrostatic @ 2.2 m)}$) between the measured pressure ($P_{(maximum @ 2.2 m)}$) and the theoretical hydrostatic pressure ($P_{(hydrostatic @ 2.2 m)}$). The pressure measured by Transducer 6 (0.890 m from the base), Transducer 5 (1.13 m from the base) and Transducer 4 (1.61 m from the base) showed a K_0 of 96.5 %, 88.7 % and 78.3 % between the measured pressure and the theoretical hydrostatic pressure, shown in Figure 5-28.

Casting Height of 2.6 Meter

At the casting height of 2.6 m, the lateral formwork pressure was equal or close to the theoretical hydrostatic pressure. The maximum lateral pressure measured at the base of the wall element by Transducer 7 showed pressures ($P_{(maximum @ 2.6 m)}$) equal to the theoretical hydrostatic pressure

($P_{(hydrostatic @ 2.6 m)}$). The pressure measured by Transducer 6, Transducer 5, Transducer 4, Transducer 3 showed a K_0 of 97.4 %, 90.4 %, 84.6 % and 42.2 %, shown in Figure 5-29.

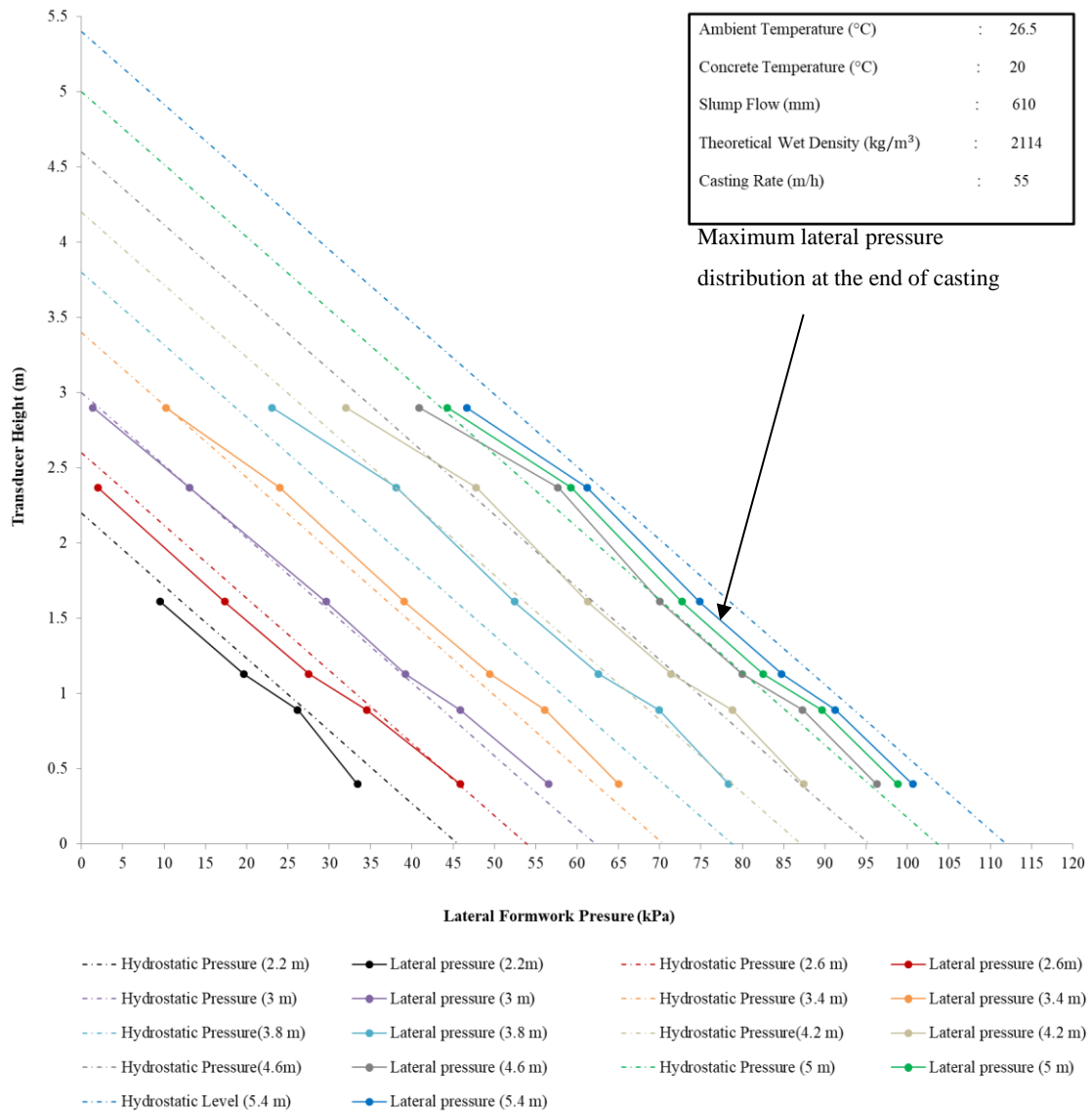


Figure 5-27: Lateral pressure distribution at various heights during casting for Wall 6 (SCC-BP-R55).

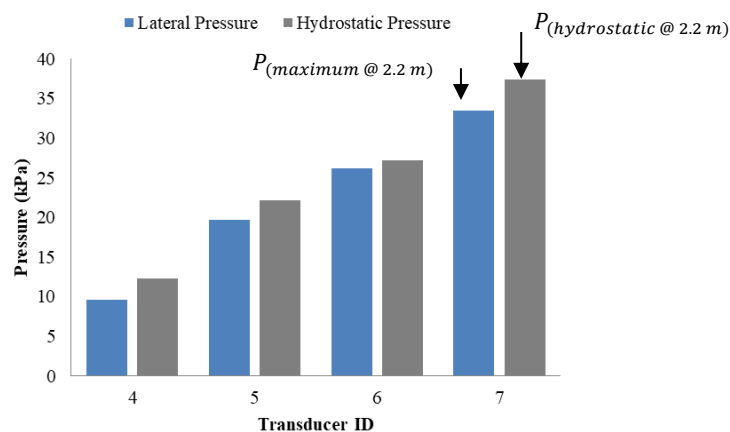


Figure 5-28: Pressure comparison at the casting height of 2.2 m for Wall 6 (SCC-BP-R55).

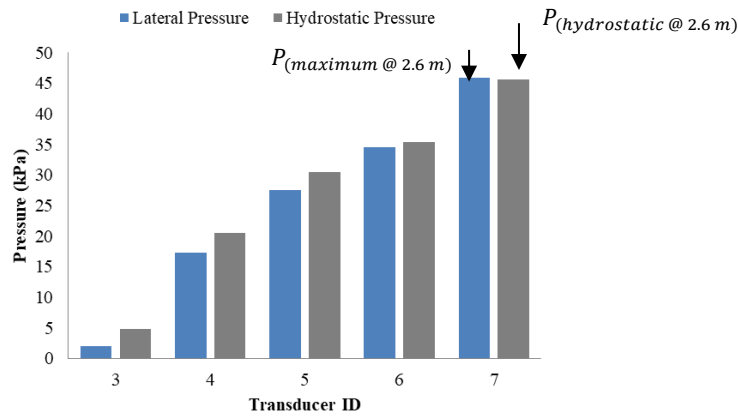


Figure 5-29: Pressure comparison at the height of 2.6 m for Wall 6 (SCC-BP-R55).

Casting Height of 3 Meter

The lateral pressure at the casting height of 3 m was above the theoretical hydrostatic pressure. The maximum lateral pressure measured near the base of the wall element (0.398 m from the base) by Transducer 7, showed 105 % of hydrostatic pressure ($K_0 = P_{(maximum @ 3 m)} / P_{(hydrostatic @ 3 m)}$) between the measured pressure ($P_{(maximum @ 3 m)}$) and the theoretical hydrostatic pressure ($P_{(hydrostatic @ 3 m)}$). The pressure measured by Transducer 6 (0.890 m from the base), Transducer 5 (1.13 m from the base), Transducer 4 (1.61 m from the base), Transducer 3 (2.368 m from the base) and Transducer 2 (2.898 m from the base) showed a K_0 of 105 %, 101 %, 103 %, 99.7 % and 67.7 %, between the measured pressure and the theoretical hydrostatic pressure, shown in Figure 5-30.

Casting Height of 3.4 Meter

At 3.4 meters from the base of the wall, the lateral formwork pressure measured was above to the theoretical hydrostatic pressure. The lateral pressure measured at base of the wall by Transducer 7, showed 105 % of hydrostatic pressure ($K_0 = P_{(maximum @ 3.4 m)} / P_{(hydrostatic @ 3.4 m)}$) between the measured pressure ($P_{(maximum @ 3.4 m)}$) and the theoretical hydrostatic pressure ($P_{(hydrostatic @ 3.4 m)}$). The pressure measured by Transducer 6, Transducer 5, Transducer 4, Transducer 3 and Transducer 2 showed a K_0 of 108 %, 105 %, 105 %, 112 % and 98.3 % between the measured pressure and the theoretical hydrostatic pressure, shown in Figure 5-31.

Casting Height of 3.8 to 4.6.Meter

At 3.8 m, 4.2 m and 4.6 m from the base of the wall, the lateral formwork pressures measured were above the theoretical hydrostatic pressure. The variation of the pressure values for the casting height of 3.8 m are shown in Figure 5-32 (a), for the casting height of 4.2 meters the pressures are shown

in Figure 5-32 (b) and for the casting height of 4.6 m the pressures are shown in Figure 5-32 (c). Refer to Table 5-4 for a summary of the percentage hydrostatic for each transducer at the various casting heights.

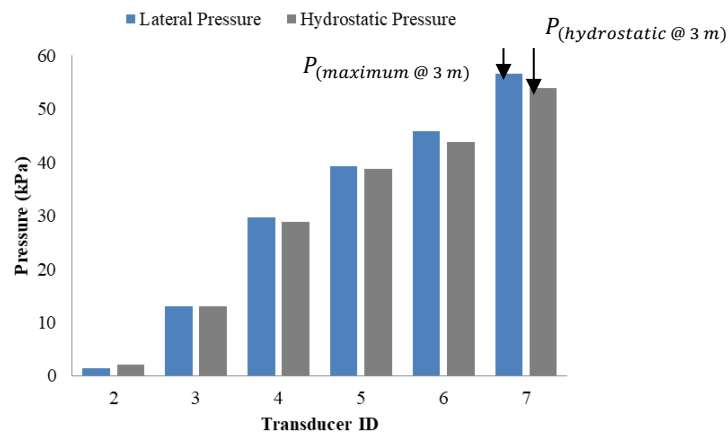


Figure 5-30: Pressure comparison at the casting height of 3 m for Wall 6 (SCC-BP-R55).

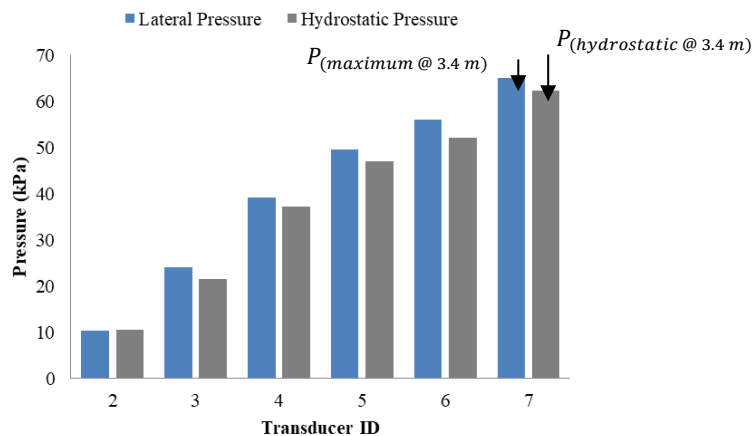


Figure 5-31: Pressure comparison at the casting height of 3.4 m for Wall 6 (SCC-BP-R55).

Casting Height of 5 Meter

The lateral pressure at the casting height of 5 m was above the theoretical hydrostatic level. The maximum lateral pressure measured near the base of the experimental wall by Transducer 7, showed 104 % of hydrostatic pressure ($K_0 = P_{(maximum @ 5 m)} / P_{(hydrostatic @ 5 m)}$) between the measured pressure ($P_{(maximum @ 5 m)}$) and the theoretical hydrostatic pressure ($P_{(hydrostatic @ 5 m)}$). The pressure measured by Transducer 6, Transducer 5, Transducer 4, Transducer 3 and Transducer 2 showed a K_0 of 105 %, 103 %, 103 %, 109 % and 102 %, shown in Figure 5-33.

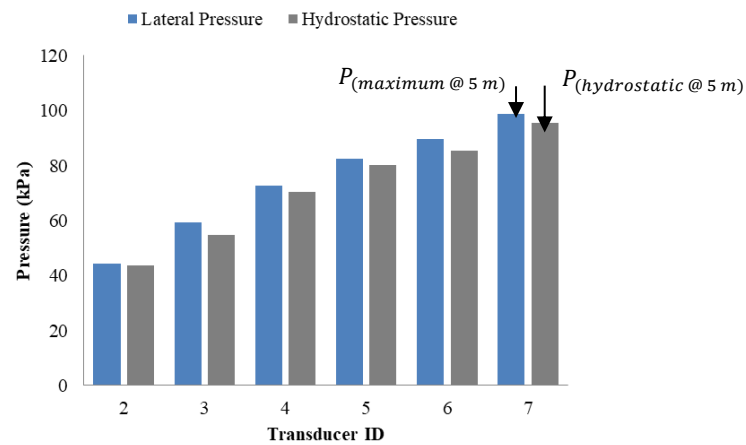


Figure 5-32: Pressure comparison at the casting height of 5 m for Wall 6 (SCC-BP-R55).

Table 5-4: Percentage hydrostatic (K_0) for the casting heights of 3.8 m to 4.6 m for Wall 6 (SCC-BP-R55).

Transducer	Height from the base (m)	Casting Heights (m)		
		3.8	4.2	4.6
2	2.898	122	124	111
3	2.368	118	123	113
4	1.61	111	116	108
5	1.13	109	113	107
6	0.890	109	115	108
7	0.398	111	117	110

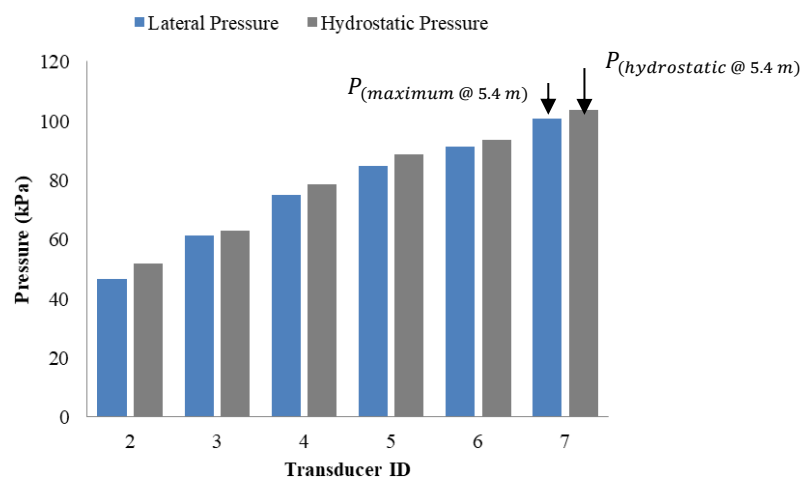


Figure 5-33: Pressure comparison at the casting height of 5.4 m for Wall 6 (SCC-BP-R55).

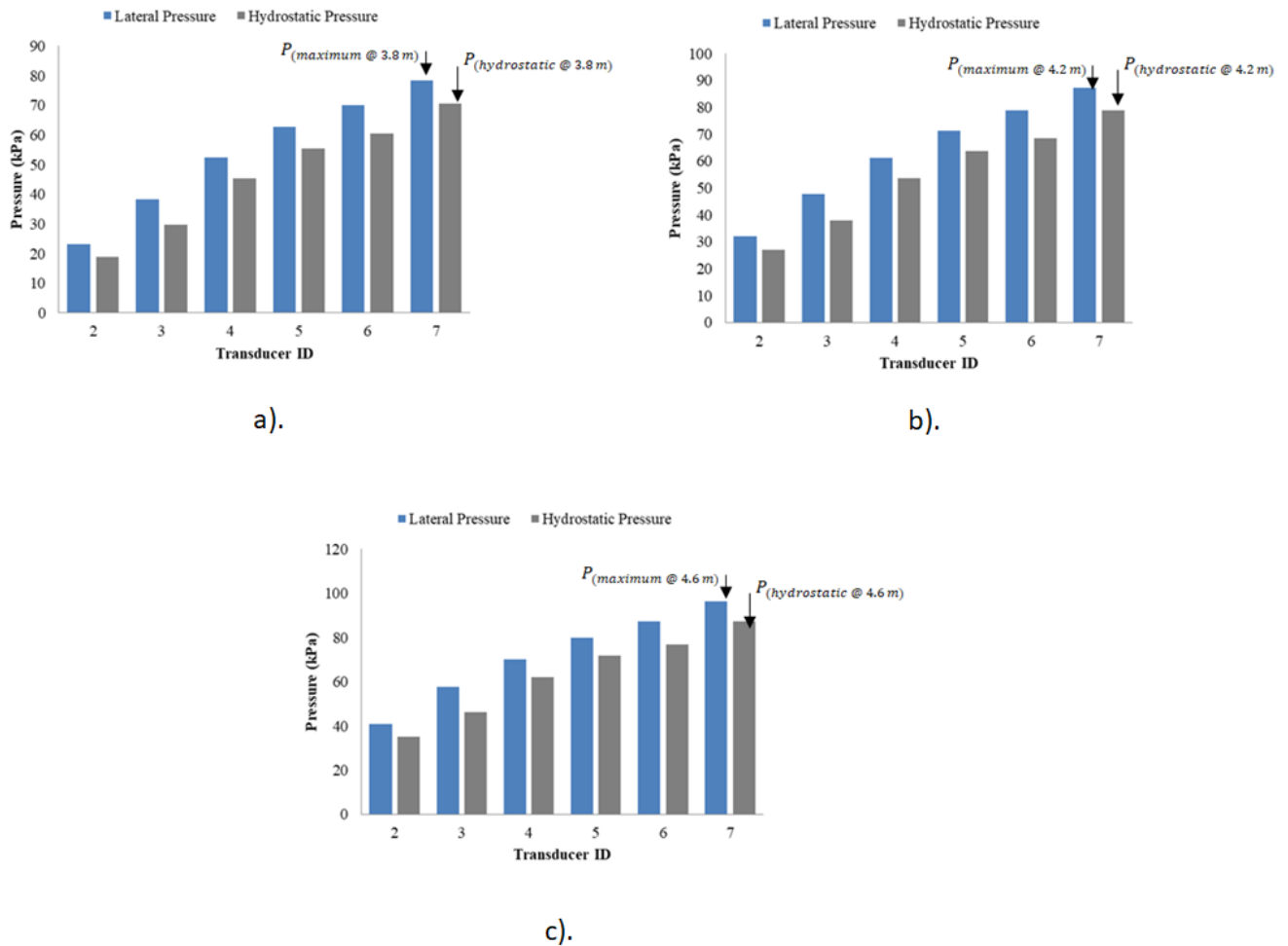


Figure 5-34: Pressure comparison at the casting height of 3.8 m to 4.6 m for Wall 6 (SCC-BP-R55).

With the 55 m/h experimental rate pumped from the base (SCC-BP-R80) it was observed the maximum lateral pressure ($P_{(maximum)}$) was greater than the hydrostatic pressure ($P_{(hydrostatic)}$) as the casting process is under way; however, as the casting process completed it was found that the lateral pressures were equal to the hydrostatic pressure.

5.4 Results Comparison and Site Observations

In the following section the results recorded and observations made from experimental investigation are compared with one another, as well as comparing the maximum measured pressure of each experimental wall with the proposed models in the literature study.

5.4.1 Comparing the Results of Wall 1, Wall 2 and Wall 3

As found with Wall 1 (SCC-TP-R80), Wall 2 (SCC-TP-WP15-R27) and Wall 3 (SCC-TP-WP15-R27) it can be concluded that implementing waiting periods in between casting sessions and lowering the casting rate, reduces the lateral formwork pressure ($P_{(maximum)}$) exerted by the SCC.

This method has shown similar results to other studies, namely that of Omran *et al.*, (2014) as highlighted in Chapter 2. This phenomenon could be because the SCC is able to set and build up an internal structure through thixotropic behaviour and hydration, thus reducing the lateral pressure exerted by the SCC.

Figures 5-35 and 5-36 shows the maximum pressure from Wall 3 (15 minute waiting periods) exhibited a 5.8 % reduction when compared to the maximum pressure from that of Wall 2 (10 minute waiting periods). The maximum pressure from Wall 1 (no waiting periods) exhibited a 10 % increase when compared to the maximum pressure from that of Wall 2 (10 minute waiting period), and 15.3 % when compared to the maximum pressure from that of Wall 3 (15 minute waiting periods). This reduction could be explained by the concrete building-up a stronger internal structure to withstand the shearing induced by the flow of the fresh concrete during casting.

Even though implementing waiting periods in between casting sessions reduces the lateral formwork pressure when casting from the top of the experimental wall, the same would not be possible for bottom-up casting. It has been suggested by Assaad *et al.* (2003) that when pumping fresh SCC from the base of the element, pauses during the casting procedure should be avoided. Assaad *et al.* (2003) states that if this is not avoided then high pumping pressures would be necessary to break down the mass that SCC built up because of its thixotropic behaviour.

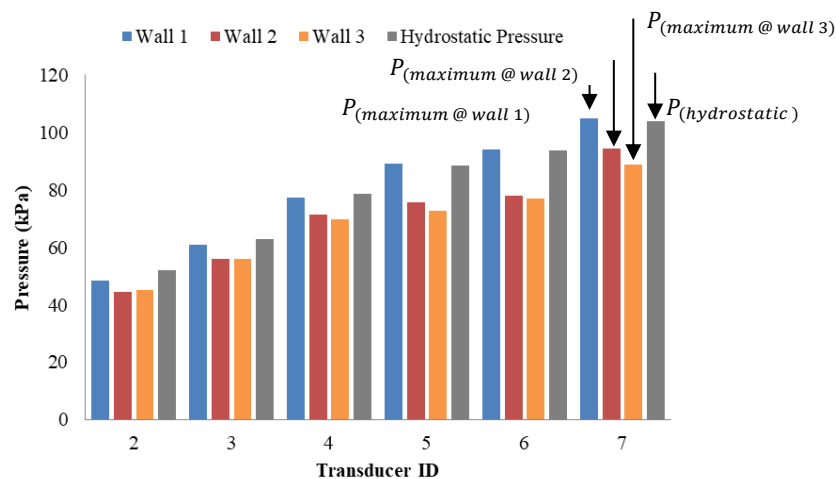


Figure 5-35: Comparison between the maximum lateral pressure distribution at end of casting for Wall 1 (SCC-TP-R80), Wall 2 (SCC-TP-WP10-R27) and Wall 3 (SCC-TP-WP15-R27).

It was also noted that when comparing Wall 2 and 3 which had the same average casting rate the concrete temperature had no significant effect on the lateral pressure at the end of the casting process, this observation was also noted by Khayat and Assaad (2006) in their investigation. No

comparison or observations could be made from the other measured parameters (slump, filling ability, etc.) due to them being kept constant.

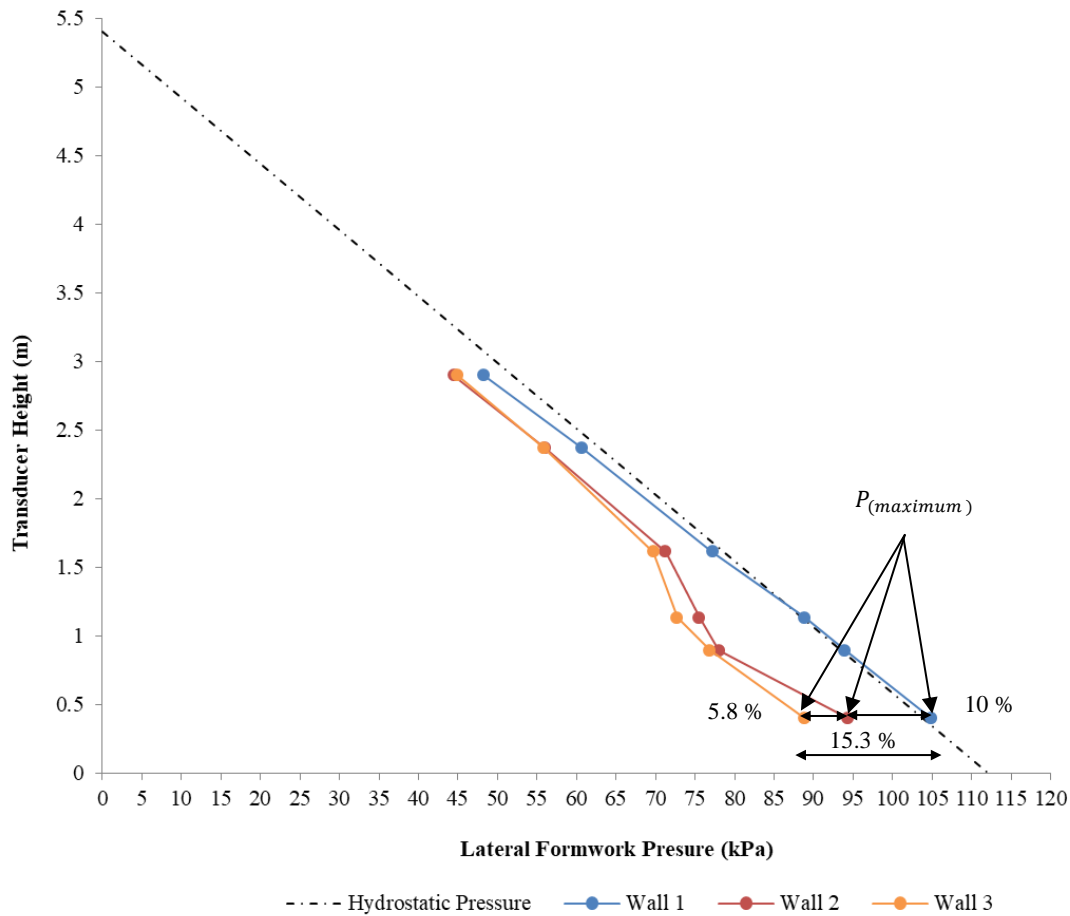


Figure 5-36: Comparison between the maximum lateral pressure distribution at end of casting for Wall 1 (SCC-TP-R80), Wall 2 (SCC-TP-WP10-R27) and Wall 3 (SCC-TP-WP15-R27).

5.4.2 Comparing the Results of Wall 1 and Wall 5

As found with Wall 1 (SCC- TP-R80) and Wall 5 (SCC-BP-R80) when pumping from the top or from the base of the experimental wall at a constant casting rate of 80 m/h, hydrostatic pressures ($P_{(hydrostatic)}$) can be expected for the maximum exerted pressure ($P_{(maximum)}$) at the end of casting, as shown in Figures 5-37 and 5-38.

However, it was found from Wall 5 (SCC-BP-R80) as the SCC was being cast the maximum exerted pressures ($P_{(maximum @ wall 5)}$) would exceed the theoretical hydrostatic pressure ($P_{(hydrostatic)}$), as shown in Figures 5-39. When comparing the exerted maximum lateral pressures of Wall 1 ($P_{(maximum @ wall 1)}$) and Wall 5 ($P_{(maximum @ wall 5)}$) at the casting height of 4.2 m from the base of the experimental wall, a 13.2 % increase in the maximum lateral pressure can be seen in Figure 5-40. Billberg (2006) states that pumping from the base of the element could cause the

lateral pressure to reach, or even exceed, full hydrostatic pressure because of the constant pump pressure and non-thixotropic behavior.

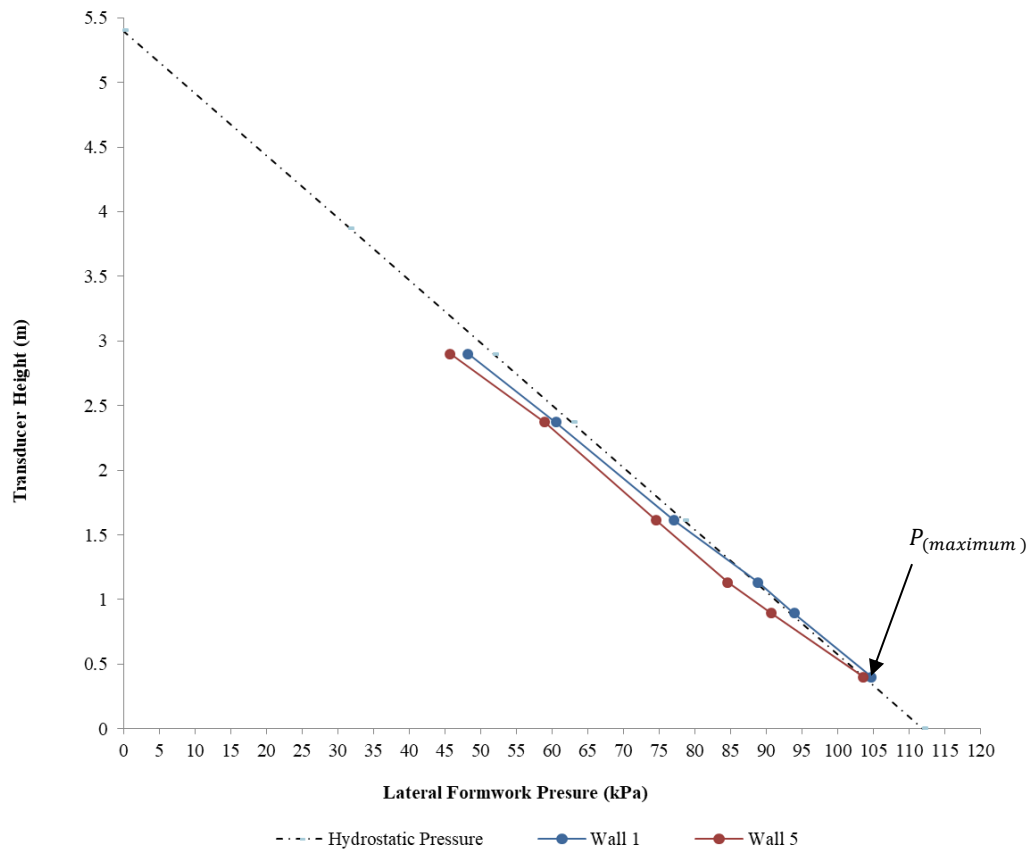


Figure 5-37: Comparison between the maximum lateral pressure distribution at end of casting for Wall 1 (SCC- TP-R80) and Wall 5 (SCC-BP-R80).

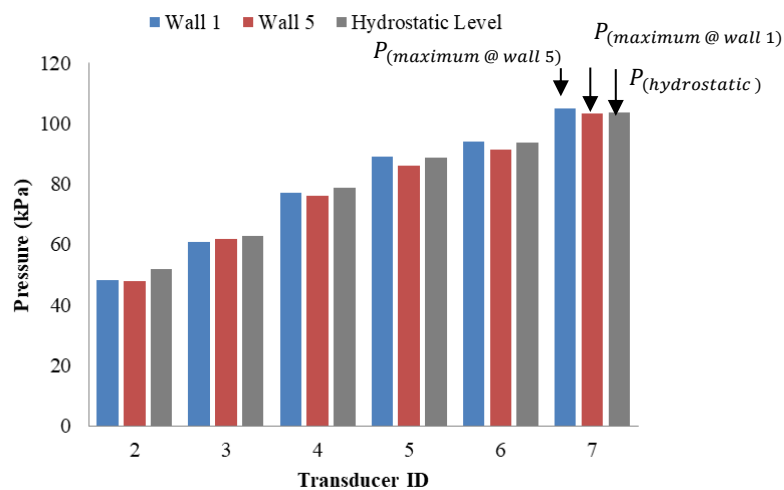


Figure 5-38: Comparison between pressures at the end of casting for Wall 1 (SCC- TP-R80) and Wall 5 (SCC-BP-R80).

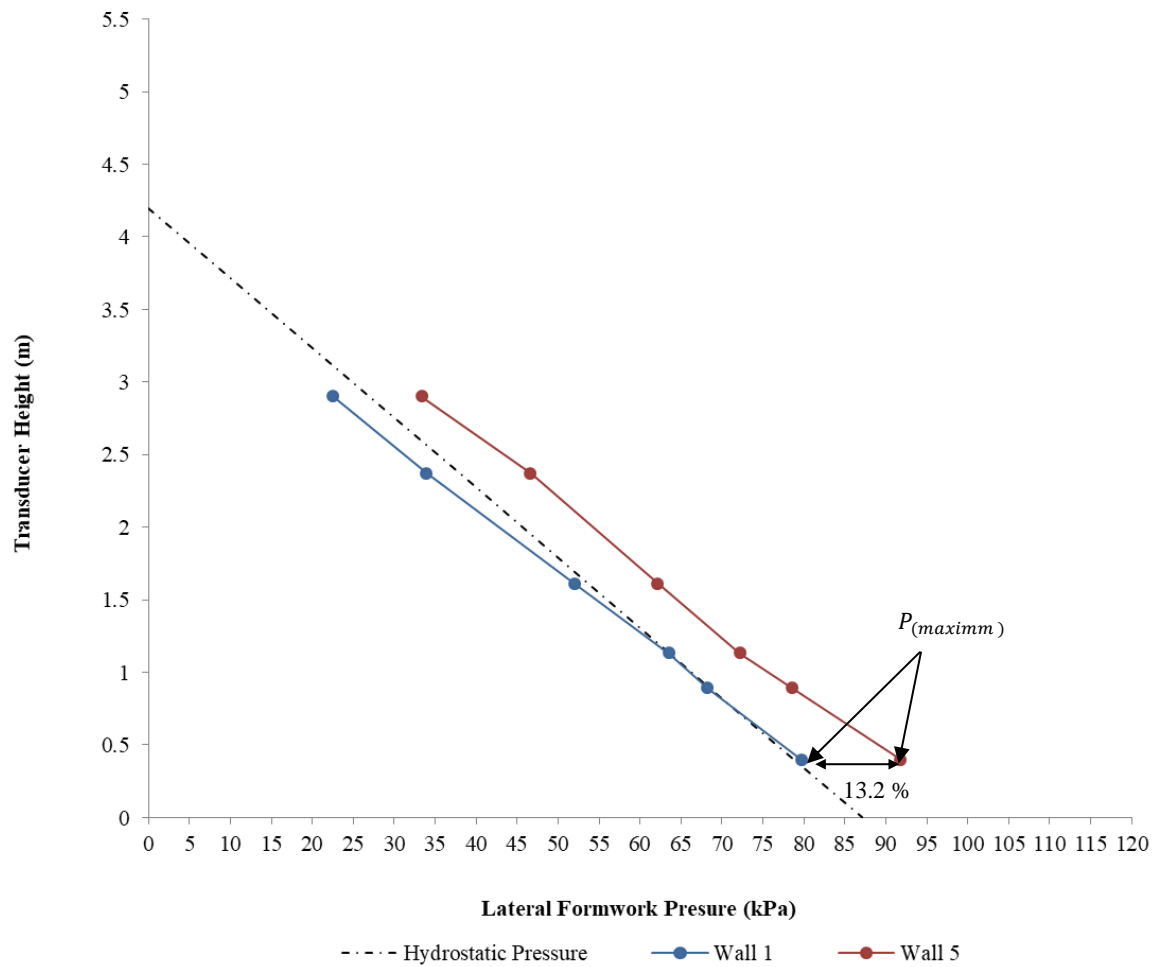


Figure 5-39: Comparison between the maximum lateral pressure distribution at a casting height of 4.2 meters for Wall 1 (SCC- TP-R80) and Wall 5 (SCC-BP-R80).

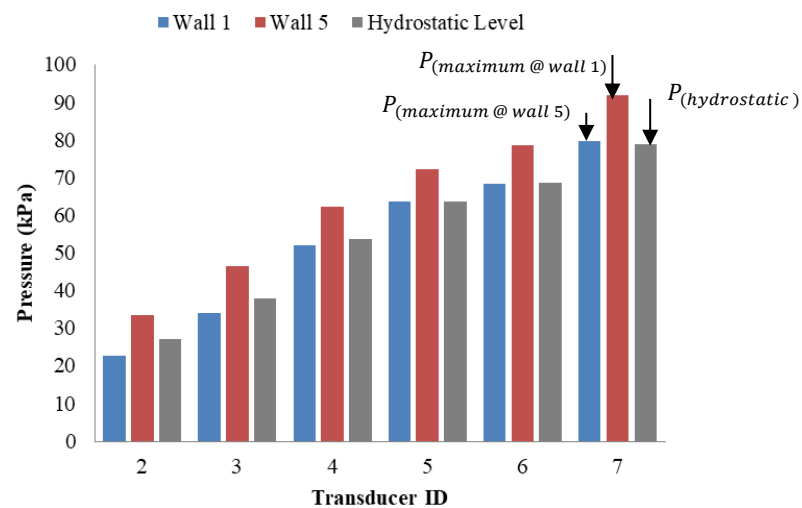


Figure 5-40: Comparison between pressures at casting height of 4.2 meters for wall 1 (SCC- TP-R80) and wall 5 (SCC-BP-R80).

A CFD analysis was performed on Ansys Fluent as shown in Figure 5-41, a simulation was created in order to investigate what effect of the additional pressures exerted by the portable pump have on the lateral pressures. The medium used in the simulation was water, as simulating the way SCC would perform was too complex for such an analysis.

In the analysis, the water was pumped into the water column at the maximum flow rate for the CIFA S8 Series PC 907 as specified in Table 3-5. From the simple simulation it was found that the pressures simulated were equal to the theoretical hydrostatic pressures. This suggests that the reason for the lateral pressures exceeding the theoretical hydrostatic pressures in the experimental investigation could be a combination of the concrete's rheology, friction between concrete and formwork panels and the pressures exerted by the portable pump.

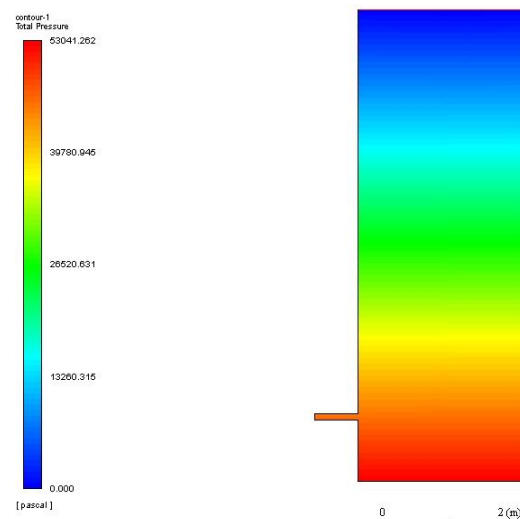


Figure 5-41: Ansys model simulating pumping pressures using water.

5.4.3 Comparing the Results of Wall 4, Wall 5 and Wall 6

As found with Wall 4 (SCC- BP-R65), Wall 5 (SCC-BP-R80) and Wall 6 (SCC-BP-R55) when pumping from the base at constant casting of 65, 80 and 55 m/h, hydrostatic pressures ($P_{(hydrostatic)}$) can be expected for the maximum exerted pressure ($P_{(maximum)}$) at the end of casting, as shown in Figures 5-42 and 5-43.

However, it was found from the three experimental walls (Wall 4, Wall 5 and Wall 6) as the SCC was being cast the maximum exerted pressures ($P_{(maximum)}$) would exceed the theoretical hydrostatic pressure ($P_{(hydrostatic)}$) as shown in Figure 5-43 during the casting process. When comparing the exerted maximum lateral pressures of Wall 4, Wall 5 and Wall 6 at the casting height of 4.2 m and at the end of casting. It can be seen from Figures 5-44 and 5-45 that there is little to no difference between the exerted pressures for the different casting rates. A reason for this could be

that as the casting rate was lowered from 80 to 55 m/h it was not sufficiently reduced for fresh SCC to undergo structural build-up through thixotropic behaviour and hydration.

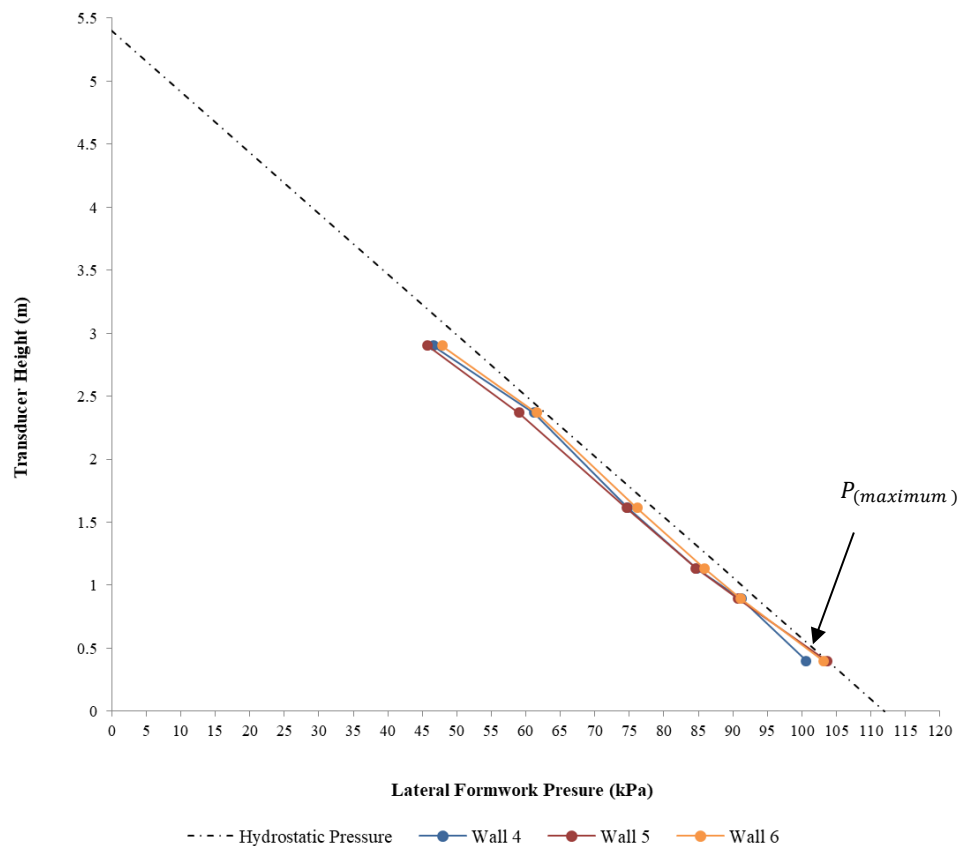


Figure 5-42: Comparison between the maximum lateral pressure distribution at end of casting for Wall 4 (SCC-BP-R55), Wall 5 (SCC-BP-R80), and Wall 6 (SCC-BP-R65).

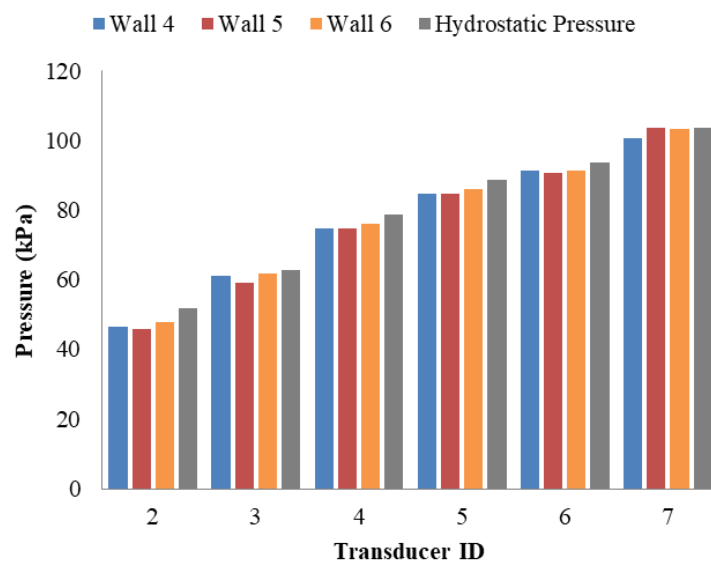


Figure 5-43: Comparison between pressures at the end of casting for Wall 4 (SCC-BP-R55), Wall 5 (SCC-BP-R80), and Wall 6 (SCC-BP-R65).

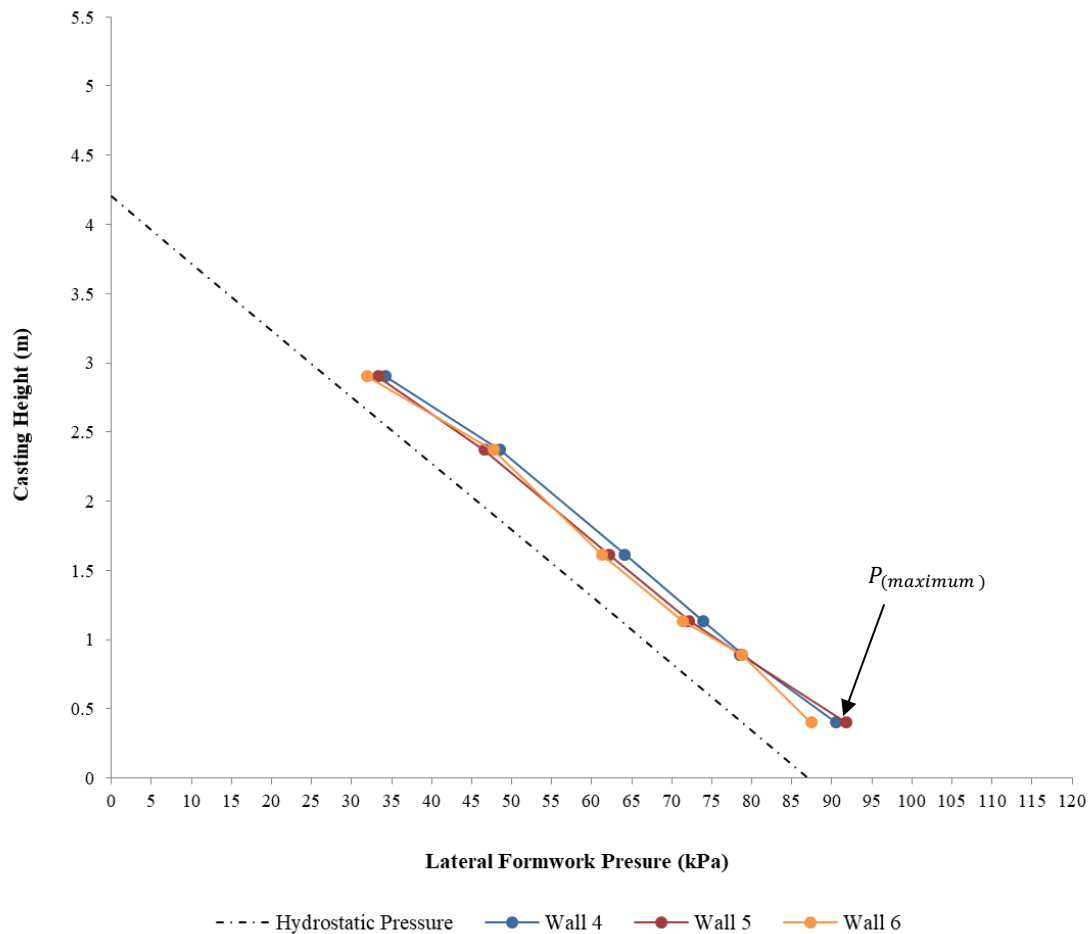


Figure 5-44: Comparison between the maximum lateral pressure distribution at a casting height of 4.2 meters for Wall 4 (SCC-BP-R55), Wall 5 (SCC-BP-R80), and Wall 6 (SCC-BP-R65).

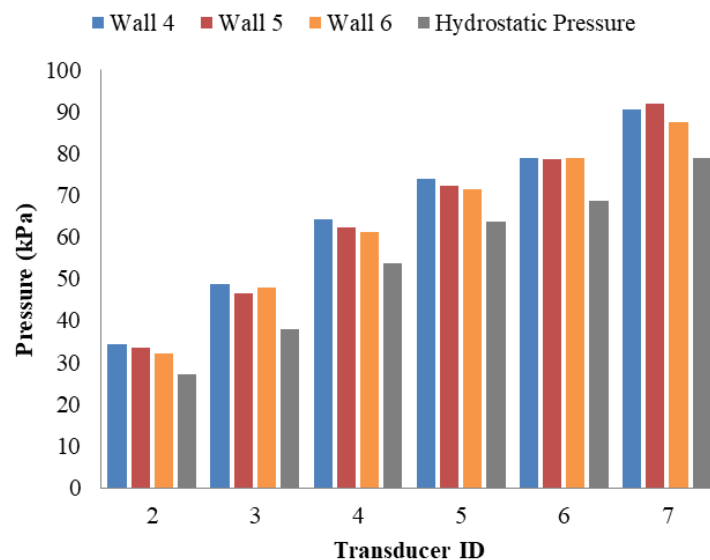


Figure 5-45: Comparison between pressures at a casting height of 4.2 meters for Wall 4 (SCC-BP-R55), Wall 5 (SCC-BP-R80), and Wall 6 (SCC-BP-R65).

5.4.4 Comparing of Results to Existing Models

This section presents the comparison of the results presented in Sections 5.4.1 to 5.4.3 to the available models discussed in the literature.

CIRIA Report 108 (1985), end of casting

The CIRIA Report 108 (1985) states when $C_1\sqrt{R} > H$ the hydrostatic pressure ($P_{(hydrostatic)}$) should be taken else Eq. 1 should be used, where C_1 is the coefficient dependent on the formwork (1 for walls and 1.5 for columns), R is the casting rate (m/h) and H is the vertical formwork height (m). Refer to Table 5-5 for the calculated parameters for CIRIA Report 108 (1985) for Walls 1 to 6 at the end of casting.

Table 5-5: CIRIA Report 108 (1985) parameters for Wall 1 to 6 at the end of casting.

Wall ID	$C_1\sqrt{R}$	H
1	8.9	5.4
2	5.2	5.4
3	5.2	5.4
4	8.1	5.4
5	8.9	5.4
6	7.4	5.4

Due to $C_1\sqrt{R} > H$ for Wall 1, Wall 4, Wall 5 and Wall 6 the predicted pressures were calculated from pgh and due to $C_1\sqrt{R} < H$ Wall 2 and Wall 3 were calculated from Eq. 1. Refer to Figure 5-46 for the comparison between the experimental data and CIRIA Report 108 (1985). The CIRIA Report 108 (1985) is a conservative method of predicting the pressures which could be exerted at the end of the casting process.

The predicted pressures for Wall 1 showed an underestimation of 1% when compared to the experimental data. For Wall 2, Wall 3 and Wall 4 the predicted pressures showed an overestimation of 9.1 %, 14.4 % and 3 % when compared to the experimental data and for Wall 5 and Wall 6 the predicted pressures were equal to the experimental data.

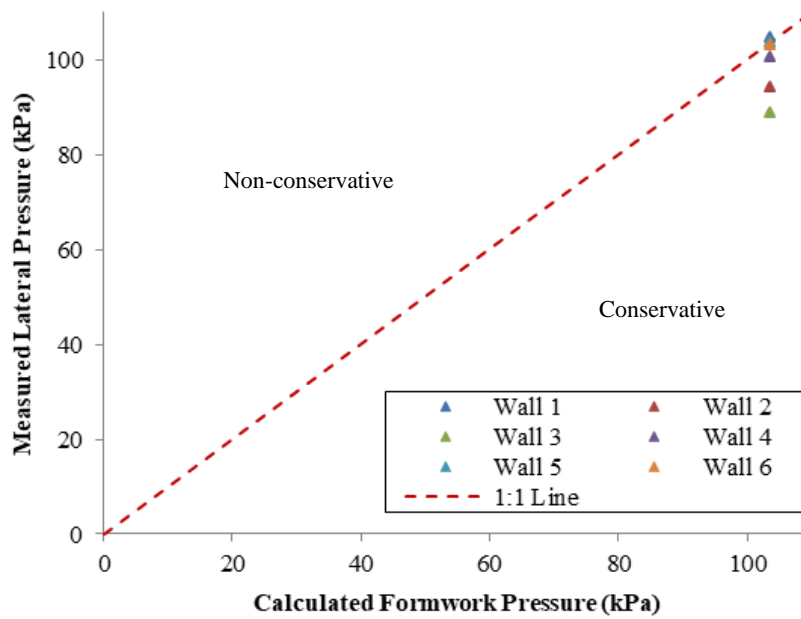


Figure 5-46: Measured pressure at the end of casting vs. CIRIA Report 108 (1985) Eq.1.

CIRIA Report 108 (1985), casting height of 4.2 meters

Refer to Table 5-6 for the calculated parameters for CIRIA Report 108 (1985) for Wall 1, Wall 4, Wall 5 and Wall 6 at a casting height of 4.2 m. Due to $C_1\sqrt{R} > H$ for Wall 1, Wall 4, Wall 5 and Wall 6 the predicted pressures were calculated from pgh . Refer to Figure 5-47 for the comparison between the experimental data and CIRIA Report 108 (1985) at a casting height of 4.2 m.

The CIRIA Report 108 (1985) is a non-conservative method of predicting the pressures which could be exerted when pumping from above when at a casting height of 4.2 m. The predicted pressure for Wall 1, Wall 4, Wall 5 and Wall 6 showed an underestimation of 1%, 14.9%, 16.5 % and 10.9 % when compared to the experimental data.

Table 5-6: CIRIA Report 108 (1985) parameters for Walls 1 to 6 at a casting height of 4.2 meters.

Wall ID	$C_1\sqrt{R}$	H
1	8.9	4.2
4	8.1	4.2
5	8.9	4.2
6	7.4	4.2

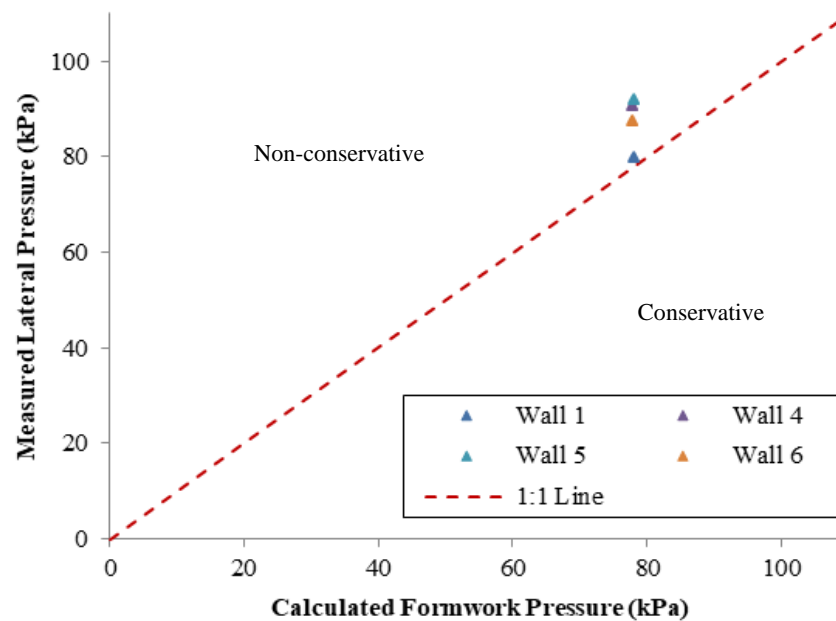


Figure 5-47: Measured pressure at a casting height of 4.2 meters vs. CIRIA Report 108 (1985) Eq.1.

CIRIA Report 108 (1985), modified casting rates

Figure 5-48 shows the comparison of the predicted pressures from the CIRIA Report 108 (1985) to the pressures from the modified casting rates of Wall 2 and Wall 3 at the end of casting. The casting rate of the SCC was artificially lowered by converting the average casting rate of 27 m/h for both walls to an equivalent constant casting rate of 4.6 m/h, where it is assumed that there are no interruptions to the casting rate and no waiting periods implemented.

This was done by taking the time to fill the wall element to be the sum of all the waiting periods and time of each casting session (C_2 was taken as 0.6 and K was calculated to 0.58). From Figure 5-47 it was found that model calculated pressures lower than the pressures from the modified casting rates. The predicted pressures for Wall 2 and Wall 3 showed an underestimation of 64 % and 54.5 % when compared to the experimental data.

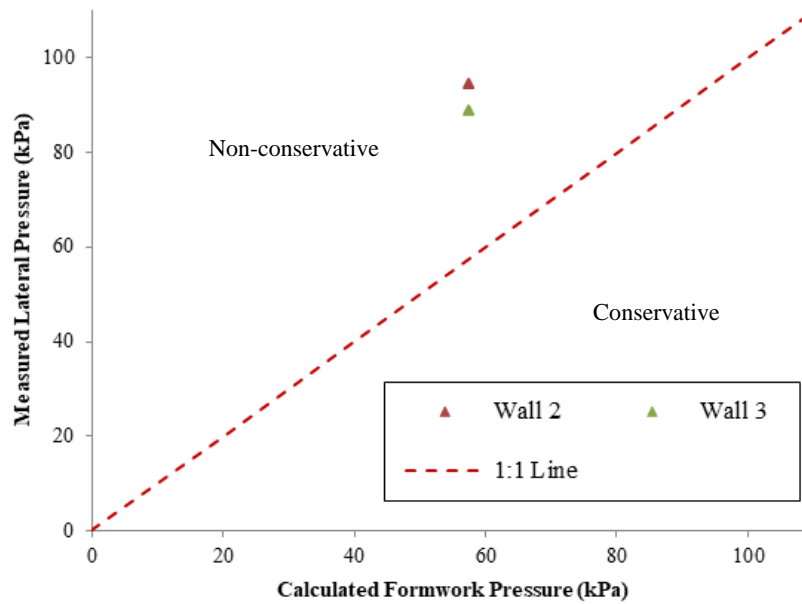


Figure 5-48: Pressures from the modified casting rates at the end of casting vs. CIRIA Report 108 (1985)

Eq.1.

Gardner (2014), end of casting

Gardner (2014) states that if $t_H = H/R < t_E / 2$ Eq.13 should be used to calculate the predicted pressures. Where t_H is the time required to fill the formwork system to the height H and t_E is the setting time (h). Refer to Table 5-7 for the calculated parameters for Gardner (2014). For Wall 1, Wall 2, Wall 3, Wall 4, Wall 5 and Wall 6 the predicted pressures were calculated from Eq.A.13 and show reasonably conservative predicted pressures at the end of the casting process, shown in Figure 5-49. The predicted pressures for Wall 1, Wall 5 and Wall 6 showed an underestimation of 2.3 %, 1.1 % and 1.2 % when compared to the experimental data. For Wall 2, Wall 3 and Wall 4 the predicted pressures showed an overestimation of 5.9 %, 11.4 % and 1.6 % when compared to the experimental data.

Table 5-7: Gardner (2014) parameters for Wall 1 to Wall 6 at the end of casting.

Wall ID	t_H	t_E
1	0.068	6
2	0.2	6
3	0.2	6
4	0.08	6
5	0.068	6
6	0.098	6

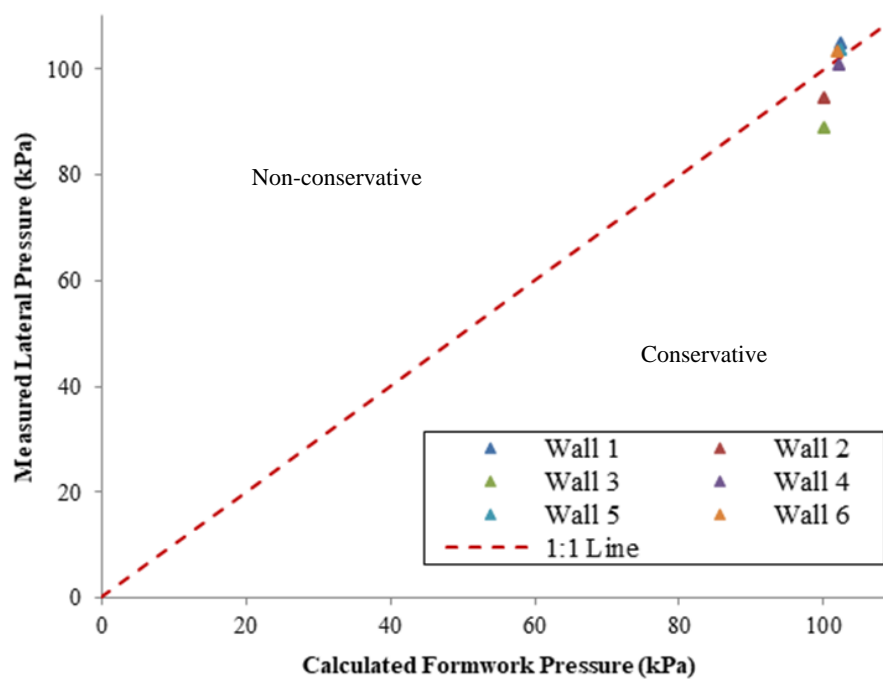


Figure 5-49: Measured pressure at the end of casting vs. Gardner (2014) Eq.13.

Gardner (2014), casting height of 4.2 meters

Refer to Table 5-8 for the calculated parameters for Gardner (2014). For Wall 1, Wall 4, Wall 5 and Wall 6 the predicted pressures were calculated from Eq.13 and shows non-conservative values for predicting the pressures which could be exerted when pumping from below, and shows slightly conservative values for predicting the pressures which could be exerted when pumping from above when at a casting height of 4.2 m, shown in Figure 5-50. The predicted pressures for Wall 1, Wall 4, Wall 5 and Wall 6 showed an underestimation of 2 %, 16.2 %, 17.6 % and 12.4 % when compared to the experimental data.

Table 5-8: Gardner (2014) parameters for Wall 1 to Wall 6 at a casting height of 4.2 meters.

Wall ID	t_H	t_E
1	0.053	6
4	0.065	6
5	0.053	6
6	0.076	6

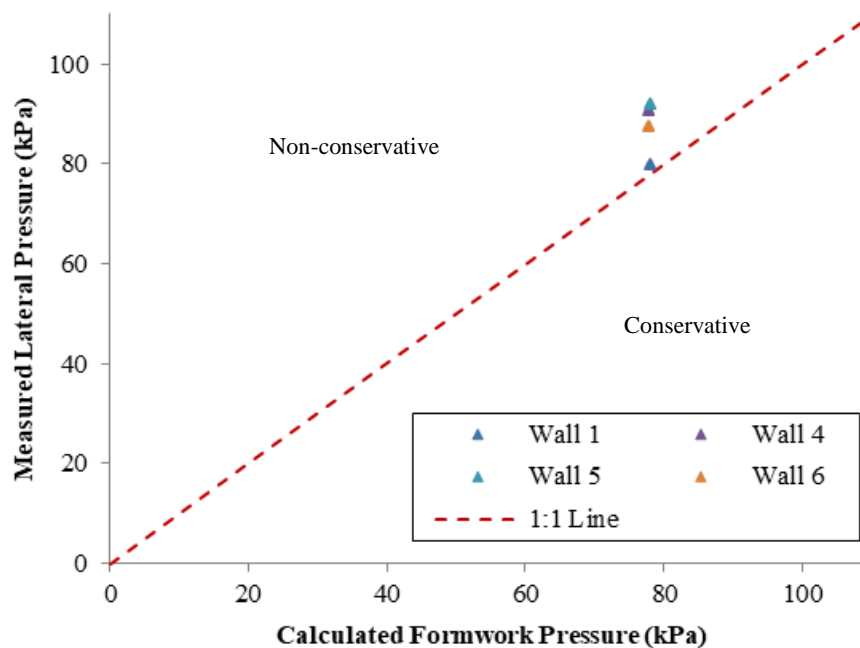


Figure 5-50: Measured pressure at a casting height of 4.2 meters vs. Gardner (2014) Eq.13.

Gardner (2014), modified casting rates

Figure 5-51 shows the comparison of the predicted pressures from Gardner (2014) to the pressures from the modified casting rates of Wall 2 and Wall 3 at the end of casting. It was found that the model calculated pressures are close to pressures from the modified casting rates, falling within the conservative zone. The predicted pressures for Wall 2 and Wall 3 showed an overestimation of 11.4% and 5.9 % when compared to the experimental data.

Omitted research models

The Models proposed by Vanhove et al. (2004), Tejeda-Dominquez (2005), Ovarlez & Roussel (2006) and Khayat & Omran (2011B) could not be compared to the experimental data, because a number of the model inputs could not be identified. This is due to the models mentioned requiring a number of tests to be performed in the laboratory on the concrete to determine the required inputs these are not tested or furnished by Lafarge. These tests could not be performed at the university's laboratory because the author could not get the required concrete mix design in order to prepare samples.

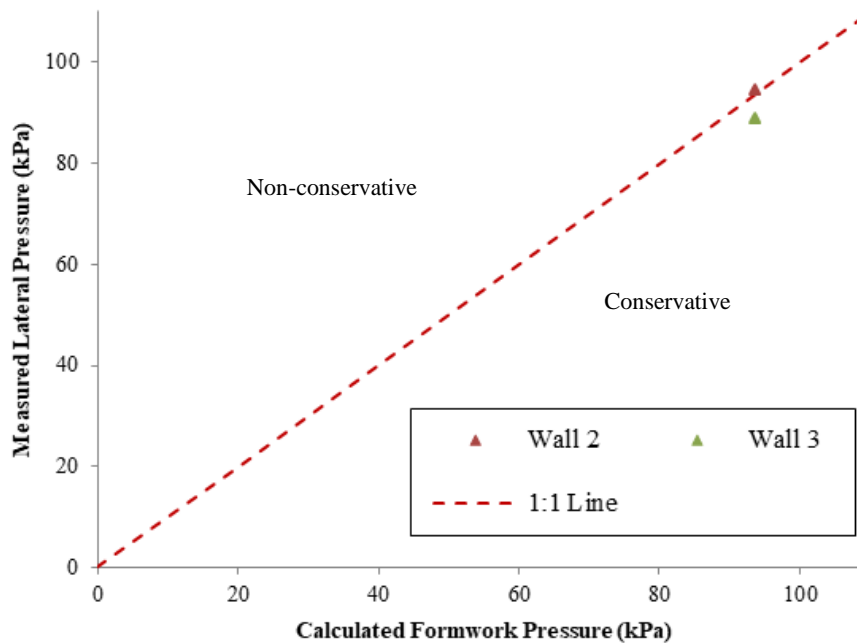


Figure 5-51: Pressures from the modified casting rates at the end of casting vs. Gardner (2014) Eq.13.

Omitted standard models

The ACI Committee 347 (2014) could not be compared to the measured lateral pressure, because the model is only valid when $R < 2.1$ m/h and $H < 4.2$ m for Eq.A.14 and when $R < 2.1$ m/h and $H > 4.2$ m for Eq.A.15. Where R is the casting rate (m/h) and H is the vertical formwork height (m). Finally the DIN 18 218 (2010) could not be compared, because the model is only valid for SCC with a consistency range (slump flow) ≤ 550 mm.

5.4.5 Site Observations

In this section the observations made on the experimental site are presented. Firstly it was found that when performing the tests on Walls 1 to 6, it was common practice for the pumping operators to cast the SCC at its highest allowable rpms despite a request for slower speeds. This would suggest it was not custom for the operators to cast the concrete at various predetermined casting rates. The formwork designer thus does not have much control over the type of equipment that is used for concrete placement

Secondly, it was found that predetermining the casting rate of the concrete was very difficult, because the pumping operators operate their cast in terms of rpms and not in terms of the flow rate (m^3/h). This would make it difficult for a formwork designer to request a specific flow rate, as the operator would not be able to set the pump to cast at the requested flow rate. Therefore, the formwork designer has limited to no influence in determining the speed of the concrete placement.

It was observed that when reaching the concrete fill height, the pump operator would reduce the pumping speed therefore reducing the casting rate near the end of casting.

Thirdly, it is probably standard industry practice, but it was once again observed that many factors can play a role in the delay or disrupt the pre-planned time and procedure of the concrete placement. During these tests these include protesting local residents, traffic, delayed readiness of formwork, weather and availability of pumps (equipment).

Finally, it was found that most of the construction personnel (site staff and pump operators) involved in the study had little to no prior knowledge of SCC, its advantages and disadvantages as well as how the concrete performs.

5.5 Conclusion

This chapter presented the results obtained from the investigation involving the top-down and bottom-up casting of SCC at high casting rates, as well as the lateral pressure obtained from interrupting the casting process and implementing predetermined waiting periods.

Top-down pumping

It was found that when casting at a rate of 80 m/h from the top of the experimental wall, the maximum lateral pressure was below the theoretical hydrostatic pressure up to a height of 4.2 meters. It was then found that the lateral pressure steadily approaches hydrostatic pressures as the SCC rises in the wall element. It was found that interrupting the casting process and implementing waiting periods of 10 and 15 minutes to achieve an average casting of 27 m/h and reduced the maximum lateral pressure induced by the SCC by 9 – 14 % when compared to the associated hydrostatic pressures.

Bottom-up pumping

From the results of the experiments in which the SCC was pumped from the base of the experimental wall at three different casting rates of 55, 65 and 80 m/h, it was seen that there was no substantial difference in the maximum lateral pressure and hydrostatic pressure.

An Ansys Fluent simulation was created modelling the pumping of water and it was found that the pressures simulated were equal to the theoretical hydrostatic pressures. It follows that increased concrete pressures was probably due to a combination of the concrete's rheology, friction between the concrete and formwork panels and the pressures exerted by the portable pump.

Comparison with existing models

A comparison of the results from Walls 1 to 6 with the models covered in the literature was presented in the chapter. It was found that the pressures predicted by the models from the CIRIA Report 108 (1985) and Gardner (2014) were conservative when compared to the experimental results at the end of casting.

From the CIRIA Report 108 (1985) model, the predicted pressures for Wall 1 showed an underestimation of 1% when compared to the experimental data. For Wall 2, Wall 3 and Wall 4 the predicted pressures showed an overestimation of 9.1 %, 14.4 % and 3 % when compared to the experimental data and for Wall 5 and Wall 6 the predicted pressures were equal to the experimental data.

From the Gardner (2014) model, the predicted pressures for Wall 1, Wall 5 and Wall 6 showed an underestimation of 2.3 %, 1.1 % and 1.2 % when compared to the experimental data. For Wall 2, Wall 3 and Wall 4 the predicted pressures showed an overestimation of 5.9 %, 11.4 % and 1.6 % when compared to the experimental data.

However, when comparing the prediction pressures to the experimental results at a casting height of 4.2 m it was found that the values from CIRIA Report 108 (1985) and Gardner (2014) were non-conservative when pumping from below, and slightly conservative when pumping from above.

From the CIRIA Report 108 (1985) model, the predicted pressure for Wall 1, Wall 4, Wall 5 and Wall 6 showed an underestimation of 1%, 14.9%, 16.5 % and 10.9 % when compared to the experimental data. From the Gardner (2014) model, the predicted pressure for Wall 1, Wall 4, Wall 5 and Wall 6 showed an underestimation of 1%, 14.9%, 16.5 % and 10.9 % when compared to the experimental data.

Yet, when comparing the prediction pressures to the pressures from the modified casting rates at the end of casting it was found that the values from CIRIA Report 108 (1985) were non-conservative, and the values from Gardner (2014) were conservative.

From the CIRIA Report 108 (1985) model, the predicted pressures for Wall 2 and Wall 3 showed an underestimation of 64 % and 54.5 % when compared to the experimental data. From the Gardner (2014) model, the predicted pressures for wall 2 and wall 3 showed an overestimation of 11.4% and 5.9 % when compared to the experimental data.

Lastly, the chapter covered the observations made by the author when performing the experiments. Chapter 6 summarises the conclusions from the study and any future recommendation.

Chapter 6 : Conclusion and Recommendations

6.1 Introduction

In this chapter the observations made from the experimental investigation are discussed. A summary of the results recorded during the investigation is presented, and some are highlighted and explained. Finally, recommendations are made for future research with regards to the lateral formwork pressure exerted by Self-Compacting Concrete (SCC).

6.2 Research Conclusion

Based on the investigation undertaken regarding the lateral formwork pressure exerted by SCC, the lack of understanding and knowledge, which is exacerbated by the scarcity of literature in the South African construction industry, has become clear. It is certain that more research is needed to determine the exact magnitude of, and identify the most important parameters influencing the lateral pressure of SCC.

The aims of this practical investigation were answered by the following:

From the experimental investigation it can be concluded that for high casting rates from the top of the formwork system hydrostatic pressure can be expected, as the SCC does not have the opportunity to set. However, it was found that by interrupting the casting process and implementing waiting periods so that the fresh SCC could set, the lateral pressure exerted was decreased. This phenomenon could be expected; as a result of the concrete having the opportunity to build up its internal structure through thixotropic behaviour and hydration, which gives it more resistance to the shearing caused by the concrete being pumped from the top of the wall element. It was found that when comparing Wall 2 and 3 with the same average casting rate the concrete temperature had no significant effect on the lateral pressure at the end of the casting process, this observation was also noted by Khayat and Assaad (2006) in their investigation.

It was found that, when pumping from the base of the formwork system at high casting rates, hydrostatic pressures could be expected at the end of the casting process and that lateral pressures over the hydrostatic pressures level could be expected during the casting of the SCC. That the lateral pressure exerted was over the predicted hydrostatic pressure could be attributed to a combination of the concrete's rheology, friction between concrete and formwork panels and the pressures exerted by the portable pump, thus an increase in lateral pressure could be expected as the height of the element increases.

A simple Ansys Fluent simulation was performed on a model using water as fluid to investigate the build-up of pressure when pumping from below. It was found that the pressures simulated were equal to the theoretical hydrostatic pressures. It was suggested that the reason for the pressures exceeding the theoretical hydrostatic pressures could be a combination of the concrete's rheology, friction between concrete and formwork panels and the pressures exerted by the portable pump.

In a comparison of the existing theoretical models with the experimental data, it was found that both CIRIA Report 108 (1985) and Gardner (2014) showed conservative predictions at the end of casting. However both models showed non-conservative values when predicting the pressure at a casting height of 4.2 m. When comparing the experimental values to the predicted pressures generated from the modified casting rates it was shown that CIRIA Report 108 (1985) demonstrated non-conservative values, however Gardner (2014) showed a conservative comparison.

From the investigation it was found that it was common practice for pumping operators to cast SCC at its highest allowable rpms, suggesting it was not common for the operators to cast SCC at various predetermined casting rates. It was found that predetermining the casting rate of the concrete was difficult due to the pumps being operated in rpms and not in terms of (m^3/h), making it difficult to request for a specific flow rate. It was observed that most of the construction personal (site staff and pump operators) involved in the study had little to no knowledge of SCC, its advantages and disadvantages as well as how the concrete performs.

Therefore, based on the results presented in this study and within the range of the tested parameters, it is recommended that calculations for formwork systems be based on the predicted pressures prescribed by CIRIA Report 108. However, efforts should be made to investigate the model presented by Gardner (2014) as the prediction values calculated are close to the experimental values presented in this study.

From the investigation it can be concluded that high placement rates result in high pressures. More field work is necessary in order to gain more insight into the lateral pressure problem, by investigating different pumping rates, pumping equipment and element dimensions. Because of the challenging situations in the South African construction industry, the requirement for a code of standards must be further investigated in order to save money when constructing formwork systems. In addition, a programme should be launched to educate the industry of characteristics and benefits of SCC.

The objectives of the practical investigation were completed by:

1) Literature review

From the literature it was found that most of the investigations were being performed in the laboratory. The study therefore concentrated on performing experiments under site conditions by investigating the placement methods (top-down and bottom-up pumping), casting rates and casting methods (constant casting and implementing waiting periods).

2) SCC mix

During the course of the investigation it was found that Agilia Vertical was a suitable SCC to use in full-scale wall elements. This was supplied by Lafarge and used in all experiments on this study.

3) Placement methods:

After consulting industry practitioners it was found that SCC was either cast from the top or from the base of formwork systems via the use of a concrete boom and portable pump.

4) Field tests

From the gathered information field tests on full-scale walls elements were performed and practical data was gathered and compared.

5) Practical data

It was found that the formwork designer has limited influence on site procedures and casting rates. The South African industry has limited experience with SCC and the temporary works designer needs to be prudent when specifying execution procedures which may limit the lateral pressures on the formwork.

6.3 Limitations of Experimental Results

The following limitations in the experimental results should be considered, as the results and conclusions are only valid for:

- The South African construction industry
- SCC (Agilia Vertical) supplied by Lafarge
- Walls and not columns
- Walls with the dimensions of 5.4 x 2.0 x 0.25 m (for longer walls, these results would be conservative due to lower effective casting rates for longer walls)
- High casting rates (as found in the current construction industry, lower casting rates will result in lower pressures)

6.4 Research Recommendations

It is recommended that a number of areas be investigated in future research studies to better understand the lateral pressure exerted on formwork by SCC. It should be kept in mind that numerous parameters beyond the scope of this research study are known to influence the lateral pressure exerted by SCC on formwork and should be investigated.

A further study recommended for research is to investigate the effect of South African produced SCC mixes on the lateral pressure, by quantifying the effect of the individual ingredients of the paste (i.e. aggregate characteristics; fly ash; cement; silicon fume; Viscosity-modifying Admixture (VMA) and superplasticiser and to quantify the thixotropy of the mixes and correlate it with the casting rate and method of placement. Thus, it is recommended that further research be carried out on how to develop more varying SCC mixes for the South African construction industry, in order to make an adequate prediction of formwork pressure.

Another recommendation is to investigate the concrete pumping line from the pump to the wall inlet, when the fresh concrete is pumped from the base of the formwork, to determine whether it has any influence on the flow characteristics of the fresh concrete. There is still limited research available on the characteristics of fresh concrete and its properties when it exits the concrete truck or the mixer. SCC is most often placed in the same way as Conventional Vibrated Concrete (CVC), and the same equipment is used to place the fresh concrete. The main difference between SCC and CVC is observed in the fresh state, as SCC has a significantly lower yield stress. Therefore, it is recommended that the influence of the flow of SCC in the pipes; and the dimensions of the pipes on the fresh properties of the SCC should be investigated, especially when pumping from the base of the formwork.

It is recommended that the effect of reinforcement on the lateral formwork pressure, when pumping SCC either from the base or from the top of the formwork system, be investigated. Finally, research is required to compare and investigate proposed models from different researchers which could not be investigated in this investigation to data generated in South Africa, in order to identify which research model should be codified for the South African construction industry.

References

- ACI Committee 237, (ACI 237R-07) (2007). Self-Consolidating Concrete. American Concrete Institute, Farmington Hills, Michigan, ACI Standard, 2007
- ACI Committee 347, (ACI 347-04) (2004). Guide to formwork for Concrete. American Concrete Institute, Farmington Hills, Michigan, ACI Standard, 2004, 32 pp.
- ACI Committee 347, (ACI 347-14) (2014). Guide to formwork for Concrete, American Concrete Institute, Farmington Hills, Michigan, ACI Standard, 2014, 35 pp.
- Assaad, J.J., Khayat, K.H., and Mesbah, H. (2003a) ‘Assessment of Thixotropy of Flowable and Self-Consolidating Concrete’. In: ACI Materials Journal, 100(1), 2003: 99 - 107
- Assaad, J.J., Khayat, K.H. and Mesbah, H. (2003b). ‘Variation of formwork pressure with thixotropy of self-consolidating concrete’. In: ACI Material Journal.2003, 100: 29-37.
- Assaad, J.J. (2004). ‘Formwork Pressure of Self-Consolidating Concrete – Influence of Thixotropy’. Dissertation Doctoral in Civil Engineering, Sherbrooke University, Quebec Canada.
- Assaad, J.J., and Khayat, K.H. (2004). ‘Formwork Pressure of Self-Consolidating Concrete – Influence of Thixotropy. Progress in Concrete. Conference Paper January 2004.
- Assaad, J.J., and Khayat, K.H. (2005a). ‘Formwork Pressure of Self-Consolidating Concrete made with various binder types and contents’. In: ACI Materials Journal, 103(4), 2006: 280-287.
- Assaad, J.J., and Khayat, K.H. (2005b). ‘Kinetics of Formwork pressure drop of SCC containing various types and contents of binder’. In: Cement and Concrete Research, 2005, 35: 1522 1530.
- Assaad, J.J., and Khayat, K.H. (2005c). ‘Effect of Coarse Aggregate Characteristics on Lateral Pressure exerted by Self-Consolidating Concrete’. In: ACI Materials Journal, 102(3): 145 153.
- Assaad, J.J., and Khayat, K.H. (2006a). ‘Effect of viscosity-enhancing admixture on formwork pressure and thixotropy of self-consolidating concrete’. In: ACI Materials Journal, 103-M31, 2006: 280-287.
- Assaad, J.J, and Khayat, K.H. (2006b). ‘Effect of mixture consistency on formwork pressure exerted by highly flowable concrete’. In: Journal Material Civil Engineering, 18(6), 2006: 786 792.
- Assaad, J.J. and Khayat, K.H. (2006c). ‘Effect of casting rate and concrete temperature on formwork pressure of Self-Consolidating concrete’. In: Materials and Structures, 39, 2006: 333 341.

ASTM C1611/C1611M-14 (2014). Standard Test Method for Slump Flow of Self-Consolidating Concrete. ASTM International American Standard Test Methods.

ASTM C494/C494M-17 (2017). Standard Specification for Chemical Admixtures for Concrete. American Standard Test Methods.

Badman, C., Bareño, J., Baur, K., Boster, C., Calvert, C., et al. (2003). Interim Guidelines for the use of Self-Consolidating Concrete in Precast/Prestressed Concrete Institute Chicago, Member Plants TR-6-03.

Barnes, H.A., Hutton, J.F., and Walters, K. (1989). 'An Introduction to Rheology, Elsevier, Amsterdam, 1989, 199.

Barnes, H.A. (1997). 'Thixotropy – A Review'. In: Journal of Non-Newtonian Fluid Mechanics, 70 (1-2), May 1997 : 1 – 33.

Barnes, H.A., and Nguyem Q.D. (2001). 'Rotating Vane Rheometry – a Review.' Journal of Non-Newtonian Fluid Mechanics, 98 (1) : 1 – 14.

Billberg, P. (2003). 'Form Pressure generated by Self-Compacting Concrete'. In: Proceeding of the 3rd International RILEM Symposium on Self-Compacting Concrete, Eds. Wallevik, O., and Nielsson, I., Reykjavik, Iceland, August 2003: 271 -280.

Billberg, P. (2005). 'Development of SCC static yield stress at rest and its effect on the lateral form pressure, Proceedings of the Second North American Conference on the Design and use of Self-Consolidating Concrete and the Fourth International RILEM Symposium of Self-Compacting Concrete, edited by S.P. Shah, October 30 – November 3, 2005, Chicago, USA.

Billberg, P. (2006). 'Form pressure generated by SCC – influence of thixotropy and structural behaviour at rest'. PhD dissertation, Royal Institute of Technology, Stockholm, 2006.

Billberg, P. (2012). 'SCC Mixture Design and its Influence on Rheology. Factors affecting the rheology of SCC and how to control it'. RILEM TC-FPC "Form pressure generated by fresh concrete" International Workshop on Self-Compacting Concrete, Stockholm, June 1st 2012.

Bokelman, K., Bastiaanse, G., Du Plessis, G., Heymann, F., Huber, U., Koorn, H. and Wium, J. (2011). 'South African Football Stadiums for the 2010 FIFA World Cup'. In: Structural Engineering International 1/2011.

- Bonen, D. and Shah, S. (2005). 'Fresh and hardened properties of self-consolidating concrete, Journal of Progress in Structural Engineering and Materials, No. 7. New Jersey: John Wiley & Son Ltd: 14-26.
- Brameshuber, W., and Uebachs, S. (2003). 'Investigation on the Formwork Pressure using Self-Compacting Concrete'. In: Proceedings of the 3rd International RILEM Symposium on Self-Compacting Concrete. Eds. Wallevik, O., and Nielsson, I., Reykjavik, Iceland, August 2003: 281 – 287.
- BS 5975: 2008+A1: (2011). Code of practice for temporary works procedures and the permissible stress design of falsework. British Standards Institution, London, UK, 2008.
- BS EN 12812:2008. (2008) Falsework – Performance Requirements and General Design. British Standards Institution, London, UK, 2008.
- Cauberg, N. and Desmyter, J. (2007). 'Measuring the Formwork pressure of Self-Compacting Concrete'. Belgium Building Research Institute (BBRI), 2007.
- CIFA, Technical Data Sheet, Portable Concrete Pump PC907/612 S8. [Online] Available: www.cifa.com/portable-pump/-/13/104. [Accessed 2017, June 29].
- CIFA, Technical Data Sheet, K31L Truck mounted concrete boom pump. [Online] Available: www.cifa.com/truck-mounted-pumps. [Accessed 2017, June 29].
- CIRIA Report 108 (1985). Concrete Pressure on Formwork. Construction Industry Research and Information Association. London, 1985, 31 pp.
- Deb, S. (2013). 'An insight into Formwork Pressures using Self-Consolidating Concrete'. In: The Masterbuilder, April 2013.
- Delf Consulting Engineers Pty Ltd. Road Structures – N4 Bakwena Toll Road Bridge Extensions. [Online] Available: www.delfengineers.com/images/bridges/brdg2.gif. [Accessed 2017, May 9].
- De Schutter, G. (2005). Guidelines for testing fresh Self-Compacting Concrete. European Research Project: Measurement of Properties of fresh Self-Compacting Concrete, 2001 – 2004. Growth Contract No. GRD2-2000-30024.
- De Schutter, G., Feys, D., and Verhoeven, R. (2010). 'Ecological profit for a concrete pipe factory due to self-compacting concrete technology'. Zachar J. et al., editors. Proceedings of the 2nd International conference on sustainable construction materials and technologies, 2, Ancona, 2010: 1281 – 1287.

- DIN 18218: 2010-01. Formwork Pressures DIN German Standard updated 2010. Concrete International 32, 6: 27-29.
- Domone, P. (2009). 'Proportioning of Self-compacting concrete – the UCL method'. UCL Department of Civil, Environmental and Geomatic Engineering.
- Drewniok, M.P., Cygan, G., and Golaszewski, P. (2017). 'Influence of the rheological properties of SCC of the formwork pressure'. In: Procedia Engineering 192 (2017) : 124 – 129.
- DYWIDAG Systems International. The Nelson Mandela Bridge – A New landmark for Johannesburg. [Online] Available: <https://www.dywidag-systems.com/projects/project-details/article/nelson-mandela-bridge-johannesburg-south-africa.html> [Accessed 2017, May 9].
- EN B. 2006. 206-1 (2000). Concrete Part 1: Specification, Performance, Production and Conformity. British Standards Institution, London, UK: 1-20.
- Felekoğlu, B., Tosun, K., Baradan, B., Altun, A., and Uyulgan, B. (2006). 'The effects to fly ash and limestone fillers on the viscosity and compressive strength of self-compacting concrete repair mortars. In: Cement, Concrete Research 2006, 36: 1719 - 1726.
- Ferron, R.P., Gregori, A., Sun, Z., and Shah, S.P. (2007). 'Rheological method to evaluate structural build-up in self-consolidating concrete cement pastes, ACI Materials Journal, 104 (3) (2007) : 242-250.
- Feys, D. (2008). 'How Self-Compacting Concrete can be destroyed'. Doctoral dissertation, Departments of Structural and Civil Engineering, Ghent University, Gent, Belgium.
- Galeota, D., Giammatteo, M.M., Gregori, A., Marino, R. and Shah, S.P. (2007). 'Formwork Pressure of Self-Compacting Concrete'. 5th International RILEM Symposium on Self-Compacting Concrete. 3 – 5 September, 2007, Ghent, Belgium.
- Gambhir, M.L. (2013). Concrete Technology, Fifth edition. Published by: McGraw Hill Education (India), Private Limited, New Dehli, 2013.
- Gardner, N.J. (1980). 'Pressure of Concrete against Formwork'. In: ACI Journal, Technical Paper, Title No. 76-35, July 1979: 809-820.
- Gardner, N.J. (1985). 'Pressure of Concrete on Formwork – A Review'. In: ACI Journal, Technical Paper, Title No. 82-69, 1985: 744-752.

- Gardner, N.J. (2014). 'Pressure of Self-Consolidating Concrete on formwork. A new model for lateral pressure determination'. In: Concrete International July, 2014: 53-50.
- Geel, A., Beushausen, H., and Alexander, M. (2007). 'The current status of Self-Compacting Concrete in South Africa'. In: Concrete Beton Journal, September 2014, p. 11.
- Giammatteo, M.M., Gregori, A., and Totani, G. (2007). 'In-situ measurement of formwork pressures generated by Self-Compacting Concrete'. In: WIT Transactions on Modelling and Simulation, 46, 2007.
- Graubner, C-A, Boska, E., Motzko, C., Proske, T., and Dehn, F. (2012). 'Formwork pressure induced by highly flowable concretes – design approach and transfer into practice'. In: Structural Concrete 13(1), 2012: 51 – 60.
- Haddadou, N., Chaid, R., Ghernouti, Y., Adjou, N, and Bouzoualegh, M. (2015). 'Fresh and hardened properties of self-compacting concrete with different mineral additions and fibers'. In: Journal Material Structure, (2015) 2: 41 – 50.
- Hurd, M.K. (2005). 'Formwork for concrete'. 7th ed. Farmington Hills: American Concrete Institute: 2005.
- Janssen, H. (1895). 'Versuche uber Getreidedruck in Silozelle' (Silo Theory). VDI Zeitschrift, 39: 1045 – 1049.
- Jooste, P. (2004). 'Significant project: Bridge 2235 – N4 Platinum Toll Highway, Midrand': The Concrete Society of Southern Africa, 2004. In: Concrete Beton, 2004.
- Jooste, P. (2009). 'Self-Compacting Concrete'. In: Concrete/Beton, 1(1): 18-19, 20-23.
- Khayat, K.H., Saric-Coric, M., and Liotta, F. (2002). 'Assessment of thixotropy and impact on stability of cementitious grout and concrete, ACI Materials Journal, 99 (3) (2002): 234-241.
- Khayat, K.H., Assaad, J.J., Morin, R., and Thibeault, M. (2005). 'Performance of Self-Consolidating Concrete in Repair of Concrete Wall Elements'. In: Proceedings of the 2nd North American Conference on the Design and Use of Self-Consolidating Concrete (SCC 2005), and the 4th International RILEM Symposium on Self-Compacting Concrete, (eds.) Shah, S.P., Chicago, 2205, : 1003 – 1012.
- Khayat, K.H., and Assaad, J.J. (2006). 'Effect of w/cm and High-Range Water-Reducing Admixture on Formwork Pressure and Thixotropy of Self-Consolidating Concrete'. In: ACI Materials Journal 103(3), 2006: 186-193.

- Khayat, K.H., Bonen, D., Shah, S., and Taylor, P. (2007). 'SCC Formwork Pressure – Task 1: Capturing existing knowledge on Formwork Pressure exerted by SCC', February, 13, 2007.
- Khayat, K.H., and Assaad, J.J. (2008). 'Measurement systems for determining formwork pressure of highly-flowable concrete'. In: *Materials and Structures*, (2008), 14(1): 37 – 46.
- Khayat, K.H. and Omran, A.F. (2009). 'State-of-the-Art Review of Form Pressure Exerted by Self-Compacting Concrete'. December, 2009.
- Khayat, K.H., Omran, A.F. and Pavate, A. (2010). 'Inclined Plane Test Method to determine Structural Build-up at rest of Self-Consolidating Concrete. In: *ACI Material Journal*, 107, (5): 515-522.
- Khayat, K.H. and Omran, A.F. (2011). 'Field Monitoring of SCC Formwork Pressure and Validation of Prediction Models'. In: *Journals of Concrete International*. 33(6): 33-39.
- Khayat, K.H., Omran, A.F., Naji, S., Billber, P., and Yahia, A. (2012a). 'Field Oriented Test Methods to Evaluate Structural Build-Up at Rest of Flowable Mortar and Concrete. *RILEM Materials and Structures*, 45, (10): 1547-1564.
- Khayat, K.H., Omran, A., and Magdi, W.A. (2012b). 'Evaluation of thixotropy of Self-Consolidating Concrete and influence on concrete performance'. *Anais do 54º Congresso Brasileiro de Concreto – CBC2012-54CBC*.
- Khrapko, M. (2007). 'Self-Compacting concrete – A Solution for Technology Hungry Concrete Construction'. In: *Proceedings of Civil Engineering Testing Conference*, 2008, New Zealand.
- Kim, S.G. (2010). 'Effect of heat generation from cement hydration on mass concrete placement'. Master of Science Graduate Thesis and Dissertation. 11675, Civil Engineering (Geotechnical Engineering), Iowa State University.
- Koehler, E.P. (2009). Use Rheology to Specify, Design and Manage Self-Consolidating Concrete, In: 9th International Conference on Superplasticizers and 10th International Conference on Recent, Seville, Spain, October 2009 : 609 – 623.
- Koehler, E.P. and Fowler, D.W. (2003). Summary of Concrete Workability Test Methods. Technical Research Report No. ICAR 105-1, August 2003.
- Lange, D.A., Birch, B., Hennen, J., Liu, Y-S., Tejeda-Domingues, F., and Struble, L. (2008). 'Modelling Formwork Pressure of SCC'. 3rd North American Conference on the Design and Use of

- Self-Consolidating Concrete 2008: Challenges and Barriers to Applications, S.P. Shah, ed., 2008: 295-300.
- Lange, D.A., Liu, Y-S, and Henschen, J. (2009). 'Modeling Formwork Pressure of SCC'. 2nd International Symposium on Design, Performance and Use of Self-Consolidating Concrete, SCC 2009-China, June 5 -7 2009, Beijing, China.
- Lange, D. (2012). 'Mechanisms of SCC Formwork Pressure'. In: International Workshop, Self-Compacting Concrete, Section 3 - Formwork Pressure, Stockholm, Sweden, June 1, 2012.
- Lapasin, R., Papo, A., and Rajgelj, S. (1983). 'Flow Behaviour of Fresh Cement Pastes. A Comparison of Different Rheological Instruments and Techniques'. In: Cement and Concrete Research, 13, 1983 : 349 – 356.
- Leeman, A., and Hoffmann, C. (2003). 'Pressure of Self-Compacting Concrete on the Formwork'. In: Materials and Systems for Civil Engineering EMPA Activities 2003 Betonwerk und Fertigteil-Technik/ Concrete Plant and Precast Technology, 69(11), November, 2003: 48- 55.
- Leeman, A., Hoffmann, C., and Winnefeld, F. (2005). 'Influence of the Mix Design on the Formwork Pressure of Self-Compacting Concrete'. In: Proceeding of the 2nd North American Conference on the Design and use of Self-Consolidating Concrete (SCC) and the 4th International RILEM Symposium on Self-Compacting Concrete, Eds. Shah, S.P., Chicago, 2005: 635 - 640.
- Leeman, A., Hofmann, C., and Winnefeld, F. (2006). 'Pressure of Self-Consolidating Concrete on Formwork'. In: Concrete International, 28(2): 27 – 31.
- Liu, F. (2014). 'Early-age hydration studies of Portland cement'. Dissertation of Doctor of Philosophy, Department of Civil and Environmental Engineering, University of Louisville, Louisville, Kentucky.
- Macklin, C. (1946). 'Pressure of Plastic Concrete on Forms'. In: USA Proceedings of the Society for Experimental Stress Analysis, 4(1), 1946: 112 – 122.
- Malherbe, J. and Wium, J. (2016) 'An economic evaluation methodology to compare the use of Self-Compacting concrete with normal concrete. *Concrete/Beton*, Number 146, September 2016:22-29.
- Moses, E.E., and Perumal, S.B. (2016). 'Hydration of Cement and its Mechanisms'. IOSR Journal of Mechanical and Civil Engineering (IOSR-JMCE) 13(6), Version 1, (Nov-Dec, 2016): 17 -31.

- McCarthy, R., and Silfwerbrand, J. (2011). 'Comparison of three methods to measure formwork pressure when using SCC'. In: Concrete International, 2011, 33(6): 27-32.
- Nehdi, M. and Rahman, M.A. (2004). 'Estimating rheological properties of cement pastes using various rheological models for different test geometry, gap and surface friction, In: Cement and Concrete Research, 34 : 1993 – 2007.
- Nemati, K.M. (2005). 'Temporary Structures – Formwork for Concrete'. ATCE-II Advanced topics in Civil Engineering, Tokyo Institute of Technology, Tokyo, Japan.
- NRMCA (2016). National Ready Mix Concrete Association. Concrete Work, Annual Convention, 10 -12 April, 2016. Loews Coronado Bay Resort, San Diego, CA, USA.
- Omran, A.F. (2009). 'Formwork Pressure Exerted by Self-Consolidating Concrete'. University of Sherbrooke, Quebec Canada, Department of Civil Engineering, June, 2009.
- Omran, A.F. and Khayat, K.H. (2014). 'Choice of thixotropic index to evaluate formwork pressure characteristics of self-consolidating concrete'. Cement and Concrete Research, 63(2014):89-97.
- Omran, A.F., and Khayat, K.H. (2013). 'Portable Pressure device to evaluate formwork pressure exerted by flowable concrete'. In: Material Civil Engineering, 2013, 25(6): 731 -740.
- Omran, A.F., Elaguab, Y.M., and Khayat, K.H. (2014). 'Effect of placement characteristics on SCC lateral pressure variations'. In: Construction and Building Materials, 2014, 66: 507 -514.
- Omran, A.F. and Khayat, K.H. (2016). 'Effect of Formwork Characteristics on SCC Lateral Pressure'. In: Journal of Materials in Civil Engineering, November, 2016.
- Ouchi, M. (2001). 'Self-Compacting concrete: development, applications and key technologies'. In: 26th Conference on Our World in Concrete & Structures: 27 – 28 August 2001, Singapore.
- Ovarlez, G. and Roussel, N. (2006). 'A Physical model for the prediction of lateral stress exerted by Self-Compacting Concrete on Formwork'. RILEM Material and Structures., 2006, 39, (2): 269 279.
- Ozawa, K., Naekawa, K., Kunishima, M., and Okamura. H. (1989). 'Development of high-performance concrete based on the durability design of concrete structures'. In: Proceedings 2nd East Asia and Pacific Conference on Structural Engineering and Construction (EASEC-2), 1989: 445 – 450 (Japanese).

- Perrot, A., Amziane, S. Ovarlez, G., and Roussel, N. (2009). 'Formwork pressure: Influence of Steel Rebars'. In: Cement and Concrete Research, 2009, 39: 524-528.
- Petersen, M. (2008). 'High-Performance and Self-Compacting Concrete in house building – Field tests and theoretical studies of possibilities and difficulties'. Doctoral thesis, Report TVBM-1027, Lund Institute of Technology, Lund University, Division of Building Materials.
- Proske, T., and Graubner, C-A, (2002a). 'Self-compacting concrete – pressure on formwork and ability to deaerate'. In: Darmstadt Concrete, 2002, 17: 1 – 15.
- Proske, T., and Graubner, C-A, (2002b). 'Pressure on formwork using SCC – experimental studies and modelling'. In: Proceedings of the 5th International RILEM Symposium on Self-Compacting Concrete, 2007, 17(2002): 1 -15.
- Puente, I., Santilli, A. and Lopez, A. (2010). 'Lateral pressure over formwork on large dimension concrete blocks'. In: Engineering Structures, 2010, 32: 195- 206
- Putzmeister, Technical Data Sheet – 36Z Meter Truck mounted concrete boom pump. [Online] available: <http://www.putzmeisteramerica.com/products/boom-pumps/boom-pumps-36z-meter-truck-mounted-concrete-boom-pump>. [Accessed 2017, June 29].
- Robert, H. (2007). Think Formwork – Reduce Costs. In: Structure Magazine, April 2007.
- Roby, H.G. (1935). 'Pressure of Concrete on Formwork'. In: Civil Engineering, 5, March, 1935, 162 pp.
- Roussel, N. 2006. A thixotropy model for fresh fluid concretes: Theory, validation and applications. Cement and Concrete Research, 36, (2006), pp. 1797 – 1806.
- Roussel, N., Geiker, M., Dufour, F., Thrane, L.N. and Szabo, P. (2007). 'Computational modelling of concrete flow: General overview. In: Cement and Concrete Research, Elsevier, 2007, 37: 1298 – 1307.
- SANS 10162-1 Ed 2.1 (2011). The structural use of steel. Part 1: Limit-states design of hot-rolled steel work. South African National Standards, Pretoria.
- SANS 1083 Ed 2.4 (2014). Aggregates from natural sources – Aggregates for concrete. South African National Standards, Pretoria.
- SANS 1491-1 (1989). Portland cement extenders – Part 1: Ground granulated blast furnace slag. South African National Standards, Pretoria.

SANS 50197 Ed 2. (2013). Cement, Part 1: Composition, specification and conformity criteria for common cements. South African National Standards, Pretoria.

SANS 5863 Ed 2.1 (2006). Concrete tests – Compressive strength of hardened concrete. South African National Standards, Pretoria.

Schwartzentruber, L.D., Roy, R.L., and Cordin, J. (2006). 'Rheological Behaviour of Fresh Cement Pastes formulated form Self-Compacting Concrete (SCC).' Cement and Concrete Research, 36 (7) : 1203 – 1213.

Senouci, A.B. and Al-Ansari, M.S. (1996). 'Optimum Design of Concrete Slab Forms'. In: Engineering Journal of University of Qatar, 9, 1996: 79 – 93.

Shaughnessy, R., and Clark, P.E. (1988). 'The rheological behaviour of fresh cement pastes, Cement and Concrete Research, 18 : 327 – 341.

Smith, R.C. and Andres, C.K. (1993). 'Principles and Practices of Heavy Construction' 4th Ed. Prentice Hall a division of Simon & Schuster, Englewood Cliff, New Jersey 07632.

Stanton, T.E. (1937). 'Measurement Pressure on Forms from Fresh Concrete'. In: Concrete, 45, 1937:11 – 16.

Szwabowski, J. 'Influence of three-phase structure on the yield stress of fresh concrete in Rheology of fresh cement and concrete, In: Proceedings of the International Conference organised by the British Society of Rheology, P.F.G. Banfill (eds.) Spon Press, London. 1991, : 241 – 248.

Szecszy, R., and Mohler, N. (2009). 'Self-Consolidating Concrete'. In: Concrete Technology, : 24.

Tattersall, G.H. and Banfill, P.G.F. (1983). The Rheology of Fresh Concrete, Pitmans Books Limited, London (1983).

Tejeda-Dominguez, F. (2005). 'Laboratory and field study of self-consolidating concrete formwork pressure'. M.Sc. Thesis. University of Illinois at Urbana-Champaign, 2005.

Tejeda-Dominguez, F., Lange, D.A., and D'Ambrosia, M.D. (2005). 'Formwork Pressure of Self-Consolidating Concrete (SCC) in Tall Wall Field Applications'. 84th Annual Meeting Transportation Research Board, Washington, DC, January 2005.

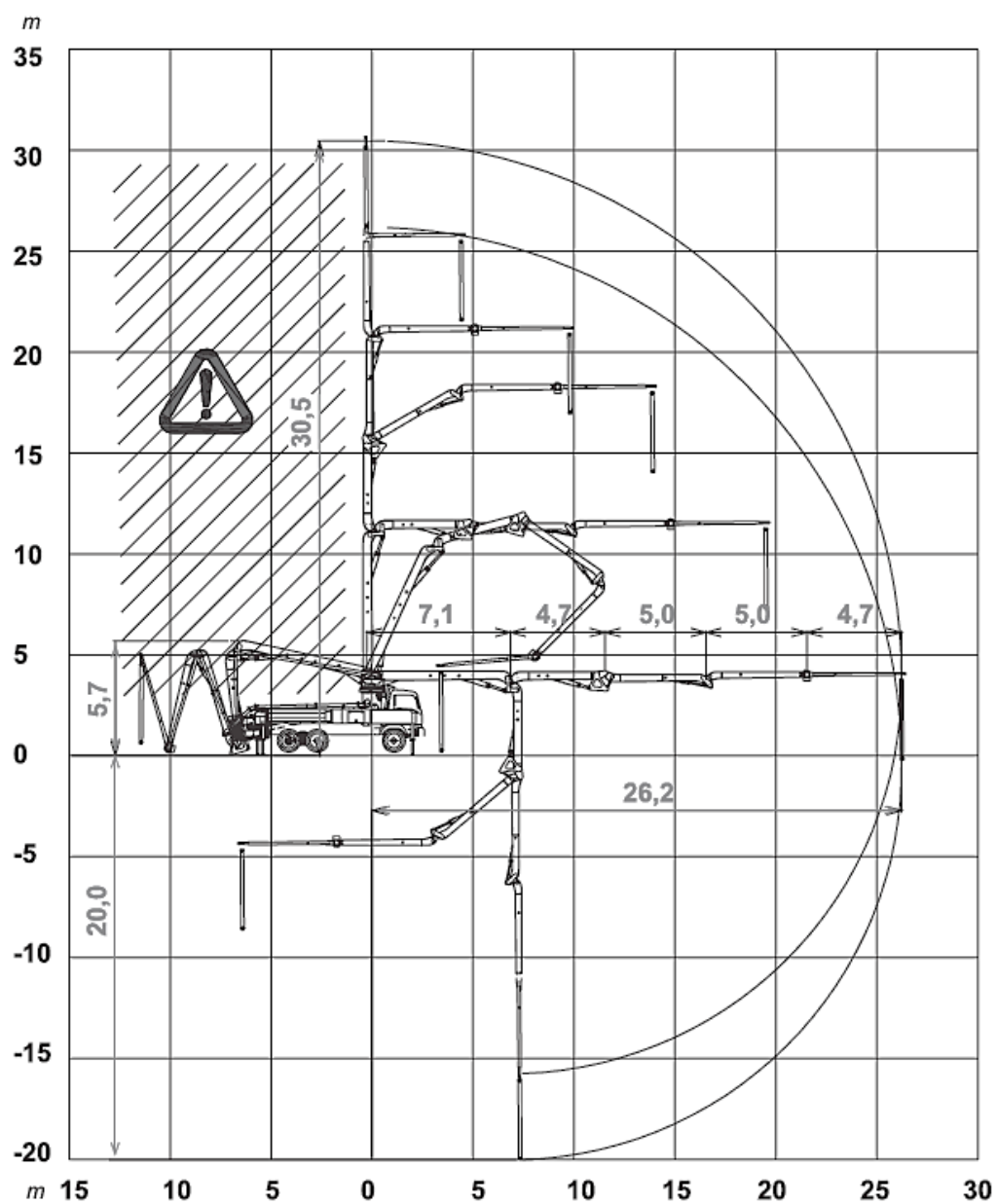
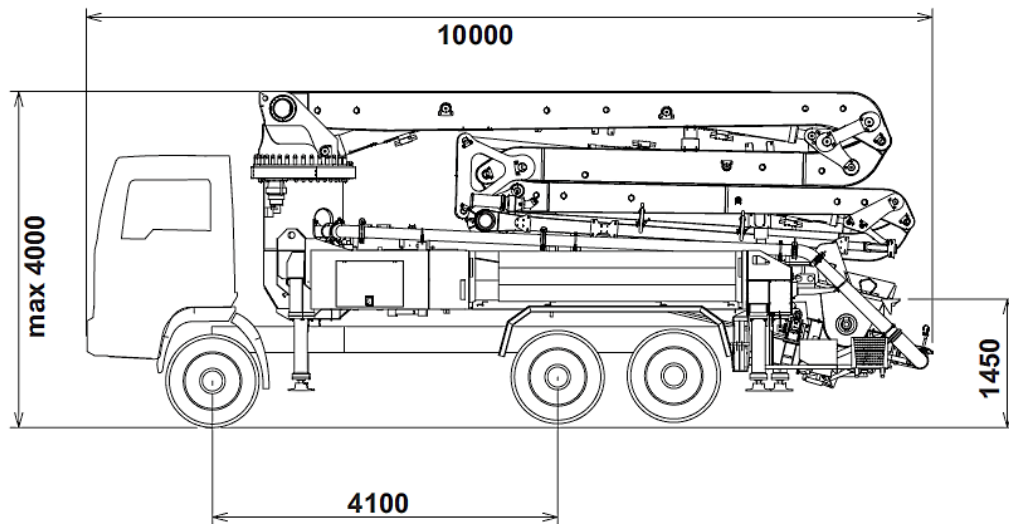
The Constructor, Civil Engineering Home. 'Concrete Formwork Checklist at site: Formwork checklists for walls'. [Online] Available: <https://theconstructor.org/concrete/concrete-formwork-checklist-at-site/9200/>. [Accessed 2017 August 16].

- Thrane, L.N., Pade, C. and Nielsen, C.V. (2008). 'Guidelines for mix design of Self-compacting concrete. Publisher: Danish Technological Institute, Concrete. Gregersensevej, DK-2630, Taastrup.
- Tichko, S., Van De Maele, J., Vanmassenhove, N., De Schutter, G., Vierendeels, J., Verhoeven, R. and Troch, P. (2014). 'Numerical simulation of formwork pressure while pumping self-compacting concrete bottom-up'. In: *Engineering Structures*. 70: 218–233.
- Tichko, S., De Schutter, G., Troch, P., Vierendeels, J., Verhoeven, R., Lesage, K. & Cauberg, N. (2015). 'Influence of the viscosity of self-compacting concrete and the presence of rebars on the formwork pressure while filling bottom-up'. In: *Engineering Structures*. 101: 698–714.
- Tregger, N.A., Ferrara, L. and Shah, S.P. (2008). 'Identifying Viscosity of Cement Paste from Mini-Slump-Flow Test'. *ACI Material Journal*, 105 (6): 558 – 566.
- Turk, K. (2012). 'Viscosity and hardened properties of self-compacting mortars with binary and ternary cementitious blends of fly ash and silica fume'. In: *Construction and Building Material* 37 (2012) : 326 -334.
- Vanhove, Y., Djelal, C., and Magnin, A. (2000). 'Friction Behaviour of a Fluid Concrete against a Metallic surface'. In: *International Conference on Advances in Mechanical Behaviour, Plasticity and Damage*, Elsevier Science Ltd, Euromat 2000, Tours, November 2000 (1): 679 – 684.
- Vanhove, Y., Djelal, C., and Magnin, A. (2004). 'Prediction of Lateral pressure exerted by self-compacting concrete on formwork'. In: *Magazine of Concrete Research*, 56, 1, February: 55–62.
- Van Waarde, F. (2007). 'Formwork pressures when casting Self-Compacting Concrete – A practical and numerical investigation'. Master's Thesis, Technical University of Delft, Concrete Structures, Faculty of Civil Engineering, March 2007.
- Wallevik, J. (2003). 'Rheology of Particle Suspensions, (Phd Thesis), Department of Structural Engineering, Norwegian University of Science and Technology, Trondheim, Norway, 2003, 397.

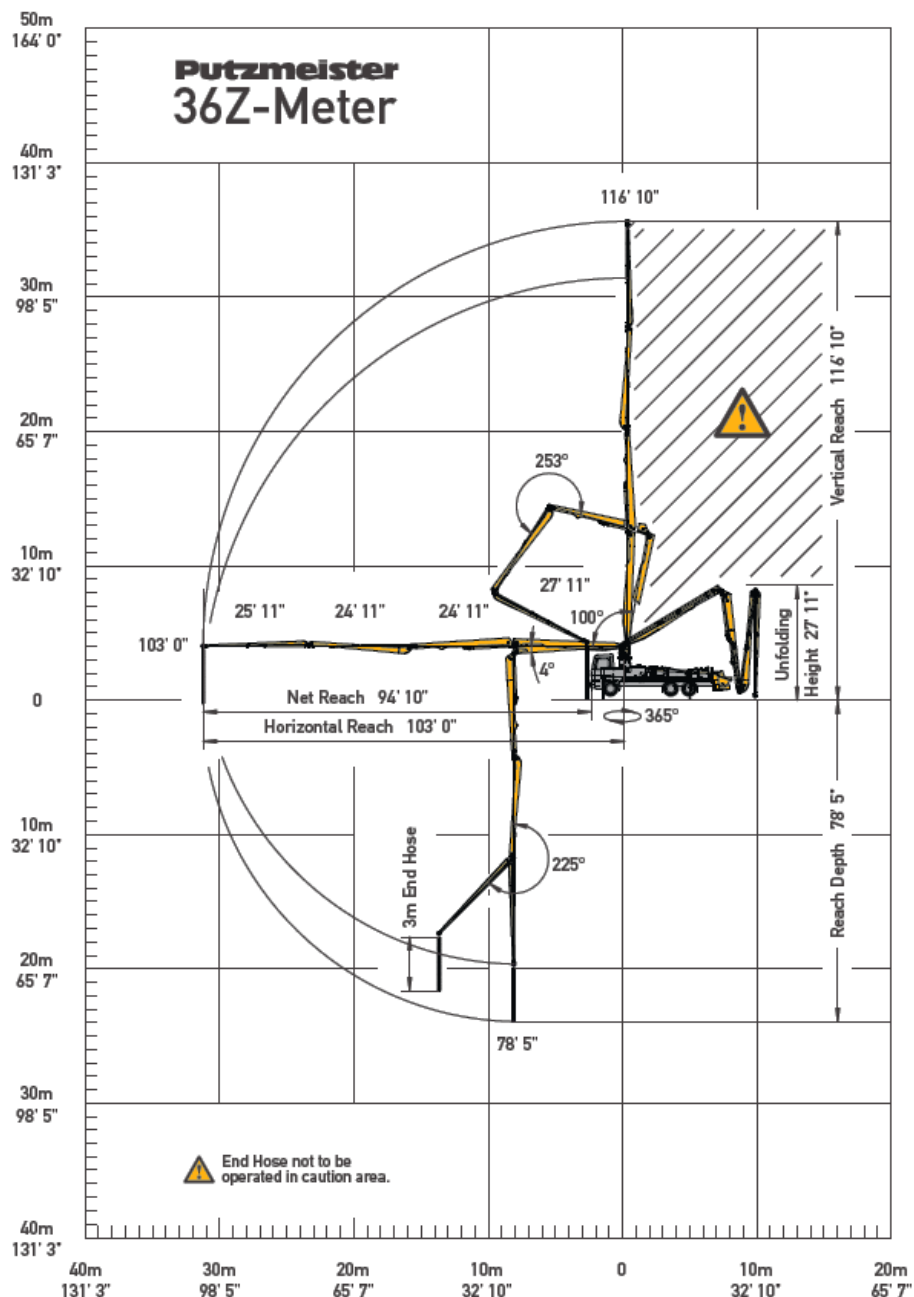
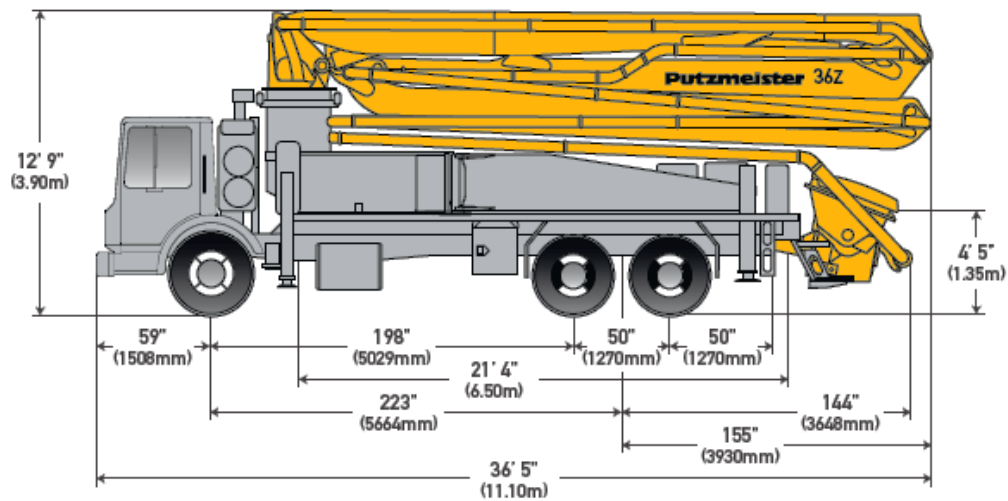
Bibliography

- Bhattacharya, K., Freund, B., Proske, T., Pandey, A.D., Lahiri, S.K., Sinha, A., Busetty, V.K., & Ravi, C. 2014. 'Numerical Modelling of Concrete Pressure on Vertical Formworks'. International Journal of Research (IJR), 1, 5, June 2014. ISSN 2348-6848.
- Das, A. 2014. 'Risk and Reliability Associated with use and re-use of vertical formwork'. Master of Science thesis in Civil Engineering, Oregon State University.
- Deng, Y. & Morcous, G. 2011. 'Construction Challenges of Cast-In-Place Self-Consolidating Concrete. 47th ASC Annual International Conference Proceedings.
- Djelal, C., Vanhove, Y., & Magnin, A. 'Correlation between friction coefficient and lateral pressure exerted by concretes on formwork'. Tribology, 1, 3, (2007).
- Gambatese, J.A., Barbosa, A.R. & Das, A. 2014. 'Use and Re-use of Formwork: Safety Risks and Reliability Assessment', (CPWR Small study No. 13-2-PS). Final Report. School of Civil and Construction Engineering, Oregon State University.
- Gregori, A., Raissa, Ferron, R.P., Sun, Z & Shah, S.P. 2008.'Experimental Simulation of Self-Consolidating Concrete Formwork Pressure, ACI Materials Journal, Title No. 105-M12, Technical Paper, January-February, 2008.
- Khayat, K.H., Assaad, J., Mesbah, H., & Lessard. 2004. 'Effect of section width and casting rate on variations of formwork pressure of self-consolidating concrete'. Materials and Structures, 37, 2004: 1- 6.
- Kwon, S.H., Phung, Q.T., Park, H.Y., Kim, J.H., & Shah, S.P. 2011. Cement and Concrete Research, 41, (2011): 90 – 101.
- Lopez-Arquillos, A., Rubio-Romero, J.C. and Gambatese, A.G.F. 2014. 'Safety Risk Assessment for vertical concrete formwork activities in civil engineering construction work' A Journal of Prevention, Assessment & Rehabilitation, 49,(2): 183-192.
- Teixeira, S., Santilli, A., & Puente, I. 2016. 'Analysis of casting rate for the validation of models developed to predict the maximum lateral pressure exerted by self-compacting concrete on vertical formwork. Journal of Building Engineering, 6, (2016): 215-224.

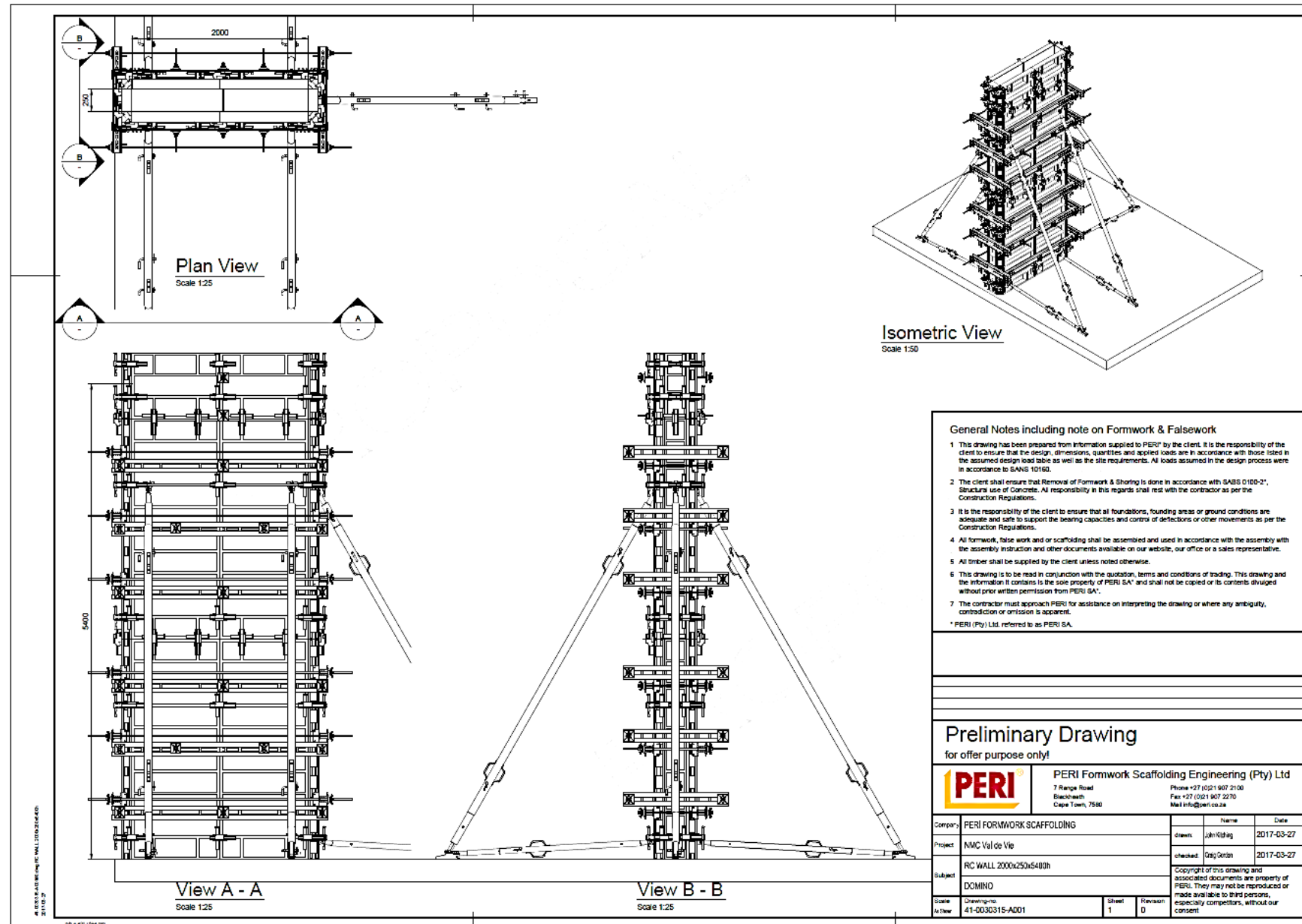
Annexure A : Additional CIFA K31L Information



Annexure B: Additional Putzmeister 36Z-Meter Information



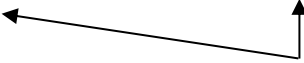
Annexure C: Experimental Formwork System Design Drawing



Annexure D : Pressure Readings for Wall 1

Transducer ID	Height from the base of the formwork system							
	2.2 m		2.6 m		3 m		3.4 m	
	Lateral Pressure (kPa)	Hydrostatic Pressure (kPa)	Lateral Pressure (kPa)	Hydrostatic Pressure (kPa)	Lateral Pressure (kPa)	Hydrostatic Pressure (kPa)	Lateral Pressure (kPa)	Hydrostatic Pressure (kPa)
#1	-	-	-	-	-	-	-	-
#2	-	-	-	-	0.06	2.1	3.51	10.4
#3	-	-	0.19	4.8	4.84	13.1	15.8	21.4
#4	0.10	12.2	10.5	20.5	21.4	28.8	32.3	37.1
#5	9.755	22.2	21.7	30.5	32.8	38.8	43.9	47.1
#6	15.25	27.2	26.75	35.5	37.9	43.8	48.4	52.1
#7	27.45	37.4	37.9	45.7	49.1	53.9	59.8	62.3
#8	26.9	37.4	37.8	45.7	46.6	53.9	57.5	62.3

Transducer ID	Height from the base of the formwork system									
	3.8 m		4.2 m		4.6 m		5 m		5.4 m	
	Lateral Pressure (kPa)	Hydrostatic Pressure (kPa)	Lateral Pressure (kPa)	Hydrostatic Pressure (kPa)	Lateral Pressure (kPa)	Hydrostatic Pressure (kPa)	Lateral Pressure (kPa)	Hydrostatic Pressure (kPa)	Lateral Pressure (kPa)	Hydrostatic Pressure (kPa)
#1	-	-	-	-	-	-	-	-	-	-
#2	11.1	18.7	22.6	27.0	32.2	35.3	42.4	43.6	48.3	51.9
#3	23.0	29.7	33.9	38.0	43.8	46.3	54.7	54.6	60.7	62.9
#4	40.1	45.4	52.1	53.7	60.2	62.0	71.6	70.3	77.2	78.6
#5	51.5	55.4	63.5	63.7	71.3	71.9	82.4	80.3	88.9	88.6
#6	56.7	60.3	68.3	68.6	76.5	76.9	87.4	85.2	93.9	93.5
#7	68.5	70.6	79.7	78.9	88.1	87.2	97.7	95.4	104.8	103.74
#8	65.9	70.6	78.4	78.9	80.9	87.2	83.1	95.4	80.04	103.74


 Transducer problems

Annexure E : Pressure Readings for Wall 2 and Wall 3

Transducer ID	Height from the base of the formwork system		
	Maximum lateral pressure		
	Lateral Pressure (kPa) SCC-TP-WP10-R27	Lateral Pressure (kPa) SCC-TP-WP15-R27	Hydrostatic Pressure (kPa)
#1	-	-	-
#2	44.5	45.0	51.9
#3	55.9	55.9	62.9
#4	71.3	69.7	78.6
#5	75.6	72.8	88.6
#6	77.9	76.9	93.5
#7	94.3	88.8	103.7
#8	89.5	84.9	103.7

Annexure F : Pressure Readings for Wall 4

Transducer ID	Height from the base of the formwork system							
	2.2 m		2.6 m		3 m		3.4 m	
	Lateral pressure (kPa)	Hydrostatic Pressure (kPa)	Lateral pressure (kPa)	Hydrostatic Pressure (kPa)	Lateral pressure (kPa)	Hydrostatic Pressure (kPa)	Lateral pressure (kPa)	Hydrostatic Pressure (kPa)
#1	-	-	-	-	-	-	-	-
#2	-	-	-	-	0.7	2.1	11.6	10.4
#3	-	-	2.9	4.8	13.0	13.1	24.2	21.4
#4	9.3	12.2	19.7	20.5	29.6	28.8	39.9	37.1
#5	19.6	22.2	30.1	30.5	40.7	38.8	49.9	47.1
#6	25.5	27.2	35.6	35.5	46.1	43.8	55.7	52.1
#7	36.7	37.4	46.4	45.7	57.3	53.9	66.9	62.3
#8	39.3	37.4	48.9	45.7	58.6	53.9	68.2	62.3

Transducer ID	Height from the base of the formwork system									
	3.8 m		4.2 m		4.6 m		5 m		5.4 m	
	Lateral pressure (kPa)	Hydrostatic Pressure (kPa)	Lateral pressure (kPa)	Hydrostatic Pressure (kPa)	Lateral pressure (kPa)	Hydrostatic Pressure (kPa)	Lateral pressure (kPa)	Hydrostatic Pressure (kPa)	Lateral pressure (kPa)	Hydrostatic Pressure (kPa)
#1	-	-	-	-	-	-	-	-	-	-
#2	23.6	18.7	34.3	27.0	41.3	35.3	45.6	43.6	47.9	51.9
#3	37.7	29.7	48.6	38.0	55.0	46.3	59.6	54.6	61.6	62.9
#4	53.1	45.4	64.2	53.7	69.9	62.0	74.6	70.3	76.2	78.6
#5	63.3	55.4	73.9	63.7	79.0	71.9	83.8	80.3	85.9	88.6
#6	68.8	60.3	78.9	68.6	84.6	76.9	88.8	85.2	91.2	93.5
#7	80.7	70.6	90.6	78.9	96.9	87.2	101.3	95.4	103.2	103.74
#8	81.1	70.6	92.1	78.9	96.5	87.2	101.6	95.4	103.3	103.74

Annexure G : Pressure Readings for Wall 5

Transducer ID	Height from the base of the formwork system							
	2.2 m		2.6 m		3 m		3.4 m	
	Lateral pressure (kPa)	Hydrostatic Pressure (kPa)	Lateral pressure (kPa)	Hydrostatic Pressure (kPa)	Lateral pressure (kPa)	Hydrostatic Pressure (kPa)	Lateral pressure (kPa)	Hydrostatic Pressure (kPa)
#1	-	-	-	-	-	-	-	-
#2	-	-	-	-	4.79	2.1	16.5	10.4
#3	-	-	4.10	4.8	15.9	13.1	27.5	21.4
#4	10.9	12.2	22.2	20.5	34.5	28.8	44.2	37.1
#5	18.9	22.2	32.4	30.5	44.9	38.8	53.7	47.1
#6	24.3	27.2	36.6	35.5	50.8	43.8	59.4	52.1
#7	35.9	37.4	50.23	45.7	64.7	53.9	71.9	62.3
#8	-	-	-	-	-	-	-	-



Transducer failure

Transducer ID	Height from the base of the formwork system									
	3.8 m		4.2 m		4.6 m		5 m		5.4 m	
	Lateral pressure (kPa)	Hydrostatic Pressure (kPa)	Lateral pressure (kPa)	Hydrostatic Pressure (kPa)	Lateral pressure (kPa)	Hydrostatic Pressure (kPa)	Lateral pressure (kPa)	Hydrostatic Pressure (kPa)	Lateral pressure (kPa)	Hydrostatic Pressure (kPa)
#1	-	-	-	-	-	-	-	-	-	-
#2	22.8	18.7	33.4	27.0	39.2	35.3	43.5	43.6	45.8	51.9
#3	35.1	29.7	46.6	38.0	52.52	46.3	56.9	54.6	59.1	62.9
#4	50.6	45.4	62.2	53.7	67.2	62.0	71.9	70.3	74.7	78.6
#5	60.25	55.4	72.2	63.7	76.8	71.9	82.2	80.3	84.7	88.6
#6	65.9	60.3	78.6	68.6	82.9	76.9	88.1	85.2	90.8	93.5
#7	78.6	70.6	91.9	78.9	95.9	87.2	101.7	95.4	103.7	103.74
#8	-	-	-	-	-	-	-	-	-	-



Transducer failure

Annexure H : Pressure Readings for Wall 6

Transducer ID	Height from the base of the formwork system							
	2.2 m		2.6 m		3 m		3.4 m	
	Lateral pressure (kPa)	Hydrostatic Pressure (kPa)	Lateral pressure (kPa)	Hydrostatic Pressure (kPa)	Lateral pressure (kPa)	Hydrostatic Pressure (kPa)	Lateral pressure (kPa)	Hydrostatic Pressure (kPa)
#1	-	-	-	-	-	-	-	-
#2	-	-	-	-	1.44	2.1	10.2	10.4
#3	-	-	2.03	4.8	13.1	13.1	24.0	21.4
#4	9.58	12.2	17.4	20.5	29.6	28.8	39.1	37.1
#5	19.7	22.2	27.5	30.5	39.2	38.8	49.5	47.1
#6	26.2	27.2	34.6	35.5	45.9	43.8	56.1	52.1
#7	33.5	37.4	45.9	45.7	56.6	53.9	65.1	62.3
#8	-	-	-	-	-	-	-	-



Transducer failure

Transducer ID	Height from the base of the formwork system									
	3.8 m		4.2 m		4.6 m		5 m		5.4 m	
	Lateral pressure (kPa)	Hydrostatic Pressure (kPa)	Lateral pressure (kPa)	Hydrostatic Pressure (kPa)	Lateral pressure (kPa)	Hydrostatic Pressure (kPa)	Lateral pressure (kPa)	Hydrostatic Pressure (kPa)	Lateral pressure (kPa)	Hydrostatic Pressure (kPa)
#1	-	-	-	-	-	-	-	-	-	-
#2	23.1	18.7	32.1	27.0	40.9	35.3	44.3	43.6	46.7	51.9
#3	38.2	29.7	47.8	38.0	57.7	46.3	59.3	54.6	61.2	62.9
#4	52.5	45.4	61.3	53.7	70.1	62.0	72.7	70.3	74.9	78.6
#5	62.6	55.4	71.4	63.7	80.0	71.9	82.6	80.3	84.8	88.6
#6	69.9	60.3	78.8	68.6	87.3	76.9	89.7	85.2	91.3	93.5
#7	78.4	70.6	87.5	78.9	96.3	87.2	98.8	95.4	100.7	103.74
#8	-	-	-	-	-	-	-	-	-	-



Transducer failure

Annexure I : Humanities Ethical Approval



UNIVERSITEIT • STELLENBOSCH • UNIVERSITY
Jou kennisvenoot • your knowledge partner

Approval Notice New Application

24-Mar-2017
Labuschagne, Jean-Claude J

Proposal #: SU-HSD-004110
Title: Hydrostatic Pressure Induced by Self-Compacting Concrete on Formwork

Dear Mr Jean-Claude Labuschagne,

Your **New Application** received on **01-Mar-2017**, was reviewed
Please note the following information about your approved research proposal:

Proposal Approval Period: 24-Mar-2017 -23-Mar-2020

Please take note of the general Investigator Responsibilities attached to this letter. You may commence with your research after complying fully with these guidelines.

Please remember to use your **proposal number** (SU-HSD-004110) on any documents or correspondence with the REC concerning your research proposal.

Please note that the REC has the prerogative and authority to ask further questions, seek additional information, require further modifications, or monitor the conduct of your research and the consent process.

Also note that a progress report should be submitted to the Committee before the approval period has expired if a continuation is required. The Committee will then consider the continuation of the project for a further year (if necessary).

This committee abides by the ethical norms and principles for research, established by the Declaration of Helsinki and the Guidelines for Ethical Research: Principles Structures and Processes 2004 (Department of Health). Annually a number of projects may be selected randomly for an external audit.

National Health Research Ethics Committee (NHREC) registration number REC-050411-032.

We wish you the best as you conduct your research.

If you have any questions or need further help, please contact the REC office at 218089183.

Included Documents:

DESC Report
REC: Humanities New Application

Sincerely,

Clarissa Graham
REC Coordinator
Research Ethics Committee: Human Research (Humanities)

Annexure J : Institutional Permission letter (PERI)



PERI Formwork Scaffolding Engineering (Pty) Ltd
15 Range Road, Blackheath 7580 Western Cape, P O Box 2668, Bellville 7535, South Africa
Phone: 27 (0) 907 2100; Fax: +27 (0) 907 2270

INSTITUTIONAL PERMISSION LETTER

INSTITUTION NAME & ADDRESS: PERI Formwork & Scaffolding Capital Place, Block F 15 - 21 Neutron Avenue Technopark Stellenbosch 7600 South Africa

INSTITUTION CONTACT PERSON: Riaan Brits

INSTITUTION CONTACT NUMBER: 021 880 7777

INSTITUTION EMAIL ADDRESS: riaan.brits@peri.co.za

TITLE OF RESEARCH PROJECT: Lateral Pressure Induced by Self-Compacting Concrete on Formwork

ETHICS APPLICATION REFERENCE NUMBER: SU-HSD-004110

RESEARCHER: Jean-Claude Labushagne

DEPT NAME & ADDRESS: Faculty of Engineering Stellenbosch University Cnr Banhoek Road & Joubert Street Stellenbosch 7600 South Africa

CONTACT NUMBER: 0710579633

EMAIL ADDRESS: 16788125@sun.ac.za

Dear Jean-Claude Labushagne

We have reviewed your request to conduct a research project involving data related to **Technical Design**. You have permission to utilize the data for this project as define in your "Project Proposal".

The following stipulations should be observed:

- *All data supplied to the University need to be treated as confidential and maybe shared only on written agreement by PERI.*

Sincerely,

Name: Riaan Brits

Who warrants that he/she is duly authorised to sign on behalf of PERI Formwork Scaffolding Engineering (PTY) Ltd

Position: Director: Technical

Date: 03 February 2017

Signature: _____

A handwritten signature in black ink, appearing to be "Riaan Brits", is written over a horizontal line.

Annexure K : Institutional Permission letter (Lafarge)



INSTITUTIONAL PERMISSION LETTER

INSTITUTION NAME & ADDRESS: 16 Millner Road, Paarden Eiland Cape Town, South Africa

INSTITUTION CONTACT PERSON: Hennis van Zyl

INSTITUTION CONTACT NUMBER: 021 508 8000

INSTITUTION EMAIL ADDRESS: hennis.vanzyl@lafargeholcim.com

TITLE OF RESEARCH PROJECT: Lateral Pressure Induced by Self-Compacting Concrete on Formwork

ETHICS APPLICATION REFERENCE NUMBER: SU-HSD-004110

RESEARCHER: Jean-Claude Labuschagne

DEPT NAME & ADDRESS: Faculty of Engineering Stellenbosch University Cnr Banhoek Road & Joubert Street Stellenbosch 7600 South Africa

CONTACT NUMBER: 0710579633

EMAIL ADDRESS: 16788125@sun.ac.za

Dear Jean-Claude Labuschagne

We have reviewed your request to conduct a research project involving data related to Readymix Concrete. You have permission to utilize the data for this project as defined in your "Project Proposal".

The following stipulations should be observed:

- *The use of Lafarge logo or information must be approved by Lafarge before being publicised.*

Sincerely,

Name: Hennis van Zyl (name and surname of the contact person at the institution)

Who warrants that he/she is duly authorised to sign on behalf of Lafarge Industries.

Position: Area Manager

Date: 27 March 2017

Signature:

A handwritten signature in black ink, appearing to be 'H. van Zyl'.

Annexure L : Institutional Permission letter (NMC)



1 Link Close, Montague Gardens
7441 Cape Town
PO Box 36617, Champet
7442 South Africa

Facsimile +27 (0)21 551 2977
Telephone +27 (0)21 551 2640
www.nmc.co.za

INSTITUTIONAL PERMISSION LETTER

INSTITUTION NAME & ADDRESS: 1 Link Close Montague Gardens 7441 South Africa

INSTITUTION CONTACT PERSON: Tobie Cilliers

INSTITUTION CONTACT NUMBER: 082 606 6976

INSTITUTION EMAIL ADDRESS: tobie@nmc.co.za

TITLE OF RESEARCH PROJECT: Lateral Pressure Induced by Self-Compacting Concrete on Formwork

ETHICS APPLICATION REFERENCE NUMBER: SU-HSD-004110

RESEARCHER: Jean-Claude Labuschagne

DEPT NAME & ADDRESS: Faculty of Engineering Stellenbosch University Cnr Banhoek Road & Joubert Street Stellenbosch 7600 South Africa

CONTACT NUMBER: 0710579633

EMAIL ADDRESS: 16788125@sun.ac.za

Dear Jean-Claude Labuschagne

We have reviewed your request to conduct a research project involving data related to the research project. You have permission to utilize the data for this project as defined in your "Project Proposal".

The following stipulations should be observed:

- *We cannot provide or guarantee security on site. All material and equipment will be stored at own risk.*
- *All material and equipment must be removed as soon as the research is concluded.*
- *The area provided for the research must be confirmed and approved by NMC prior to commencement.*
- *Site working hours are from 07h30 – 17h15, Monday – Friday (excluding public holidays). No access to site before or after working hours.*
- All the people involved on site must report to the site office for the site specific OHS induction.
- Safety boots and safety vests to be worn at all times.

Sincerely,

a member of the **NMC** Construction Group

NMC (Pty) Ltd. REGISTRATION NO: 1983/013121/07

DIRECTORS: *CA Adonis *MS Behrenden *SL Chambers (COO/acting) *OG De Souza (COO/Civil)
*A Fourie *W Joubert *JG Lombard *MJ Mzamo *GP Robb *NC Sess *BB Simelane *RA Sparks (Chairman)
*MJ van Coller *AJ Vlok (CEO) *BB Wiersma *DJK Wiersma *SK Webber (CFO) *Gerrit Bredt

setting the construction standard

©100 GBV

ENRCA Certified: ISO 14001 & ISO 9001:2015 CERT: 18001



1 Link Close, Montague Gardens
7441 Cape Town
PO Box 36617, Chempet
7442 South Africa

Facsimile +27 (0)21 551 2977
Telephone +27 (0)21 551 2640
www.nmc.co.za

Name: Tobie Cilliers
Position: Snr Site Agent
Date: 07/04/2017
Signature:

A handwritten signature in black ink, appearing to read 'Tobie Cilliers', written over a horizontal line.

a member of the **NMC** Construction Group

NMC (Pty) Ltd. REGISTRATION NO: 1983/013121/07

DIRECTORS: *CA Adonis *MS Behardien *St Chambers (COO bulding) *GG De Sousa (COO Civil)
*A Fourie *W Joubert *JG Lombard *ML Mzama *GP Robb *NC Sass *BB Simlane *RJA Sparks (Chairman)
*MJ van Coller *AJ Vlok (CFO) *BB Wentenaar *DJK Weiss *SK Webber (CEO) *Gasp Bana

setting the construction standard

ISO 9001

DEKRA Certified: ISO 14001 & ISO 9001:2015